THE UNIVERSITY *of* EDINBURGH

Exponential Asymptotics in Wave Propagation Problems

Christopher Neal Foley

Doctor of Philosophy
University of Edinburgh
2013

Declaration

I declare that this thesis was composed by myself and that the work contained therein is my own, except where explicitly stated otherwise in the text.

(*Christopher Neal Foley*)

To my Mutz, Margaret PR Foley. This is for you.

Abstract

We use the methods of exponential asymptotics to study the solutions of a one dimensional wave equation with a non-constant wave speed $c(x,t)$ modelling, for example, a slowly varying spatio-temporal topography. The equation reads

$$h_{tt}(x,t) \;=\; \big(c^2(x,t)h_x(x,t)\big)_x, \tag{1}$$

where the subscripts denote differentiation w.r.t. the parameters x and t respectively. We focus on the exponentially small reflected wave that appears as a result of a Stokes phenomenon associated with the complex singularities of the speed. This part of the solution is not captured by the standard WKBJ (geometric optics) approach. We first revisit the time-independent propagation problem using resurgent analysis. Our results recover those obtained using Meyers integral-equation approach or the Kruskal–Segur (K–S) method. We then consider the time-dependent propagation of a wavepacket, assuming increasingly general models for the wave speed: time independent, $c(x)$, and separable, $c_1(x)c_2(t)$. We also discuss the situation when the wave speed is an arbitrary function, $c(x,t)$, with the caveat that the analysis of this setup has yet to be completed. We propose several methods for the computation of the reflected wavepacket. An integral transform method, using the Dunford integral, provides the solution in the time independent case. A second method exploits resurgence: we calculate the Stokes multiplier by inspecting the late terms of the dominant asymptotic expansion. In addition, we explore the benefits of an integral transform that relates the coefficients of the dominant solution in the time-dependent problem to the coefficients of the dominant solution in the time-independent problem. A third method is a partial differential equation extension of the K–S complex matching approach, containing details of resurgent analysis. We confirm our asymptotic predictions against results obtained from numerical integration.

Acknowledgements

In presenting this thesis, I would like to acknowledge the help and support I have received throughout my PhD.

First and foremost, I would like to thank my supervisor and sage Adri Olde Daalhuis whose mixture of patience and brilliance helped, not only to guide me throughout my work but, to shape me into a better mathematician.

Secondly, I am most grateful to my partner Mahala, my Loml. Thank you for all of your love and support throughout my PhD. I promise to return it in equal measure for the rest of our lives. (Joint secondly) I must also thank my gran and my mum whose combined wisdom and encouragement has been invaluable.

Thirdly, many thanks to both the administration and support staff at the School of Mathematics, University of Edinburgh, that contributed to making my PhD programme proceed smoothly.

Finally, I would like to thank Jacques Vanneste for his time and efforts in editing and discussing my work.

Contents

Abstract **5**

1 Introduction **11**
1.1 Stokes phenomenon, Stokes lines and turning points . . . 11
1.2 Kruskal–Segur method . . . 12
1.3 Resurgence relation . . . 13
1.4 Subdominant solution . . . 14
1.5 Physical setup . . . 14
1.5.1 Why exponentially small? . . . 16
1.6 Literature review and map of the thesis . . . 16
1.6.1 Chapter 2 . . . 16
1.6.2 Chapter 3 . . . 18

2 Exponentially small reflection **21**
2.1 Introduction to the problem . . . 21
2.2 Time independent problem . . . 22
2.2.1 K–S approach . . . 22
2.2.2 Initial set-up and the exponentially small pre-factor of the reflected solution 23
2.2.3 Complex conjugate transition points . . . 25
2.2.4 Stokes lines . . . 25
2.2.5 Matched asymptotics . . . 26
2.3 Spatially independent wave speed problem . . . 29
2.3.1 Stokes multiplier relations . . . 29
2.4 Exponential asymptotics via resurgence analysis: a time independent wave speed 30
2.5 Numerical Results . . . 33
2.5.1 Convergence to the estimate in (3.40) . . . 34
2.6 Mistakes in the literature . . . 35
2.6.1 Grimshaw . . . 36
2.6.2 Hinch . . . 38
2.7 $-1 < \alpha_1 < 0$ . . . 41
2.7.1 A calculation of an $\mathcal{O}(\epsilon)$ Stokes multiplier . . . 42
2.7.2 No Stokes phenomena . . . 45
2.8 $\alpha_1 < -1$ . . . 47
2.8.1 Inspecting the recurrence relation near x_* . . . 50
2.9 Wave reflection: a branch point order perspective . . . 51

3 Solutions to a wave equation for a spatio-temporal wave speed **53**
3.1 Preliminary results: leading order 'initial' solution . . . 53
3.1.1 Ray-tubes and localised initial data . . . 56
3.2 Exponential asymptotics via resurgent analysis . . . 57
3.2.1 Subdominant (reflected) solutions . . . 57
3.2.2 Stokes lines . . . 60
3.2.3 Recurrence relations near the turning points . . . 61
3.2.4 $b_{j0}(x,t)$ and the Stokes multiplier . . . 65
3.2.5 General solution . . . 67

3.3 Integral transform along the characteristic curve . . . 67
3.3.1 Resurgent analysis and benefits of the integral transform . . . 69
3.3.2 Subdominant Solutions . . . 71
3.3.3 $b_{j0}(x,t)$ and the Stokes multipliers . . . 72
3.4 Extending K-S (WKBJ) to compute reflection . . . 73
3.4.1 K–S Method . . . 74
3.4.2 Temporal Turning Point . . . 78
3.4.3 General solution . . . 79
3.5 Numerical tests when $c(x,t)$ is separable . . . 79
3.5.1 Time independent wave speed . . . 80
3.5.2 Spatially independent wave speed . . . 82
3.5.3 Separable wave speed profile . . . 83

4 Conclusion and future work **85**
4.1 Highlights . . . 85
4.2 Future projects . . . 86
4.2.1 $\alpha_1 = -1$: Chapman and Mahony . . . 86
4.2.2 No Stokes phenomenon . . . 87
4.2.3 Solution of (3.1) for an arbitrary spatio-temporal wave speed . . . 88

A Local matching approach for the case of special $\hat{\alpha}$ values in §3.7.1 **91**

B Fourier transform of a wave equation with a spatially varying wave speed **93**

C Conservation laws, amplitudes and general identities **107**
D Showing $C(x')$ is constant in (B.21) . . . 107
E Finding the constant V_+ . . . 108
F Conservation Law . . . 108
G Reflected wave amplitude and the Stokes multiplier . . . 109
H Dropping the Heaviside function . . . 110
I Deforming the contour in (B.58) . . . 110

Chapter 1

Introduction

This thesis is concerned with finding an estimate for the solutions of a wave equation with a spatio-temporal wave speed varying slowly in space and time. Specifically, we are interested in finding an asymptotic estimate for the exponentially small reflected waves that appear as a result of a Stokes phenomenon associated with the branch point zeros and singularities of the speed profile in the complex x-t plane (Chapter 3), c.f. Figure1.1. To do this, we use the tools of exponential asymptotics (E-A) via the methods outlined in the abstract. It is therefore useful to introduce some of the terminology and techniques connected with E-A used throughout this study.

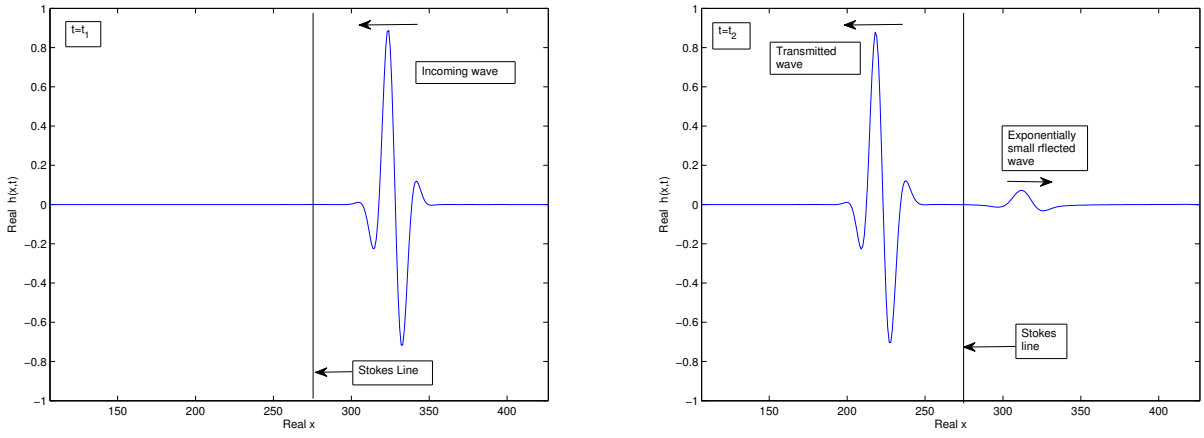

Figure 1.1: Numerical simulation, c.f. §3.5, of the 'physical' phenomenon whereby an incident wave, shown here at time $t = t_1$ in the left panel, gives rise to a transmitted wave and exponentially small reflected wave at a later time $t = t_2$ on crossing a Stokes line (right panel). The Stokes line has been inserted for illustrative purposes only. The Stokes line exists in the complex x plane and thus its location above has been chosen to indicate the point at which it crosses the real axis.

1.1 Stokes phenomenon, Stokes lines and turning points

The Stokes phenomenon plays a pervasive role in asymptotic analysis. A popular (e.g. [8], [39] [47] and [48]) introduction to the phenomenon is to inspect particular details of the solutions of the one dimensional Helmholtz (or Schrödinger) equation

$$\frac{d^2w(x)}{dx^2} + \frac{q^2(x)}{\epsilon^2}w(x) = 0, \quad \epsilon \to 0, \tag{1.1}$$

where the function $q(x)$ does not depend on ϵ and for our purposes assumed analytic on the real axis. It is noted in [47] that: a central problem for the general linear second order equation (1.1) has for a long time been connecting solutions across zeros and singular points of $q(x)$ collectively known as *transition points*. Note, [44] states that: zeros (and branch point singularities) of $q(x)$ are called *transition points* or *turning points* of the differential equation (1.1). The reason for these names is that when the variables are real and the root is a simple zero, it separates an interval in which the solutions are of exponential type from one in which they oscillate.

The asymptotic solutions of (1.1) can be found by seeking WKBJ solutions of the form

$$w(x) \sim \mathrm{e}^{\mathrm{i}\theta(x)/\epsilon} \sum_{n=0}^{\infty} \tilde{a}_n(x)\epsilon^n, \tag{1.2}$$

which upon substituting into (1.1) gives

$$w(x) \sim q^{-1/2}(x) \left(A(\epsilon)\mathrm{e}^{\frac{\mathrm{i}}{\epsilon}\int^x q(x')dx'} \sum_{n=0}^{\infty} a_n(x)\epsilon^n + B(\epsilon)\mathrm{e}^{-\frac{\mathrm{i}}{\epsilon}\int^x q(x')dx'} \sum_{n=0}^{\infty} b_n(x)\epsilon^n \right), \tag{1.3}$$

with constants $A(\epsilon)$ and $B(\epsilon)$ valid in appropriate sectors of the complex x-plane. Eq. (1.3) is an asymptotic representation of the exact solution of (1.1) bounded away from the transition points. See [44] for regions of validity of (1.3). Therefore, the constants $A(\epsilon)$ and $B(\epsilon)$ may have different values on different sides of such a transition point, and the connection problem may be phrased as that of determining the value in one section given the value in another. The fact that the constants $A(\epsilon)$ and $B(\epsilon)$ change from one region of the complex plane to another, on crossing particular rays called *Stokes lines*, is known as the *Stokes phenomenon*. The phenomenon was discovered and discussed by G. G. Stokes in a series of papers [55], [56] and [57]. Stokes lines, across which the coefficient of a subdominant solution (c.f. §1.4) 'jumps'[1] from one value to another, emanate from the transition points, x_*, of $q(x)$ and are defined by

$$\Re\{\chi(x)\} = 0, \quad \text{where} \quad \chi(x) = \int_{x_*}^{x} q(x')dx'.$$

Also of interest are the *anti-Stokes lines* where the two solutions in (1.3) are similar in size, i.e. where

$$\Im\{\chi(x)\} = 0.$$

Note that a transition or turning point, x_*, is typically a singular point for every $\tilde{a}_n(x) : n > N$, for finite positive N, in (1.2).

1.2 Kruskal–Segur method

A method of some importance in the present study is the Kruskal–Segur (K–S) method, which was outlined in the seminal work [31]. Applications of the K–S method in an ODE and PDE problem are given in Chapters 2 and 3 respectively. Therefore, we summarise the key ideas relevant to (1.1).

The K–S approach provides a method for determination of the constants $A(\epsilon)$ and $B(\epsilon)$ in (1.3) throughout a wide range of sectors in the complex plane. In the region of interest, let us assume that the term pre-factored by $A(\epsilon)$ in (1.3) is the dominant solution and $B(\epsilon)$ pre-factors the subdominant solution. Typically, we are interested in finding the value of the coefficient of the subdominant term once the dominant solution has crossed a Stokes line. This is achieved by rewriting (1.1) near a transition point x_* through a local expansion of $q(x)$ and solving the resulting ODE. The solutions found are known as the inner solutions. Then the inner solutions are connected with the WKBJ solutions (1.3) across a region containing a Stokes line and where both sets of solutions are valid (transition region), which allows for determination of $B(\epsilon)$ across the Stokes line. However, due care must be exercised when taking a K–S approach as an obvious drawback is noted: how does one determine the number of terms to take in the

[1] This 'jump' was later found to be smooth in the seminal paper by M. V. Berry, [9].

local expansion of $q(x)$ to gain the 'correct' value of $B(\epsilon)$? This matter is discussed in Chapter 2.

1.3 Resurgence relation

Resurgence plays an important role in modern asymptotic theory and a resurgence relation will be central to our analysis in Chapter 3. Texts which cover this topic include [2], [10], [20] and [54], and for applications see [7], [27], [41], [42] or [43]. Here, we aim to summarise the aspects used within this study.

We focus on the ODE (1.1) with solutions given by (1.3). Let

$$w_1(x) \sim q^{-1/2}(x)\mathrm{e}^{\frac{\mathrm{i}}{\epsilon}\int_{x_*}^{x} q(x')dx'} \sum_{n=0}^{\infty} a_n(x)\epsilon^n$$

$$\text{and} \quad w_2(x) \sim q^{-1/2}(x)\mathrm{e}^{-\frac{\mathrm{i}}{\epsilon}\int_{x_*}^{x} q(x')dx'} \sum_{n=0}^{\infty} b_n(x)\epsilon^n$$

be solutions to (1.1) bounded away from any transition points. The function $q(x)$ is assumed to contain a transition point at $x = x_*$ where $\Im\{x_*\} > 0$ and chosen so that a Stokes line emanating from x_* crosses the real axis at some location. Then on crossing a Stokes line the solution valid at $x \to \infty$, $w_1(x)$, switches on a subdominant solution of the form $\epsilon^{\mu}K(\epsilon)w_2(x)$, as illustrated in Figure 1.2. The constant $K(\epsilon)$ is known as the Stokes multiplier and μ is a real constant. Note that the Stokes multiplier can be represented as $K(\epsilon) = \sum_{n=0}^{\infty} K_n\epsilon^n$, where the K_n are constants. It can be shown that the late terms of the dominant solution, that is

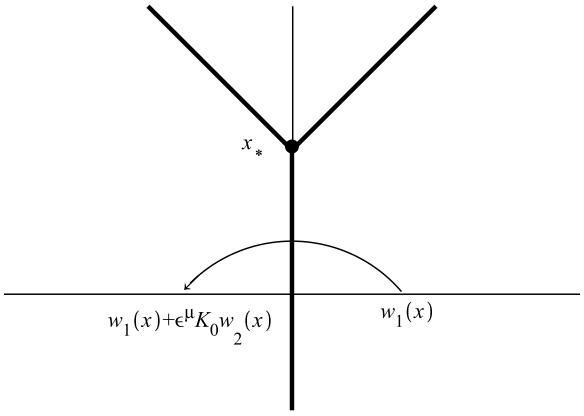

Figure 1.2: Stokes lines (bold) and the Stokes phenomenon: plot of the 'switch on' of a subdominant solution as a dominant solution crosses a Stokes curve.

a_n for $n \gg 1$, are then related to the early terms of the subdominant solution by the following asymptotic (resurgence) relation

$$a_n(x) \sim \frac{K_0}{2\mathrm{i}\pi}\frac{\Gamma(n+\mu)b_0(x)}{\big(\chi(x)\big)^{n+\mu}}, \quad n \to \infty, \tag{1.4}$$

with $\chi(x) = 2\mathrm{i}\int_{x_*}^{x} q(x')dx'$. Eq. (1.4) plays a central role in the analysis throughout this thesis. This relationship is studied in detail in [19] (see [20] also) where Dingle shows that

for a wide range of asymptotic expansions, the WKBJ method and so on, the coefficients are asymptotically of the form (1.4).

To get an idea of the origins of (1.4), note that placing (1.2) into (1.1) returns a recurrence relation where each successive term of the asymptotic approximation will require the derivative of the previous term, c.f. (2.57). Thus, if a_n contains a singularity of the form $(x-x_*)^{-(n+\mu)}$ then a_{n+1} will contain a singularity of the form $(n+\mu)(x-x_*)^{-(n+\mu+1)}$ and each new derivative adds a factor to the numerator and increases the strength of the singularity. Then, as $n \to \infty$ we expect (1.4).

1.4 Subdominant solution

So that the nomenclature used within this study is transparent and, largely, self contained we now briefly discuss the concept of a subdominant solution or solution *beyond all orders*.

As discussed in [52], "an important feature of an asymptotic series like

$$\phi(\epsilon) \sim \sum_n \phi_n \epsilon^n \tag{1.5}$$

is that every term is algebraic in ϵ. Transcendentally small terms like $\mathrm{e}^{-1/\epsilon^2}$ are smaller than every term in the series as $\epsilon \to 0$, and are not captured by it. Thus, if (1.5) is valid then

$$\phi(\epsilon) + \mathrm{e}^{-1/\epsilon^2} \sim \sum_n \phi_n \epsilon^n$$

is valid as well. Such transcendentally small [subdominant] terms are said to lie *beyond all orders* of the asymptotic expansion.

In most applications, these tiny corrections are insignificant and they can safely be neglected. However, exceptional problems in which these very small terms have great practical interest are known in many branches of science, including dendritic crystal growth, viscous fluid flow, quantum tunneling, KAM theory, and others. For these exceptional problems, conventional asymptotic analysis is simply inadequate. These problems require improved methods, designed to obtain meaningful corrections that lie beyond all orders of a conventional asymptotic expansion. The phrase *asymptotics beyond all orders* [for our purposes, exponential asymptotics] refers to the collection of such methods."

It is worth noting that a subdominant solution switched on via a Stokes phenomenon is exponentially small, e.g. the exponentially small wave packet switched in (1) as shown in Figure1.1, but on crossing the next anti-Stokes line it can become dominant.

The fact that a transcendentally small (subdominant) term, hiding behind all orders of a (divergent) asymptotic series, can have a practical effect is shown within this study. That is, it is explicitly shown within this thesis that the neglected transcendental contributions, exponentially small reflected waves, are of a *qualitatively different* nature and this gives them dominant importance in some respects.

1.5 Physical setup

We now outline the physical setup which leads to (1). In this thesis we consider the linear shallow-water equations without background rotation, i.e. no Coriolis forces. The linear shallow-water equations starting from a state of rest are derived by considering small perturbations from a basic state $h(x,0) = H(x)$ and $u(x,0) = 0$, c.f. Fig1.3. Hence, we write

$$h(x,t) = H(x) + \delta h'(x,t) + \mathcal{O}(\delta^2) \quad \text{and} \quad u(x,t) = \delta u'(x,t) + \mathcal{O}(\delta^2), \tag{1.6}$$

where $0 < \delta \ll 1$ is a small non-dimensional parameter measuring the amplitude of the flow deviations. The linearised equations are then found by substituting (1.6) into the shallow-water equations, see [12], and collecting terms linear in δ. The result is

$$h'_t(x,t) = -\left(H(x)u'(x,t)\right)_x \quad \text{and} \quad u'_t(x,t) = -g(t)h'_x(x,t). \tag{1.7}$$

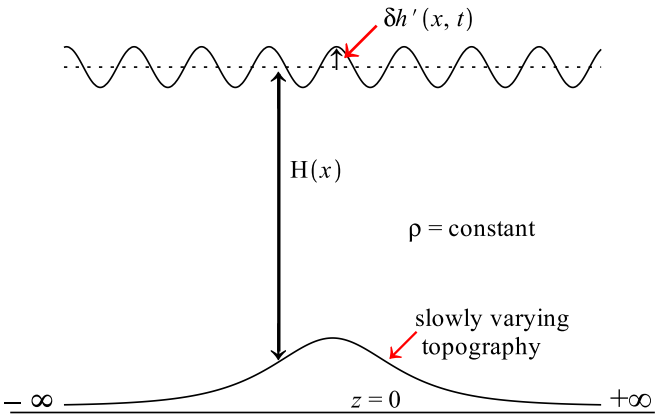

Figure 1.3: Schematic of the shallow water system.

The equations in (1.7) take into account variations in the topography, i.e. the interface of the fluid with the lower boundary, due to the single appearance of $H(x)$. We have also included a time dependent gravity $g(t)$ which can be realised experimentally in an accelerated tank. Combining (1.7) returns (1), on removing the prime, with

$$c(x,t) = \sqrt{g(t)H(x)}. \tag{1.8}$$

The approach is then to assume that $H(x)$ and $g(t)$ are slowly varying so that for all x and t the solution of (1) appears locally as a plane wave. This is a special case where the solution of (1) forms a *slowly varying wavetrain* whose amplitude varies slowly in x to account for slow variations in $c(x,t)$. In other words, the distance over which $c(x,t)$ changes significantly should appear large compared to the intrinsic length scale of the system $1/k$, where k is the wavenumber. The scale separation between the phase of the wave train and the amplitude can be exploited to derive asymptotic equations based on a small parameter which we take to be $\epsilon : \ 0 < \epsilon \ll 1$. This is the field of high wavenumber asymptotics and prompts the use of the ansatz

$$h(x,t) \ \sim \ A(x,t)\mathrm{e}^{\mathrm{i}\theta(x,t;\epsilon)/\epsilon}, \quad \theta(x,t;\epsilon) = \theta_0(x,t) + \theta_1(x,t)\epsilon + \ldots$$

to solve (1). The solution is expected to appear locally as a plane wave, hence

$$\partial_x\theta_0(x,t) \ \sim \ k(x,t) \quad \text{and} \quad \partial_t\theta_0(x,t) \ \sim \ -\omega(x,t),$$

where $\omega(x,t)$ is the frequency. It is clear that the physical setup corresponding to (1) has many more practical applications than the classical homogenous wave speed wave equation. A visit to the beach when the tide is out will invariably reveal regions where a (repeated) topography shown in Figure1.3 is present. General examples where the setup in Figure1.3 is applicable include: tsunami dynamics, compressible gas dynamics, optics and river hydraulics. Hence, the main result of the thesis, found in Chapter 3, which delivers an explicit leading order solution for both the transmitted and reflected waves in (1), for a separable wave speed as in (1.8), is of practical importance.

1.5.1 Why exponentially small?

One might ask: why do we expect to 'see' an exponentially small reflected wave appear as the initial solution of (1) crosses a Stokes line in the real x–t plane? To answer this, we consider a time independent wave speed profile, $c(x,t) = c(\epsilon x)$, in (1). The small parameter ϵ has been included in the argument of the wave speed to make clear that there are only gradual changes in the medium. Then, for infinitely differentiable wave speed functions ($c \in C^\infty$ and real x) with sufficient decay of derivatives in the far field, the WKBJ method predicts zero reflection to any order of approximation in the asymptotic expansion with respect to ϵ. The failure of shortwave asymptotics (WKBJ) to identify wave reflection was stressed by Mahony in 1967, [37]. He put forward the conjecture that in fact any reflected wave will be *transcendentally small*. This conjecture, in the setting of gradual reflection of short waves, was proved by Meyer in 1975, [38], who, on reducing (1) to a related ODE problem (e.g. (1.1)) calculates an explicit expression for the amplitude of the exponentially small reflected wave for a wide class of wave speed profiles. However, neither Meyer nor Mahony gave explicit formulae for the case where $c(x)$ has a discontinuity in its nth derivative. The matter of exponential smallness and $\mathcal{O}(\epsilon^n)$ reflection is discussed by Berry in [4].

A useful explanation of the reason for an exponentially small reflected wave is given by Hinch, [29] p137, and reads:
"when a single right-moving wave is incident on a region where the medium varies, $c(\epsilon x)$, all of its energy is transmitted and there is no reflected wave, to leading order. Now, if c has a discontinuity (where it is not slowly varying), then equating $[h]$ and $[c^2 h_x]$ on the two sides of the discontinuity yields a reflected wave with a relative magnitude of $\mathcal{O}\left(\frac{\Delta c}{c}\right)$...one can show that if $c(\epsilon x)$ has a discontinuity in its n^{th} derivative, then there will be a reflected wave of order ϵ^n. If all the derivatives of $c(\epsilon x)$ are continuous (a C^∞ function), then the reflected wave is exponentially small."
This simple explanation was also given by Berry, [4], set in the context of a Schrödinger equation with an analytic potential. The idea of exponentially small terms extends naturally to spatio-temporal wave speed profiles $c(x,t)$.

1.6 Literature review and map of the thesis

Throughout Chapters 2 and 3 we study the classical d'Alembert wave equation in a variable medium, given by (1).

1.6.1 Chapter 2

We begin by revisiting the time independent propagation problem, i.e. $c(x,t) = c(x)$, and introduce a setup corresponding to a continuously forced wave of fixed frequency whereby there exists a single incident wave at $x \to \infty$. On crossing a Stokes line a Stokes phenomenon gives rise to an exponentially small reflected wave detected at $x \to -\infty$ owing to a single transition point of $c(x)$. Determining the value of the reflected wave amplitude on the real line forms the basis of study in Chapter 2. To achieve this we assume Fourier type solutions of the form $h(x,t) = y(x)\mathrm{e}^{\mathrm{i}\omega t}$ and w.l.g. set $\omega = 1$. Then, (1) reduces to

$$\epsilon^2 \frac{d^2u(x)}{dx^2} + P(x;\epsilon)u(x) = 0, \tag{1.9}$$

$$\text{where} \quad P(x;\epsilon) = \frac{1}{c^2(x)} - \epsilon^2 \frac{c''(x)}{c(x)} \quad \text{and} \quad y(x) = \frac{u(x)}{c(x)}.$$

Eq (1.9) came into prominence in the early part of the 20th century among physicists as a type of *Schrödinger wave equation* in the theory of quantum mechanics, noted by letting $P(x;\epsilon) = E - V(x)$ in (1.9) where E is the energy and $V(x)$ a potential function. Additionally, (1.9) has importance in the area of shallow water wave mechanics, or more specifically the *gradual reflection of short waves* (c.f. §1.5).

The review paper by Berry and Mount [3], 1972, indicates that much of what is currently known about the subdominant solutions of (1.9) was known in the quantum mechanical context

well before the seminal mathematics paper of Meyer, [38], in 1975. For instance, the calculation of an exponentially small reflected wave appears in Pokrovskii *et al* in the papers [49] and [50], both 1958. However, in those papers they failed to evaluate the multiple integrals involved to correctly determine the $\mathcal{O}(1)$ coefficient of the exponentially small term. This matter was later resolved by Pokrovskii and Khalatnikov in [51]. That is, the reflected wave amplitude, R, for a general branch point order of $c(x)$, α (also known as the order of the turning point), is shown to be:

$$R \sim -2\mathrm{i}\sin\left(\frac{\alpha\pi}{2(\alpha+1)}\right)\mathrm{e}^{2\mathrm{i}W^*}, \quad W^* = \frac{1}{\epsilon}\int_0^{x_*}\frac{dx'}{c(x')}, \ \epsilon \to 0, \tag{1.10}$$

where x_* is a turning point of (1.9). Note that the object $\mathrm{e}^{2\mathrm{i}W^*}$ is exponentially small. Eq(1.10), known as the '*WKB reflection formula*', appears subsequently in Fröman and Fröman [26] in 1965. These results correspond to that of [38]. However, it is noted by Berry in [4] that "[the] continuity class [conjecture] by Mahony (1967) [was] proved by Meyer in (1975, 1976)." Therefore, although the main result of Meyer in [38], given by (1.10), was shown earlier by [51], Meyer set out a formal foundation for the criteria with which one expects and can calculate exponentially small terms along the real line.

The history suggests two things: that the Russian results took time to percolate to the west and that Meyer was interested in rigorous results.

The two main methods used in the past to recover (1.10) are: the '*complex method*', where the WKBJ solutions are traced along a path (away from any turning points) in the complex plane connecting the two regions where we aim to find connection formulae. This method was invented by Zwaan [61]. See the text [26] for deveolpments on the method. Note, in §2.6 we highlight errors in [28] and [29], both of which appear as a result of an erroneous use of the complex method in a calculation to estimate the amplitude of an exponentially small reflected wave. The second method, by which the calculation of (1.10) is possible, is a more fundamental form of the K-S method (summarised in §1.2). This method, known as the '*Uniform Approximation*' (U-A) method or equivalently *'The Method of Comparison Equations'*, was pioneered by Langer in 1937, see [35]. The method is a generalisation of the basic WKBJ method and relies on being able to obtain an approximate solution to (1.9) in terms of known solutions to the equation

$$\frac{d^2\phi(z)}{dz^2} + \Lambda(z)\phi(z) = 0, \tag{1.11}$$

where $\Lambda(z)$ is chosen to be similar in some way to $P(x;\epsilon)$, i.e. $\Lambda(z)$ is the leading order form of $P(x;\epsilon)$ local to a turning point of (1.9). Several examples of the U-A method are given in [3]. A calculation of interest is that leading to equation (4.17) in [3]; where (1.11) is the Airy equation and the resulting connection relations reveal an exponentially small reflected wave with a trigonometric Stokes multiplier. In fact, using the U-A approach the main result of [51] and [38], i.e. (1.10), can be computed very quickly. This is essentially the approach we employ in **§2.2** and hence highlights **the first objective of the thesis**: to introduce two mathematical connection methods which are simpler, more general and transparent than any advanced before [e.g. [61]–Zwaan 1929, [32]–Langer 1931, [38]–Meyer 1975 and [47]–Painter and Meyer 1982]. Simplification and clarification of connection theory, with which we determine the solutions of (1.9) across Stokes lines, is, in fact, the whole objective of the study in §2.2 and §2.4.

For the interested reader: an introduction to the U-A technique is given in [40] or the generalised method by Dingle in [18].

It is worth noting that the connection between the solutions to the Schrödinger equation and exponentially small reflection in a slowly varying wave equation (c.f. §1.5.1) is that the potential $V(x)$ be considered an analytic barrier. An analytic barrier requires that $V(x)$ is analytic on the real axis which is analogous to the condition that $c(x)$ be analytic along the real axis. Hence, the quantum mechanical literature which connects to the applied mathematics literature pertains to analytic barriers. This leads us to the topic of reflectionless potentials. For a particular class of (analytic barrier) potential profile in (1.9) there is no reflected wave. This matter is raised by Berry in [9] and subsequently elucidated by Berry and Howls in [6]. This forms the topic of interest in §2.7.1 of the thesis. However, the results of §2.7.1 further the results of [6].

As an addendum to §2.7.1 we briefly discuss a class of reflections missed by [38] but solved in [13], whereby the leading (dominant) contribution to the reflected wave is no longer coming from the turning point closest to the real axis. We use this result as a first attempt to prove the results of §2.7.1. This is achieved by noting that, when the dominant contribution is no longer coming from the turning point closest to the real axis for special values of the small parameter ϵ this 'dominant' contribution can be switched off, [13]. It is then possible to isolate the turning point closest to the real axis for such special values of ϵ. That is, for particular values of ϵ the only turning point contributing to a reflected wave will be coming from the turning point closest to the real axis. We use this approach to test the reflectionless wave speed profiles in §2.7.1 numerically.

Further reading on the methods with which to attain solutions of (1.9) can be found in [33], [34], and [37], and for a larger class of transition points in [4], [39]. **The closest results to those obtained in the thesis are:** Meyer–[13], Chapman & Mahony–[38], Berry–[4] and Berry & Howls–[6]. This is because: both [13] and [38] are concerned with the reflection of waves in a slowly varying medium and begin with a set up as outlined in §2.1 and §2.2, and [4] and [6] deal with the reflectionless profiles of §2.7.1.

1.6.2 Chapter 3

In this chapter we examine (1) for the case of a separable spatio-temporal wave speed $c(x,t) = c_1(x)c_2(t)$ and an initially quiescent medium that is disturbed in such a way as to generate a localised wave-packet. The result is a travelling wave which undergoes Stokes phenomena on crossing Stokes lines owing to the transition points of $c_1(x)$ and $c_2(t)$. The aim is then to find the form of the reflected wave solutions. This is achieved in **§3.2** where explicit estimates for the leading order transmitted and reflected waves are given. This is **the main result of the thesis**. The estimate, found initially by employing a resurgent analysis approach, is then repeated via an integral transform in §3.3 and lastly by extending the K-S method to compute reflection in §3.4. Each method successfully captures the behaviour of the reflected wave and it is therefore hoped that the methods outlined will prove useful in the analysis of a wider class of PDE. The analytical results are tested numerically via an Adams–Bashforth multistep method in §3.5. By inspecting the citations of the papers mentioned in Chapter 2, there is, or appears to be, no trace of an explicit solution to the problem of finding the exponentially small terms in (1).

There are other applications of E-A to PDE's, for instance: the aptly titled *'Exponential asymptotics and Stokes lines in a partial differential equation'* by Chapman & Mortimer, [16], is a good starting point when looking for an introduction to E-A techniques in a PDE. The goal of [16] is to investigate the exponentially small terms 'hidden' in the solutions of a PDE motivated by the geometrical model for crystal growth. The approach is to take a Fourier transform along the arclength of the solid-liquid interface and evaluate the resultant integral via steepest descents. Resurgence also plays a crucial role within their study. Another interesting paper, by Trinh *et al*, [58], is an E-A investigation into waveless ships, where it is expected that the free-surface waves produced by the ships hull are beyond-all-orders of the regular asymptotic expansions. The motion of the fluid is governed by Laplace's equation, with the kinematic condition on all boundaries, and Bernoulli's equation on the free surface where the asymptotic parameter is taken to be the Froude number ($= \epsilon$). The results confirm a conjecture by Vanden–Broeck & Tuck, 1977, that a single-cornered piecewise-linear hull will always generate a wake, and are attained by reducing the PDE to a related ODE problem before applying resurgent analysis. For an overview of divergent series and Borel re-summation in a Navier–Stokes equation see [17]. A paper concerning the non-linear Burgers equation [15] has the explicit aim of furthering our understanding of E-A techniques in the area of nonlinear partial differential equations. The authors, whose names read as a (current) 'who's who' list of british based E-A analysts, demonstrate how an E-A approach can be used to completely characterise the shock formation in a non-linear PDE. The factorial over power ansatz e.g.(1.4) plays an important role in this study. Of course, one may apply the Cole–Hopf transformation to convert the nonlinear Burgers equation into the linear heat equation and hence apply some of the techniques of Chapter 3, which may provide an alternative inspection to that of [15]. There are many more articles which develop E-A methods in a PDE environment that are worthy of

mention here. However, the list above was chosen as it reflects one of the major themes of this thesis: the application of resurgent analysis (i.e. the factorial over a power ansatz of (1.4)) to a PDE.

Note: a natural starting point, from which to inspect the solutions of (1), is to begin with the case where $c(x,t)$ is time-independent, $c(x,t) = c(x)$. This situation is outlined and solved in Appendix B where a spectral analysis approach is applied directly to (1), as opposed to assuming Fourier modes, e.g. §2.2. The approach is not in keeping with the methods of Chapter 2 and consequently the spectral analysis approach appears in Appendix B as opposed to main body of the thesis.

Chapter 2

Exponentially small reflection

2.1 Introduction to the problem

Throughout chapters 2 and 3 we study the solutions of a slowly varying wave equation whose spatio-temporal wave speed profile, $c(x,t)$, is separable:

$$\partial_t^2 h \;=\; \partial_x \left(c_1^2(x) c_2^2(t) \partial_x h \right), \tag{2.1}$$

with initial conditions

$$\begin{aligned} h(x,0) \;&=\; f(x-x_0)\mathrm{e}^{\mathrm{i}k_0 x/\epsilon}, \quad \epsilon \to 0, \\ \text{and} \quad \partial_t h(x,0) \;&=\; c_1(x)c_2(0)\partial_x h(x,0), \end{aligned} \tag{2.2}$$

where x_0 and k_0 are fixed and non zero, and $f(x-x_0)$ is some prescribed localised function around x_0, for example. Note that the second condition in (2.2) corresponds to a leftwards propagating initial wave. Additionally, we have opted to incorporate the small parameter in the initial condition. This is equivalent to the standard setup of taking $c_1(\epsilon x)c_2(\epsilon t)$, in (2.1), where ϵx and ϵt are the slow variables.

Following [38], the wave speed $c_1(x)c_2(t)$ is analytic in a neighbourhood of the real axis, in x and t, except for a countable set S_* of roots, isolated singular points or branch points collectively called "transition points" located away from the real axis. It is noted in the appendix of [38] that, "each transition point makes a separate additive contribution" to a Stokes phenomenon. Therefore, we focus on a spatial transition point at x_* (and its complex conjugate) and a temporal transition point at t_*(and its complex conjugate)[1]. $c_1(x)c_2(t)$ is strictly positive and tends to positive limits:

$$\begin{aligned} c_1(x) \in \mathbb{R} > 0 :\; x \in \mathbb{R} \quad \text{and} \quad c_1(x) \to c_{1\pm} > 0, \quad x \to \pm\infty, \\ c_2(t) \in \mathbb{R} > 0 :\; t \in \mathbb{R} \quad \text{and} \quad c_2(t) \to c_{2\pm} > 0, \quad t \to \pm\infty, \end{aligned} \tag{2.3}$$

where $c_{1\pm}$ and $c_{2\pm}$ are constants.

The set-up in (2.2) and (2.3) implies that: an incident 'initial' wave from $x \to \infty$ gives rise to a transmitted and exponentially small reflected wave on crossing a Stokes line. In this thesis, we aim to compute the amplitude of the exponentially small reflected wave using two methods: a Kruskal–Segur (K–S) method of matched asymptotics in the complex plane and resurgent analysis (R-A). A Stokes phenomenon occurs as a result of the turning points in (2.1) at

$$x = x_* \quad \text{and} \quad t = t_*. \tag{2.4}$$

Contributions from additional points are considered identically.

[1] It should be noted that: for temporal transition points the roots of $c_2(t)$ play an important role.

2.2 Time independent problem

Let $c_2(t) = 1$, then (2.1) reads

$$\partial_t^2 h = \partial_x (c_1^2(x) \partial_x h). \tag{2.5}$$

Introducing Fourier type solutions of the form

$$h(x,t) = y(x) e^{i\omega t/\epsilon} \tag{2.6}$$

and setting $\omega = 1$, leads to the ODE

$$\frac{d}{dx}(c_1^2(x)\frac{dy}{dx}) + \frac{y}{\epsilon^2} = 0. \tag{2.7}$$

Following [38], we assume the transition point nearest to the real axis is a branch point singularity, x_*, and let $\Re(x_*) = 0$ and

$$\Im(x_*) > 0. \tag{2.8}$$

The case when the transition point closest to the real axis is a root is discussed later.

The problem of finding a leading order approximation of the exponentially small reflected wave in (2.7) was solved by Pokrovskii and Khalatnikov in [51], Fröman and Fröman in [26], and Meyer in [38]. However, as noted in [13], this estimate, shown in (1.10), fails to provide a correct prediction for a wide class of speed profiles. In this section we recover the results of [51], [26] and [38], in the first instance, by employing a K–S approach which appears to be more efficient than any previous method. We then use resurgence to confirm this result and subsequently, for a particular set-up that appears to be missed by Meyer and later by Chapman & Mahony we extend the result.

2.2.1 K–S approach

In this section we apply a similar approach to [59], in the case of a more general wave speed profile.

We seek WKBJ solutions of (2.7) by placing the ansatz

$$y(x) \sim A(\epsilon) \mathrm{e}^{\mathrm{i}g_1(x)/\epsilon} \sum_{n=0}^{\infty} a_n(x)\epsilon^n + B(\epsilon)\mathrm{e}^{-\mathrm{i}g_1(x)/\epsilon} \sum_{s=0}^{\infty} b_n(x)\epsilon^n \tag{2.9}$$

into (2.7). The subscript 1 has been used to relate to the spatial wave speed $c_1(x)$ in (2.1). To leading order, the WKBJ solutions are:

$$y(x) \sim A(\epsilon) c_1^{-1/2}(x) e^{\mathrm{i}g_1(x)/\epsilon} + B(\epsilon) c_1^{-1/2}(x) e^{-\mathrm{i}g_1(x)/\epsilon}, \tag{2.10}$$

where

$$g_1(x) = \int_0^x \frac{dx'}{c_1(x')}. \tag{2.11}$$

It is noted that a change in the lower bound of $g_1(x)$ results in a change in the arbitrary functions of ϵ, $A(\epsilon)$ and $B(\epsilon)$, in (2.9). Hence, w.l.g. we set the lower bound to zero in (2.11). This matter is discussed shortly, c.f. the analysis following (2.17).

It is worth noting that the WKBJ solutions (2.9) determine the solutions of (2.7) up to arbitrary functions of ϵ. That is, the phase of the transmitted and reflected waves, $\pm g_1(x)$, as well as the coefficients $a_n(x)$ and $b_n(x)$ can be computed uniquely so that the only unknowns in (2.9) are the pre factor functions $A(\epsilon)$ and $B(\epsilon)$. In fact, the ability to compute the phase and the coefficients in the asymptotic expansions of the transmitted and reflected waves explicitly, via the WKBJ method, is possible in the ODE (2.7) environment only. More precisely, on applying the WKBJ method directly to the PDE (2.1) it is only possible to determine the phase and the coefficients of the transmitted wave uniquely, by application of the initial conditions (2.2). The phase, and therefore the coefficients in the asymptotic expansion, of the reflected wave contain an arbitrary function. For this reason we cannot take a K–S approach, using the

WKBJ solutions, directly when tackling (2.1), as additional information is required to determine the reflected wave up to an arbitrary function of ϵ. However, details that provide a platform for finding the solutions of (2.1) up to the desired level are discussed in this section.

Turning Points

The only possible candidates for turning points in (2.7) are the transition points noted in (2.4). The appearance of $c_1^{-1/2}$ in (2.10) highlights this and a detailed analysis of the recurrence relations which the coefficient functions in (2.9) satisfy confirms this.

2.2.2 Initial set-up and the exponentially small pre-factor of the reflected solution

With $x_0 > 0$ in (2.2), the initial (and dominant) solution is the object pre-factored by $A(\epsilon)$ in (2.9). We focus on finding an estimate for the amplitude of the reflected wave that exists as $x \to -\infty$. Therefore, $B(\epsilon) = 0$ as $x \to \infty$ in (2.10).Then, to the right of a Stokes line there is a single 'initial' solution

$$y_{_R}(x) \sim A_\infty c_1^{-1/2}(x) e^{\mathrm{i}g_1(x)/\epsilon}, \quad \Re(x) > 0, \tag{2.12}$$

where $A(\epsilon) = A_\infty$ has been chosen. Upon crossing a Stokes line, the dominant solution switches on a subdominant solution so that the solution of (2.7) is now

$$y_{_L} \sim A_{-\infty} c_1^{-1/2}(x) e^{\mathrm{i}g_1(x)/\epsilon} \left(1 + K(\epsilon)\mathrm{e}^{-\mathrm{i}\chi(x)/\epsilon} b_0(x)\right), \quad \Re(x) < 0, \tag{2.13}$$

where the object $\mathrm{e}^{\mathrm{i}\chi(x)}$ is subdominant and is therefore exponentially small. The form of $\chi(x)$ is determined by comparing (2.13) with the general solution of (2.7), given in (2.10), and a condition on $\chi(x)$ deduced shortly. Eq. (2.13) is the leading order form of the transmitted and reflected waves, where A_∞ and $A_{-\infty}$ are constant. (We expect and confirm later that $A_\infty = A_{-\infty}$.) The subscripts R and L here and henceforth denote solutions of (2.7) valid away from x_* to the right and left of the Stokes line, and $K(\epsilon)$ is known as the Stokes multiplier. Recall from §1.3 that $K(\epsilon)$ can be expanded in a power series of ϵ

$$K(\epsilon) = \sum_{n=0}^{\infty} K_n \epsilon^n, \tag{2.14}$$

where the K_n are constant. Figure 2.1 illustrates the setup in (2.12) and (2.13).

We now outline a procedure that determines both the solutions of (2.1) and (2.7) up to arbitrary (algebraic) functions of ϵ. That is, we go further than (2.10) by determining the exponentially small pre-factor of the subdominant solution, so that the leading order solutions of (2.7) are known up to some algebraic power of ϵ (i.e. the first non zero term in (2.14)). In the current ODE problem this approach may appear overly complicated, however, at the level of the PDE this method proves very useful.

The two terms in (2.9) provide a basis for the solutions of (2.7) in a region bounded away from any turning points (see [44] on the regions of validity of the Liouville Greens solutions). Thus, connecting the two equivalent forms in (2.10) and (2.13), we must have that

$$\begin{aligned} b_0(x) &= 1 \\ \text{and} \quad B(\epsilon)\exp\{-\mathrm{i}g_1(x)/\epsilon\} &= A_{-\infty}K(\epsilon)\exp\{\mathrm{i}(g_1(x) - \chi(x))/\epsilon\}. \end{aligned} \tag{2.15}$$

It is deduced that the function $\chi(x)$ in (2.13) must satisfy

$$\chi(x) \to 0 : \quad x \to x_*. \tag{2.16}$$

This is because: along the anti-Stokes lines the two objects in (2.13) are of the same order, whereas along the Stokes lines the initial (dominant) solution maximally dominates the term switched on. Anti-Stokes and Stokes lines emanate from the turning point at x_*, thus, as $x \to x_*$

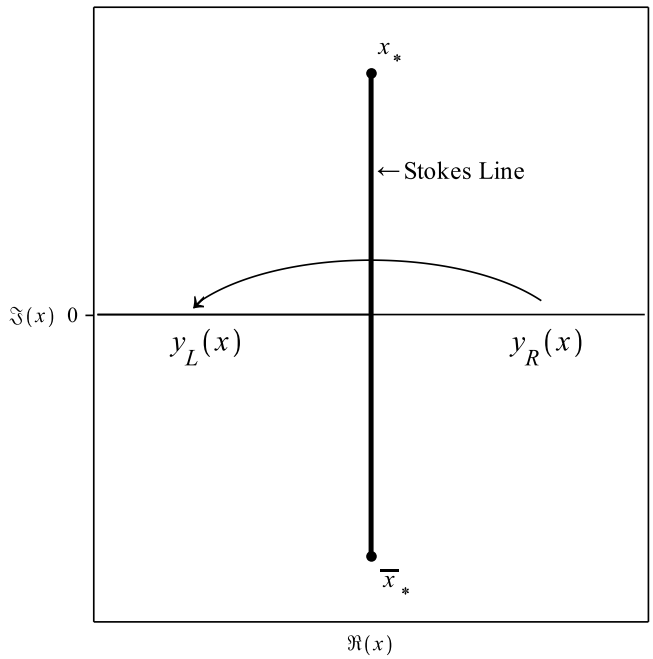

Figure 2.1: A schematic of the change in the solution of (2.7) as the initial wave, $y_{_R}(x)$, crosses the Stokes line that lies between the points at x_* and $\bar{x}_*$. The functions $y_{_R}(x)$ and $y_{_L}(x)$ are given in (2.12) and (2.13), respectively.

(2.16) is required (see [54] and the paragraph before the result (2.63) for more information on this). $\chi(x)$ in (2.13) is now determined using (2.15) and (2.16), where it is found that

$$\chi(x) \,=\, 2\big(g_1(x) - g_1(x_*)\big). \tag{2.17}$$

Eq (2.17) makes clear that a change in the lower bound of $g_1(x)$ in (2.11) from 0 to $\varphi \in \mathbb{R}/\{0\}$, will not alter any conclusion of this section. That is, let

$$g_1(x) = \int_{\varphi}^{x} 1/c(x')dx' \quad \Longrightarrow \quad \chi(x) = 2\left(\int_{\varphi}^{x} 1/c(x')dx' - \int_{\varphi}^{x_*} 1/c(x')dx'\right) = 2\left(\int_{0}^{x} 1/c(x')dx' - \int_{0}^{x_*} 1/c(x')dx'\right).$$

Hence, the exponentially small term in (2.10), and equivalently (2.13), is always $\mathrm{e}^{2\mathrm{i}\int_0^{x_*} 1/c_1(x')dx'}$. This is noted by recalling that

$$\mathrm{i}\int_{0}^{x_*} 1/c_1(x')dx' \in \mathbb{R} < 0 \quad \text{and} \quad \mathrm{i}\int_{\varphi}^{0} 1/c_1(x')dx' \in \mathrm{i}\mathbb{R}$$

hold by construct. Therefore, with (2.15) and (2.17), $B(\epsilon)$ in (2.10) is,

$$B(\epsilon) \,=\, A_{-\infty}K(\epsilon)\mathrm{e}^{2\mathrm{i}g_1(x_*)/\epsilon}. \tag{2.18}$$

Hence, using (2.14), the the leading order WKBJ solutions (2.10) are known up to some algebraic function of ϵ. Note, the solution switched on must be subdominant to the initial solution, hence,

$$\Re\left(\mathrm{i}g_1(x_*)\right) < 0. \tag{2.19}$$

Eq. (2.19) provides a condition with which to identify the active transition point, whose Stokes line crosses the real axis.

2.2.3 Complex conjugate transition points

To fix ideas we will consider two examples of speed profiles, namely:

$$\text{(i)}\ c_1(x) = \left(\frac{2+x^2}{1+x^2}\right)^{\alpha_1} \tag{2.20}$$

$$\text{and}\quad \text{(ii)}\ c_1(x) = (1+\operatorname{sech}(x))^{\alpha_1}\,. \tag{2.21}$$

These profiles were chosen for mathematical convenience as they include complex conjugate transition points[2] and satisfy the conditions set out in §2.1. Neither (2.20) or (2.21) are known to represent any particular physical situation.

In the case of complex conjugate transition points, the approach of prioritising the transition point closest to the real axis, to find the leading order behaviour of the reflected wave, requires modification. That is, from the results of [13], [38] and a similar approach in [41] one may have concluded that: when complex conjugate transition points are present (e.g. at $x_* = \mathrm{i}$ and $\bar{x}_* = -\mathrm{i}$ in (2.20)) there will be a double Stokes line crossing the real axis. For example, one Stokes line starting at x_* and terminating at $\bar{x}_*$ and the other oppositely directed. The result being two subdominant terms are switched on. However, the condition in (2.19) clearly restricts this idea. As an example, let $c_1(x)$ be given by (i) in (2.20), therefore $x_* = \mathrm{i}$, then,

$$\mathrm{i}g_1(\mathrm{i}) = -\int_0^1 \left(\frac{1-x^2}{2-x^2}\right)^{\alpha_1} dx < 0,$$

hence,

$$\mathrm{i}g_1(-\mathrm{i}) = -\mathrm{i}g_1(\mathrm{i}) > 0.$$

This is true in general and thus: in the case of complex conjugate transition points, one transition point is actively contributing to a Stokes phenomenon along the real axis in view of (2.19).

Local behaviour of the wave speed

To set the Stokes line that crosses the real axis to be the imaginary axis, between x_* and $\bar{x}_*$, we prescribe the leading order behaviour of $c_1(x)$ near x_* to be

$$c_1(x) \sim \gamma \mathrm{i}^{-\alpha_1}(x-x_*)^{-\alpha_1} : \quad x \to x_* \quad \text{and} \quad \alpha_1 \in (-1,0)\cup(0,\infty), \tag{2.22}$$

where $\gamma \in \mathbb{R} > 0$. The importance that $\alpha_1 > -1$ emerges from our study. This is the local behaviour when $c_1(x)$ has complex conjugate transition points.

2.2.4 Stokes lines

Along a Stokes line, the initial (dominant) solution must maximally dominate the reflected (subdominant) solution, thus the Stokes lines are lines along which

$$\begin{aligned} &\Im\{\mathrm{i}g_1(x)\} = 0, \\ \text{and}\quad &\Re\{\mathrm{i}\chi(x)\} > 0. \end{aligned} \tag{2.23}$$

With the particular choice of a symmetric wave speed setup, i.e. (i) or (ii) in (2.20),

$$g_1(\mathrm{i}x) \in \mathrm{i}\mathbb{R} : \quad x \in \mathbb{R}$$

and $[x_*, \bar{x}_*]$ is a Stokes line for x_*.

Note that, switching the direction of the initial wave amounts to switching the sign of the phase, (2.11), in (2.13). The result is a sign switch of $\chi(x)$ in (2.17), which rotates the Stokes

[2]Conjecture: it may be the case that any function that is real along the real line (thus whose coefficients in a Taylor series are real) and is singular somewhere in the complex plane, always contains complex conjugate transition points.

lines by π radians. The upshot is that: the relevant turning point, whose Stokes line crosses the real axis, is now $\bar{x}_*$. Figure(2.2) illustrates this point.

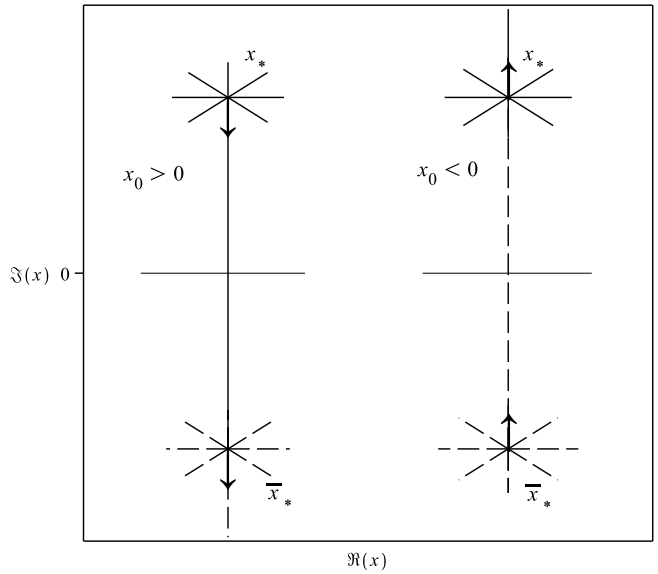

Figure 2.2: Plotted are schematics of the Stokes lines (solid and dashed) associated with turning points at x_* and $\bar{x}_*$, respectively. Stokes lines near the turing points have been exaggerated for illustrative purposes. The arrows denote the direction of the Stokes lines along the imaginary axis from each of the turning points. When $x_0 > 0$ the initial wave travels toward decreasing x and the Stokes line which crosses the real axis is coming from x_*. When $x_0 < 0$, the situation is reversed. The vertical arrows make clear the reversing of the Stokes lines due to a sign change of x_0.

2.2.5 Matched asymptotics

Solutions of (2.7) near the turning point x_*

We now focus on finding the solutions of (2.7) near the transition point at x_*. The aim is to match the local solutions of (2.7) with (2.12) and (2.13) across the Stokes line that lies below x_*, c.f. Fig2.2. Introducing

$$\eta = \mathrm{i}\epsilon^{-1/(\alpha_1+1)}(x - x_*), \quad \alpha_1 > -1, \tag{2.24}$$

(2.11) and (2.22) become:

$$\begin{aligned} c_1(x) &\sim \gamma\epsilon^{-\alpha_1/(\alpha_1+1)}\eta^{-\alpha_1}, \quad x \to x_* \\ \text{and} \quad g_1(x) &\sim g_1(x_*) - \frac{\mathrm{i}\epsilon\eta^{\alpha_1+1}}{\gamma(\alpha_1+1)}, \quad x \to x_*. \end{aligned} \tag{2.25}$$

Using (2.24) and (2.25), the (leading order) $\mathcal{O}(1)$ version of (2.7) local to x_* is

$$\frac{d}{d\eta}\left(\frac{1}{\eta^{2\alpha_1}}\frac{dy}{d\eta}\right) - \frac{1}{\gamma^2}y = 0. \tag{2.26}$$

This is a modified Bessel equation whose solution can be shown to be

$$y \sim \eta^{\alpha_1+\frac{1}{2}}\left(CH^{(1)}_{\nu_1}\left(\frac{\mathrm{i}\eta^{\alpha_1+1}}{\gamma(\alpha_1+1)}\right) + DH^{(2)}_{\nu_1}\left(\frac{\mathrm{i}\eta^{\alpha_1+1}}{\gamma(\alpha_1+1)}\right)\right), \tag{2.27}$$

where C and D are constants, and

$$\nu_1 = \frac{2\alpha_{_1}+1}{2\alpha_{_1}+2}. \tag{2.28}$$

$H^{(1)}_{\nu_1}$ and $H^{(2)}_{\nu_1}$ are Hankel functions of the first and second kind, with the following large-z asymptotic relations

$$H^{(1)}_{\nu}(z) \sim \sqrt{\frac{2}{\pi z}} e^{\mathrm{i}(z-\frac{\nu\pi}{2}-\frac{\pi}{4})} \quad \text{for} -\pi < \arg z < 2\pi \quad \text{and} \quad |z| \to \infty, \tag{2.29}$$

$$H^{(2)}_{\nu}(z) \sim \sqrt{\frac{2}{\pi z}} e^{-\mathrm{i}(z-\frac{\nu\pi}{2}-\frac{\pi}{4})} \quad \text{for} -2\pi < \arg z < \pi \quad \text{and} \quad |z| \to \infty, \tag{2.30}$$

from [23] and [24] respectively. We aim to match (2.12) and (2.13) to (2.27) along the anti-Stokes lines (closest to the Stokes line along the imaginary axis), where the two terms in (2.27) have comparable size. At $x = x_*$, these are lines tangent to:

$$\eta_{_R} \,=\, \tau \mathrm{e}^{\mathrm{i}\pi/(2(\alpha_{_1}+1))} \quad \text{and} \quad \eta_{_L} \,=\, \tau \mathrm{e}^{-\mathrm{i}\pi/(2(\alpha_{_1}+1))}. \tag{2.31}$$

Note that, the anti-Stokes lines near x_* lie above and below the real axis in the η-plane, from the transform (2.24).

Matching solutions along the anti-Stokes lines

Along (2.31), (2.12) and (2.13) are:

$$y_{_R}(x) \,\sim\, A_\infty \frac{\tau^{\alpha_{_1}/2}}{\sqrt{\gamma}} \epsilon^{\alpha_{_1}/2(\alpha_{_1}+1)} \mathrm{e}^{\mathrm{i}\pi(\nu_1-1/2)/2} \mathrm{e}^{\mathrm{i}g_1(x_*)/\epsilon} \exp\left\{\mathrm{i}\frac{\tau^{\alpha_{_1}+1}}{\gamma(\alpha_{_1}+1)}\right\}, \quad \eta \,=\, \eta_{_R}, \tag{2.32}$$

and

$$\begin{aligned} y_{_L}(x) \,\sim\, & A_{-\infty} \frac{\tau^{\alpha_{_1}/2}}{\sqrt{\gamma}} \epsilon^{\alpha_{_1}/2(\alpha_{_1}+1)} \mathrm{e}^{-\mathrm{i}\pi(\nu_1-1/2)/2} \mathrm{e}^{\mathrm{i}g_1(x_*)/\epsilon} \exp\left\{-\mathrm{i}\frac{\tau^{\alpha_{_1}+1}}{\gamma(\alpha_{_1}+1)}\right\} \\ & \times \left(1 + K(\epsilon) \exp\left\{2\mathrm{i}\frac{\tau^{\alpha_{_1}+1}}{\gamma(\alpha_{_1}+1)}\right\}\right), \quad \eta \,=\, \eta_{_L}, \end{aligned} \tag{2.33}$$

where (2.17) has been used. Importantly, along $\eta = \eta_{_R}$ the arguments of the Hankel functions in (2.27) have

$$\arg\left(\frac{i\eta_{_R}^{\alpha+1}}{\gamma(\alpha+1)}\right) = \pi.$$

This is within the range of (2.29) but lies outside of (2.30). To remedy the situation we use the connection relation

$$H^{(2)}_{\nu_1}\left(\frac{\tau^{\alpha_{_1}+1}}{\gamma(\alpha_{_1}+1)} e^{i\pi}\right) = 2\cos(\nu_1\pi) H^{(2)}_{\nu_1}\left(\frac{\tau^{\alpha_{_1}+1}}{\gamma(\alpha_{_1}+1)}\right) + e^{i\nu_1\pi} H^{(1)}_{\nu_1}\left(\frac{\tau^{\alpha_{_1}+1}}{\gamma(\alpha_{_1}+1)}\right), \tag{2.34}$$

deduced from [22]. Eq. (2.34) is an important relation, as it is with this connection formula that a Stokes phenomenon is deduced. That is, if $\cos(\nu_1\pi) = 0$, when $\nu_1 \in -(2\mathbb{N}+1)/2$ in (2.34), a Stokes phenomenon is not detected. This matter is resolved in §2.7.

Placing (2.34) into (2.27) along $\eta_{_R}$,

$$y_{_R} \sim \tau^{\frac{\alpha_{_1}}{2}} \sqrt{\frac{2\gamma(\alpha_{_1}+1)}{\pi}} \mathrm{e}^{\mathrm{i}\pi(\nu_1-1/4)} \left(D \exp\left\{\mathrm{i}\frac{\tau^{\alpha_{_1}+1}}{\gamma(\alpha_{_1}+1)}\right\} + E \exp\left\{-\mathrm{i}\frac{\tau^{\alpha_{_1}+1}}{\gamma(\alpha_{_1}+1)}\right\}\right), \tag{2.35}$$

where

$$E = C\mathrm{e}^{-\frac{\mathrm{i}\pi}{2}(2\nu_1+1)} + 2D\cos(\nu_1\pi)\mathrm{e}^{\frac{\mathrm{i}\pi}{2}}.$$

Equating (2.32) and (2.35), we find $E = 0$. Therefore,

$$C = 2D\cos(\nu_1\pi)e^{i\pi\nu_1}, \tag{2.36}$$

and

$$A_\infty = D\sqrt{\frac{2(\alpha_1+1)}{\pi}}\gamma\epsilon^{\frac{-\alpha_1}{2(\alpha_1+1)}}\mathrm{e}^{-\mathrm{i}g_1(x_*)/\epsilon}\mathrm{e}^{\mathrm{i}\nu_1\pi/2}. \tag{2.37}$$

Following the same process along η_L we have that,

$$\arg\left(\frac{i\eta_L^{\alpha+1}}{\gamma(\alpha+1)}\right) = 0.$$

Therefore, both (2.29) and (2.30) can be used directly. Hence,

$$y_L \sim D\tau^{\frac{\alpha_1}{2}}\sqrt{\frac{2\gamma(\alpha_1+1)}{\pi}}\mathrm{e}^{\mathrm{i}\frac{\pi}{4}}\exp\left\{-\mathrm{i}\frac{\tau^{\alpha_1+1}}{\gamma(\alpha_1+1)}\right\}\left(1-2\mathrm{i}\cos(\nu_1\pi)\exp\left\{2\mathrm{i}\frac{\tau^{\alpha_1+1}}{\gamma(\alpha_1+1)}\right\}\right). \tag{2.38}$$

Comparing with the WKBJ solution (2.33) gives

$$A_{-\infty} = D\sqrt{\frac{2(\alpha_1+1)}{\pi}}\gamma\epsilon^{-\alpha_1/(2(\alpha_1+1))}e^{-\mathrm{i}g_1(x_*)/\epsilon}\mathrm{e}^{\mathrm{i}\nu_1\pi/2} = A_\infty,$$

and the Stokes multiplier in (2.13) is found to be

$$K(\epsilon) \sim -2\mathrm{i}\cos(\nu_1\pi) \quad \nu_1 \neq \frac{2n+1}{2},\ n = 0, 1, 2\ldots \tag{2.39}$$

Placing (2.17) and (2.39) into (2.15) gives

$$B(\epsilon) \sim -2\mathrm{i}\cos(\nu_1\pi)\mathrm{e}^{2\mathrm{i}g_1(x_*)/\epsilon}A_{-\infty}, \quad x \to -\infty, \tag{2.40}$$

where ν_1 has the same restrictions as in (2.39). Eq. (2.40) is the main result of this section and represents the leading order estimate of the reflected wave amplitude in (2.7) (c.f. (1.10) the 'WKB reflection formula'). Eq. (2.40) recovers the estimate given in [38]. Note, the exponential term in (2.40) is exponentially small, see §(2.2.3). Let $A_\infty = 1$, then the solution of (2.7) to the left of a Stokes line, (2.13), and along the real axis is

$$y_L \sim c^{-1/2}(x)\left(\mathrm{e}^{\mathrm{i}g_1(x)/\epsilon} - 2\mathrm{i}\cos(\nu_1\pi)\mathrm{e}^{2\mathrm{i}g_1(x_*)/\epsilon}\mathrm{e}^{-\mathrm{i}g_1(x)/\epsilon}\right): \quad \nu_1 \neq -(2\mathbb{N}+1)/2.$$

Then, solutions of (2.5) (in terms of the Fourier modes) are

$$\begin{aligned} h_R(x,t) &\sim c_1^{-1/2}(x)\mathrm{e}^{\mathrm{i}(t+g_1(x))/\epsilon}, \quad x \to \infty, \\ \text{and} \quad h_L(x,t) &\sim c_1^{-1/2}(x)\left(\mathrm{e}^{\mathrm{i}(t+g_1(x))/\epsilon} + K(\epsilon)\mathrm{e}^{\mathrm{i}(t-g_1(x))/\epsilon}\right), \quad x \to -\infty. \end{aligned} \tag{2.41}$$

Switching the Initial Setup

If we have that $x_0 < 0$ in (2.2), then the initial (and dominant) solution of (2.7) is the object pre-factored by $B(\epsilon)$ in (2.9). Setting $A(\epsilon) \to 0$ as $x \to -\infty$ in (2.10)

$$y_L(x) \sim B_{-\infty}c^{-1/2}(x)\mathrm{e}^{-\mathrm{i}g_1(x)/\epsilon}, \quad x \to -\infty, \tag{2.42}$$

to the left of a Stokes line and

$$y_R \sim B_\infty c^{-1/2}(x)\mathrm{e}^{-\mathrm{i}g_1(x)/\epsilon}\left(1 + K(\epsilon)\mathrm{e}^{\mathrm{i}\chi(x)/\epsilon}\right), \quad x \to \infty, \tag{2.43}$$

to the right. The fact that $A(\epsilon) \neq 0$ as $x \to \infty$ in (2.10), results from a Stokes phenomenon associated with the turning point at $\bar{x}_*$. This setup up is the complex conjugate of the setup in (2.12) and (2.13). Hence, the Stokes multipliers are complex conjugates of one another.

Therefore,

$$K(\epsilon) \sim 2\mathrm{i}\cos(\nu_1\pi)$$

and the amplitude of the reflected wave is

$$A(\epsilon) \sim 2\mathrm{i}\cos(\nu_1\pi)\mathrm{e}^{-2\mathrm{i}g_1(\bar{x}_*)/\epsilon}, \quad x \to \infty. \tag{2.44}$$

2.3 Spatially independent wave speed problem

We now investigate the solutions to (2.1) when $c_1(x) = 1$. That is,

$$\frac{\partial_t^2 h}{c_2^2(t)} = \partial_x^2 h. \tag{2.45}$$

We again approach the problem by assuming Fourier type solutions

$$h(x,t) = y(t)\mathrm{e}^{\mathrm{i}kx/\epsilon}, \tag{2.46}$$

and immediately set $k = 1$. Hence, (2.45) is

$$\frac{d^2y}{dt^2} + c_2^2(t)y/\epsilon^2 = 0. \tag{2.47}$$

In this situation, we focus on the setup where the roots of $c_2(t)$ are the closest transition points, (2.4), to the real axis. Prescribing the local behaviour of $c_2(t)$ as

$$c_2(t) \sim \sigma\mathrm{i}^{\alpha_2}(t - t_*)^{\alpha_2} : \quad t \to t_*, \tag{2.48}$$

where $\sigma \in \mathbb{R} > 0$ and $\alpha_2 > -1$. The similitude of (2.47) with (2.7) permits one to immediately identify that: a leftward propagating initial wave gives rise to a reflected wave whose amplitude is

$$B(\epsilon) \sim -2\mathrm{i}\cos(\nu_2\pi)\mathrm{e}^{2\mathrm{i}g_2(t_*)/\epsilon}, \quad x \to -\infty,$$

and a rightward propagating initial wave gives rise to a reflected wave whose amplitude is

$$A(\epsilon) \sim 2\mathrm{i}\cos(\nu_2\pi)\mathrm{e}^{2\mathrm{i}g_2(\bar{t}_*)/\epsilon}, \quad x \to \infty.$$

The following have been used

$$g_2(t) = \int_0^t c_2(t')dt' \quad \text{and} \quad \nu_2 = \frac{2\alpha_2 + 1}{2(\alpha_2 + 1)}.$$

Therefore, the Stokes multipliers are

$$K(\epsilon) \sim (-)^j 2\mathrm{i}\cos(\nu_2\pi) : \quad \alpha_2 \neq \frac{2n+1}{2},\ n = 0, 1, 2\ldots, \tag{2.49}$$

with $j = 1$ or $j = 2$ pertaining to an initial wave travelling toward decreasing or increasing x.

2.3.1 Stokes multiplier relations

Let the subscript lj represent a spatial or temporal speed profile, where $l = 1$ refers to spatial and $l = 2$ temporal, and j represent the relevant complex conjugate turning point (one of) whose associated Stokes line crosses the real axis, i.e. $j = 1$ corresponds to x_* and $j = 2$ corresponds to $\bar{x}_*$. Then, the Stokes multipliers are:

$$\begin{aligned} K_{1j}(\epsilon) &\sim (-)^j 2\mathrm{i}\cos(\nu_1\pi) \\ \text{and} \quad K_{2j}(\epsilon) &\sim (-)^j 2\mathrm{i}\cos(\nu_2\pi), \end{aligned} \tag{2.50}$$

where

$$\nu_l \;=\; \frac{2\alpha_l+1}{2(\alpha_l+1)} \notin -(2\mathbb{N}+1)/2.$$

Eq. (2.50) proves useful when comparing the Stokes multipliers of chapters 2 and 3.

2.4 Exponential asymptotics via resurgence analysis: a time independent wave speed

We now return to the problem of finding the leading order approximation to the reflected wave due to a spatial transition point in (2.7) with a new approach. We begin with the slowly varying WKBJ anzatz in (2.9)

$$y(x) \;\sim\; c_1^{-1/2}(x)\left(A(\epsilon)\mathrm{e}^{\mathrm{i}g_1(x)/\epsilon}\sum_{n=0}^{\infty}a_n(x)\epsilon^n + B(\epsilon)\mathrm{e}^{-\mathrm{i}g_1(x)/\epsilon}\sum_{n=0}^{\infty}b_n(x)\epsilon^n\right), \tag{2.51}$$

where the phase $g_1(x)$ is given in (2.11).

Recurrence relations

The coefficient functions a_n and b_n in (2.51) satisfy recurrence relations. To find these we substitute

$$y(x) \;=\; c_1^{-1/2}(x)e^{\pm\mathrm{i}g_1(x)/\epsilon}Y_{\pm}(x;\epsilon), \tag{2.52}$$

into (2.7), which yields

$$\pm\frac{2\mathrm{i}}{\epsilon}\frac{dY_{\pm}}{dx} \;=\; Q_1(x)Y_{\pm} - \left(c_1Y_{\pm}'\right)', \tag{2.53}$$

where

$$Q_1(x) = \frac{(c_1')^2}{4c_1} + c_1''/2 \tag{2.54}$$

and the prime denotes differentiation w.r.t. x. Eq. (2.54) makes clear that

$$Q_1(x) \to \infty \quad \text{as} \quad x \to x_*. \tag{2.55}$$

Substituting $Y_+(x;\epsilon)$ with $\sum_n a_n\epsilon^n$ and $Y_-(x;\epsilon)$ with $\sum_n b_n\epsilon^n$ into (2.53), at $\mathcal{O}(\epsilon^{-1})$:

$$\begin{aligned} a_0'(x) \;&=\; 0 \implies \quad a_0(x) \;=\; 1, \\ \text{and} \quad b_0'(x) \;&=\; 0 \implies \quad b_0(x) \;=\; 1. \end{aligned} \tag{2.56}$$

In general,

$$2\mathrm{i}\frac{d}{dx}a_{n+1}(x) \;=\; Q_1(x)a_n(x) - \left(c_1a_n'(x)\right)', \tag{2.57}$$

and

$$2\mathrm{i}\frac{d}{dx}b_{n+1}(x) \;=\; -Q_1(x)b_n + \left(c_1b_n'(x)\right)'. \tag{2.58}$$

If an initial solution undergoes a Stokes Phenomenon, the solution of (2.7) on crossing the Stokes line will be of the general form (2.51) and the dominant and subdominant solutions satisfy (2.56), (2.57) and (2.58), respectively. It is clear from (2.55) that both (2.57) and (2.58) are singular at the spatial transition points in (2.4). Hence, x_* and $\bar{x}_*$ are indeed turning points of (2.7).

Since the setup is the same as (2.12) and (2.13) the transition point nearest to the real axis, whose Stokes line crosses the real axis, is the branch point singularity at $x = x_*$. Recall that the initial solution to the right of a Stokes line is

$$y_{_R}(x) \;\sim\; c_1^{-1/2}(x)\mathrm{e}^{\mathrm{i}g_1(x)/\epsilon}\sum_{n=0}^{\infty}a_n(x)\epsilon^n, \qquad \Re(x) > 0, \tag{2.59}$$

and to the left of a Stokes line,

$$y_{_L}(x) \sim c_1^{-1/2}(x)\mathrm{e}^{\mathrm{i}g_1(x)/\epsilon}\left(\sum_{n=0}^{\infty}a_n(x)\epsilon^n + K(\epsilon)\mathrm{e}^{-\chi(x)/\epsilon}\sum_{n=0}^{\infty}b_n(x)\epsilon^n\right), \qquad \Re(x) < 0. \quad (2.60)$$

The subscripts R and L are once again used to denote the solutions of (2.7) to the right and left of a Stokes line. Comparing (2.60) and (2.51) it follows that

$$K(\epsilon)\mathrm{e}^{\mathrm{i}g(x)-\chi_1(x)/\epsilon} = B(\epsilon)\mathrm{e}^{-\mathrm{i}g(x)/\epsilon}. \quad (2.61)$$

To determine $K(\epsilon)$ to leading order and $\chi(x)$ uniquely, we utilise a resurgence relation of the form

$$a_n(x) \sim -\frac{K(\epsilon)}{2\pi\mathrm{i}}\frac{b_0(x)\Gamma(n+\mu)}{(\chi(x))^{n+\mu}}, \quad n \to \infty. \quad (2.62)$$

Eq. (2.62) is a typical resurgence relation that relates the late terms of the initial solution to the early terms of a subdominant solution switched on as the initial solution crosses a Stokes line. The negative pre-factor of $K(\epsilon)$ is due to the orientation with which the turning point x_* is approached. This detail was highlighted in figure(2.2). That is, suppose we are interested in the point at x_* as a turning point of (2.7) then the Stokes line which crosses the real axis is the imaginary axis (between x_* and $\bar{x}_*$) travelling toward decreasing $\Im\{x\}$. Now, switching the point of interest to $\bar{x}_*$ results in a direction change of the Stokes line toward increasing $\Im\{x\}$. The relationship in (2.62) implies that $\mathrm{e}^{-\chi(x)/\epsilon} \to$ constant as $x \to x_*$ in (2.60). Hence,

$$\chi(x) \to 0 \quad \text{as} \quad x \to x_*, \quad (2.63)$$

in (2.60). Whence,

$$\chi(x) = 2\mathrm{i}\int_{x_*}^{x}\frac{dx'}{c_1(x')}, \quad (2.64)$$

using (2.61). With (2.56) and inspecting (2.57) and (2.62) near x_*, the leading order value of $K(\epsilon)$ is determined.

Late-term analysis

Using (2.22), (2.54) near x_* is

$$Q_1(x) \sim \gamma\mathrm{i}^{-\alpha_{_1}}\frac{\alpha_{_1}}{4}(3\alpha_{_1}+2)(x-x_*)^{-(\alpha_{_1}+2)}, \quad x \to x_*, \quad (2.65)$$

with $\alpha_{_1}$ as in (2.22). Re-arranging (2.57), becomes

$$a_{n+1}(x) = -\frac{\mathrm{i}}{2}\int^{x}\left(Q_1(x)a_n(x) - \frac{d}{dx}\left(c(x)a_n'(x)\right)\right)dx.$$

Recalling that $a_0(x) = 1$ from (2.56), then as $x \to x_*$,

$$a_1(x) \sim -\frac{\gamma}{8}\frac{3\alpha_{_1}^2+2\alpha_{_1}}{\alpha_{_1}+1}\mathrm{i}^{-\alpha_{_1}-1}(x-x_*)^{-(\alpha_{_1}+1)}. \quad (2.66)$$

Motivated by (2.65) and (2.66), we trial

$$a_n(x) \sim d_n(x-x_*)^{-(\alpha_{_1}+1)n}, \quad x \to x_*, \quad (2.67)$$

as the leading order behaviour of the a_n's near x_*. The d_n's are constant and $d_0 = 1$ from (2.56). Substituting (2.67) into (2.57) gives

$$a_{n+1}(x) \sim P\left(n - \frac{\alpha_{_1}}{2(\alpha_{_1}+1)}\right)\left(n + \frac{3\alpha_{_1}+2}{2(\alpha_{_1}+1)}\right)(x-x_*)^{-(n+1)(\alpha_{_1}+1)}\frac{d_n}{n+1}, \quad (2.68)$$

where,

$$P = \frac{\gamma}{2}(\alpha_{_1}+1)\mathrm{i}^{-\alpha_{_1}-1}. \tag{2.69}$$

Comparing (2.67) and (2.68),

$$\begin{aligned} d_n &= P(n-\nu_1-1/2)\,(n+\nu_1-1/2)\frac{d_{n-1}}{n} \\ &= \frac{P^n}{\Gamma(n+1)}\frac{\Gamma\left(n+\frac{1}{2}-\nu_1\right)\Gamma\left(n+\frac{1}{2}+\nu_1\right)}{\Gamma\left(\frac{1}{2}-\nu_1\right)\Gamma\left(\frac{1}{2}+\nu_1\right)}: \quad \nu_1 \neq -\frac{2n+1}{2},\ n=0,1,2\ldots \end{aligned} \tag{2.70}$$

where ν_1 was given in (2.28). The reflection formula, see [21], gives

$$\Gamma(1/2-\nu_1)\Gamma(1/2+\nu_1) = \frac{\pi}{\cos(\nu_1\pi)} \tag{2.71}$$

and using the identity

$$\frac{\Gamma(n+a)\Gamma(n+b)}{\Gamma(n+1)} \sim \sum_{k=0}^{\infty}(-1)^k\frac{(1-a)_k(1-b)_k}{k!}\Gamma(n+a+b-k-1), \quad n\to\infty, \tag{2.72}$$

in [45], we find

$$\frac{\Gamma(n-\nu_1+1/2)\Gamma(n+\nu_1+1/2)}{\Gamma(n+1)} \sim \Gamma(n), \quad n\to\infty.$$

Therefore, (2.70) is now

$$d_n \sim P^n\Gamma(n)\frac{\cos(\nu_1\pi)}{\pi}, \quad n\to\infty.$$

Thus,

$$a_n(x) \sim P^n\Gamma(n)\frac{\cos(\nu_1\pi)}{\pi}(x-x_*)^{-n(\alpha_{_1}+1)}, \quad n\to\infty. \tag{2.73}$$

Near to x_*, (2.64) is

$$\begin{aligned} \chi(x) &\sim 2\mathrm{i}^{\alpha_{_1}+1}\frac{(x-x_*)^{\alpha_{_1}+1}}{\gamma(\alpha_{_1}+1)} \\ &= P^{-1}(x-x_*)^{\alpha_{_1}+1}, \end{aligned}$$

having used (2.65) and (2.69). Hence, the rhs of (2.62) as $x\to x_*$ is

$$-\frac{K(\epsilon)}{2\pi\mathrm{i}}\frac{b_0(x)\Gamma(n+\mu)}{(\chi(x))^{n+\mu}} \sim -\frac{K(\epsilon)}{2\pi\mathrm{i}}P^{n+\mu}\Gamma(n+\mu)(x-x_*)^{-(\alpha_{_1}+1)(n+\mu)}\epsilon^{\mu}, \tag{2.74}$$

using (2.56). Comparing (2.73) and (2.74) in (2.62) gives $\mu=0$ and

$$K(\epsilon) \sim -2\mathrm{i}\cos(\nu_1\pi): \quad \nu_1 \neq -(2\mathbb{N}+1)/2. \tag{2.75}$$

By applying the same technique which leads to (2.75), it can be shown that

$$K(\epsilon) \sim (-)^j 2\mathrm{i}\cos(\nu_1\pi),$$

where the subscript j is used as in (2.50). Therefore, the exponentially small pre-factor of the subdominant solution is

$$\begin{aligned} B(\epsilon) &\sim -2\mathrm{i}\cos(\nu_1\pi)\mathrm{e}^{2g_1(x_*)/\epsilon}, \quad x\to-\infty, \\ \text{and} \quad B(\epsilon) &\sim 2\mathrm{i}\cos(\nu_1\pi)\mathrm{e}^{-2g_1(x_2)/\epsilon}, \quad x\to\infty. \end{aligned} \tag{2.76}$$

Then, (2.76) recovers the results in (2.40) and (2.44).

Temporal equation

It is prudent to state, for reference in chapter 3, particular details encountered when applying a resurgence approach to find the solutions of (2.47).

The WKBJ solutions of (2.47) are:

$$y \sim c_2^{-1/2}(t)\left(A(\epsilon)\mathrm{e}^{\mathrm{i}g_2(t)/\epsilon}\sum_{n=0}^{\infty}a_n(t)\epsilon^n + B(\epsilon)\mathrm{e}^{-\mathrm{i}g_2(t)/\epsilon}\sum_{n=0}^{\infty}b_n(t)\epsilon^n\right), \tag{2.77}$$

where,

$$a_0 = 1, \qquad b_0 = 1,$$

and

$$\begin{aligned} 2\mathrm{i}a'_{n+1}(t) &= Q_2(t)a_n(t) - \left(\frac{a'_n(t)}{c_2(t)}\right)', \\ 2\mathrm{i}b'_{n+1}(t) &= -Q_2(t)b_n(t) + \left(\frac{b'_n(t)}{c_2(t)}\right)', \end{aligned} \tag{2.78}$$

with

$$Q_2(t) = \frac{c_2''(t)}{2(c_2(t))^2} - \frac{3(c_2'(t))^2}{4(c_2(t))^3}. \tag{2.79}$$

the prime denotes differentiation w.r.t. t. Following the same technique that leads to (2.75), gives:

$$K(\epsilon) \sim (-)^j 2\mathrm{i}\cos(\nu_2\pi). \tag{2.80}$$

Eq. (2.80) returns the temporal result in (2.50).

2.5 Numerical Results

We compare the asymptotic result (2.40) with the amplitude of the reflected wave obtained by solving (2.7) numerically, using MATLAB's ODE45 solver. We consider the two examples of speed profiles given in (2.20) and (2.21),

$$\text{(i) } c_1(x) = \left(\frac{2+x^2}{1+x^2}\right)^{\alpha_1} \quad \text{and} \quad \text{(ii) } c_1(x) = (1+\operatorname{sech}(x))^{\alpha_1},$$

with $\alpha_1 > 0$. The case of $-1 < \alpha_1 < 0$ is discussed in §2.7. Hence, in (i) $x_* = \mathrm{i}$ and in (ii) $x_* = \frac{\pi}{2}$. Let $A(\epsilon) = 1$ in (2.9), then, the reflected wave amplitude is captured numerically by re-arranging (2.10), where to leading order it is found that

$$|B(\epsilon)| \sim \frac{\sqrt{c_1(x)}}{2}\left|y(x) + \epsilon\mathrm{i}c_1(x)y'(x)\right|, \quad x \to -\infty.$$

The numerical result is then compared with the analytical result in (2.40),

$$|B(\epsilon)| \sim 2|\cos(\nu_1\pi)|\mathrm{e}^{2\mathrm{i}g_1(x_*)/\epsilon}, \quad x \to -\infty.$$

The numerical and analytical data from the simulation was collected at $x = -100$.

It is clear the from the results presented in Figures (2.3)-(2.6) that the asymptotic estimate (2.40) has the correct gradient, i.e. the exponent $2\mathrm{i}g_1(x_*)/\epsilon$ appears correct in (2.40). Additionally, as ϵ decreases the asymptotic estimate converges toward the numerical for both speed profiles.

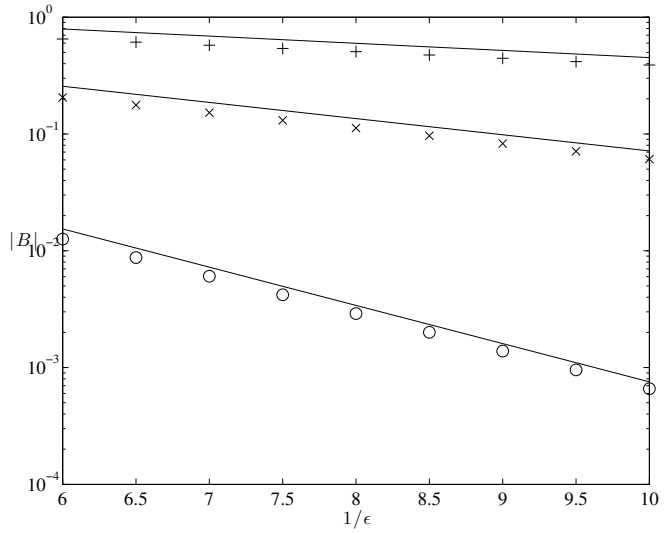

Figure 2.3: Numerical estimate of the amplitude of the reflected wave as a function of $1/\epsilon$ for c_1 given by (i); $\circ$ when $\alpha_1 = 1$, $\times$ when $\alpha_1 = 2$ and $+$ when $\alpha_1 = 3$. The straight lines show the asymptotic estimate (2.50).

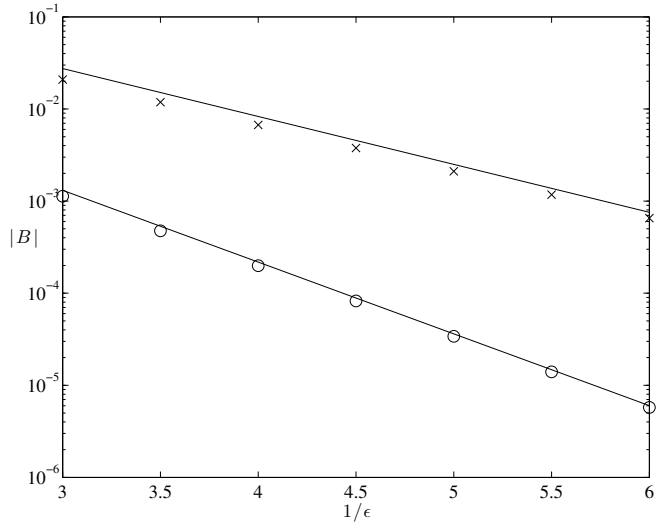

Figure 2.4: Numerical estimate of the amplitude of the reflected wave as a function of $1/\epsilon$ for c_1 given by (i); $\circ$ when $\alpha_1 = 1/10$ and $\times$ when $\alpha_1 = 1/2$. The straight lines show the asymptotic estimate (2.50).

2.5.1 Convergence to the estimate in (2.40)

There appears to be a noticeable difference in the accuracy of the estimate in (2.40) with regards to the two speed profiles at $x = -100$, most notably from Figure 2.3 and Figure 2.5. This is due to the rate at which the chosen wave speed approaches its limiting value. Figure 2.7 illustrates that the speed profile in (2.21) approaches its limiting value much more rapidly than (2.20). In fact, taking $-x$ as the large parameter, it follows that

$$\frac{2+x^2}{1+x^2} = 1 + x^{-2} + \text{l.o.t}, \quad x \to -\infty$$

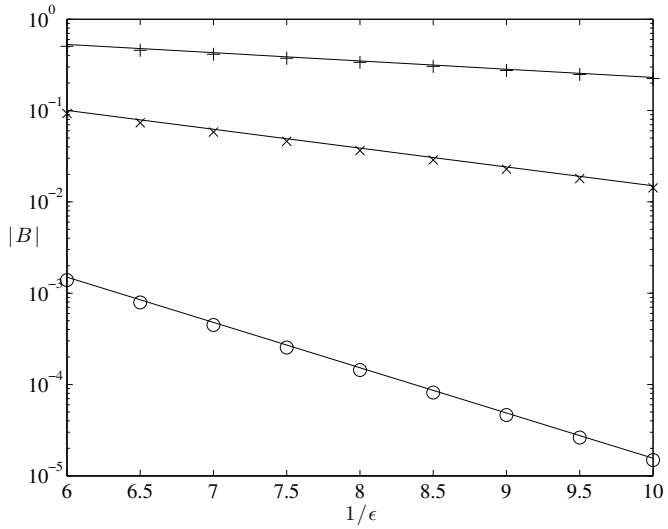

Figure 2.5: Numerical estimate of the amplitude of the reflected wave as a function of $1/\epsilon$ for c_1 given by (ii); $\circ$ when $\alpha_1 = 1$, $\times$ when $\alpha_1 = 2$ and $+$ when $\alpha_1 = 3$. The straight lines show the asymptotic estimate (2.50).

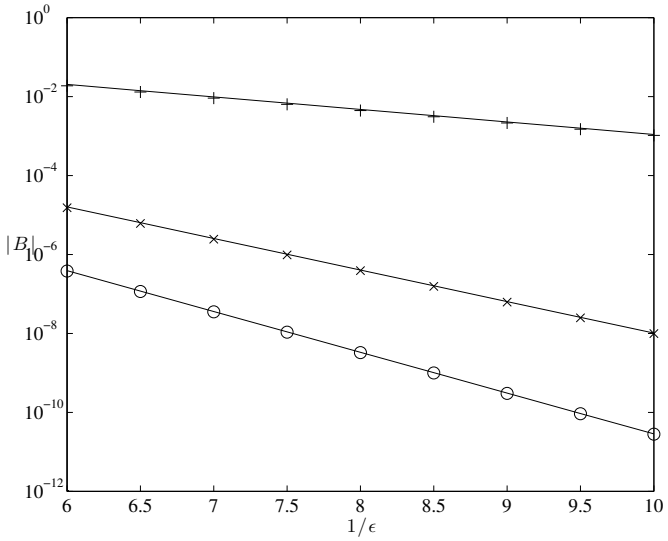

Figure 2.6: Numerical estimate of the amplitude of the reflected wave as a function of $1/\epsilon$ for c_1 given by (ii); $\circ$ when $\alpha_1 = 1/4$, $\times$ when $\alpha_1 = 1/2$ and $+$ when $\alpha_1 = 3/2$. The straight lines show the asymptotic estimate (2.50).

$$1 + \operatorname{sech}(x) = 1 + 2\mathrm{e}^x + \text{l.o.t}, \quad x \to -\infty,$$

therefore, profile (ii) converges exponentially towards the limiting value of 1.

2.6 Mistakes in the literature

Here we focus on the results of [28] and [29], whose results differ from that of (2.50) due to assumptions made about the behaviour of the solutions of (2.7) deduced away from turning points and (importantly) maintained near the turning points of (2.7). In doing so, [28] and [29], highlight some of the subtleties involved in turning point analysis.

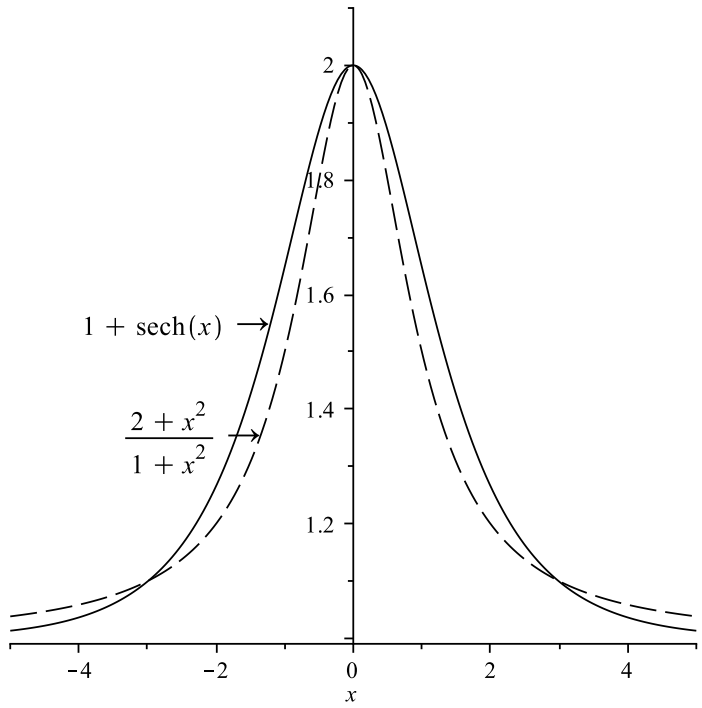

Figure 2.7: A plot of the behaviour of $c_1(x)$ as (i) dashed line and (ii) solid line. Note the obvious difference in the rate at which the function tends to the limiting value of 1.

2.6.1 Grimshaw

We sketch the approach of [28]; correcting the erroneous pre-factor which seems to miss an $\hat{\alpha}$ (order of singularity) dependence. The method of [28] is to introduce

$$X = g_1(x) = \int_0^x \frac{dx'}{c_1(x')} \quad \text{and} \quad y(x) = c_1^{-1/2}(x)v(X) \tag{2.81}$$

into (2.7). Therefore, (2.7) reduces to,

$$v'' + (\epsilon^{-2} - Q)v = 0. \tag{2.82}$$

The prime denotes differentiation w.r.t. X and

$$Q(X) = \frac{c''(X)}{2c(X)} - \left(\frac{c'(X)}{2c(X)}\right)^2, \tag{2.83}$$

with $c(X) = c_1(x)$ in (2.7). Henceforth, the turning points X_j associated with the branch point singularities and roots of $c(X)$, are considered. Assuming that $Q(X)$ is smooth, WKBJ solutions are assumed and are found to be

$$v_\pm(X) = \exp\left\{\pm \mathrm{i}\left[X/\epsilon - \epsilon\hat{Q}(X)/2\right]\right\}\left(1 + \mathcal{O}(\epsilon^2)\right), \quad \text{where} \quad \hat{Q}(X) = \int_{-\infty}^{X} Q(X')dX'.$$

The $\pm$ corresponds to a wave to the right and a wave to the left, respectively. Starting with the setup as in (2.12) and (2.13), which, using the notation of [28], is

$$\begin{aligned} v(X) &\sim T\mathrm{e}^{\mathrm{i}X/\epsilon}, \quad X \to \infty, \\ v(X) &\sim \mathrm{e}^{\mathrm{i}X/\epsilon} + R\mathrm{e}^{-\mathrm{i}X/\epsilon}, \quad X \to -\infty, \end{aligned} \tag{2.84}$$

where T and R are the so called transmission and reflection coefficients and the formulation implies the presence of a Stokes phenomenon. [28] then introduces an integral equation for $v(\hat{X})$ deduced from (2.82), namely

$$v(X) \;=\; A\mathrm{e}^{\mathrm{i}X/\epsilon} + B\mathrm{e}^{-\mathrm{i}X/\epsilon} + \frac{\epsilon}{2\mathrm{i}}\int_{-\infty}^{\infty} \mathrm{e}^{\mathrm{i}|X-X'|/\epsilon} Q(X')v(X')dX'. \tag{2.85}$$

Applying the boundary conditions, (2.84), it is deduced that $B = 0$ in (2.85) and

$$R \;=\; -\frac{\epsilon}{2\mathrm{i}}\int_{-\infty}^{\infty} \mathrm{e}^{\mathrm{i}X'/\epsilon} Q(X')v(X')dX'. \tag{2.86}$$

It is now assumed that: $v(X)$ can be replaced by its WKBJ approximation in (2.84), i.e. $v \sim \mathrm{e}^{\mathrm{i}X/\epsilon}$ as $x \to -\infty$, and (given that $Q(X)$ is assumed smooth) the integral is then dominated by the singularities of Q (i.e. X_j). However, it is not permissible to make such a substitution for $v(X)$ as the singular points of Q are the turning points of (2.82) and thus the approximations in (2.84) are singular at X_j, a matter that gives rise to a Stokes Phenomenon in (2.85) in the first instance.

Ignoring this, [28] implies the local behaviour of the wave speed profile to be

$$c(X) \;\sim\; \hat{\gamma}(X - X_j)^{-\hat{\alpha}}, \quad \hat{\alpha} \neq 0, \tag{2.87}$$

where $\hat{\gamma}$ is constant.

Note, when inspecting the solutions of (2.82) independent of (2.7), $\hat{\alpha}$ does not have the same range restrictions as $\alpha_{_1}$ in (2.22). This detail proves very useful when confirming an asymptotic estimate of the Stokes multiplier numerically for special values of $\hat{\alpha}$ when $K(\epsilon) \leq \mathcal{O}(\epsilon)$, see §2.7.1 for more details. Such a situation arose when investigating the solutions of (2.7), where the estimate in (2.39) was not valid for $\alpha_{_1} \in -1 + \frac{1}{2\mathbb{N}+1}$.

Eq(2.83) near the turning point is:

$$Q(X) \;\sim\; \hat{\alpha}(\hat{\alpha}+2)(X - X_j)^{-2}/4. \tag{2.88}$$

The contour in (2.85) is then deformed such as to take into account the turning points at X_j. Hence,

$$R \;\sim\; \mathrm{i}\epsilon\frac{\hat{\alpha}}{8}(\hat{\alpha}+2)\mathrm{e}^{2\mathrm{i}X_j/\epsilon}\sum_j \oint \frac{\mathrm{e}^{2\mathrm{i}(X'-X_j)}}{(X'-X_j)^2}dX'. \tag{2.89}$$

Therefore,

$$R_{\mathrm{G}} \;\sim\; -\mathrm{i}\frac{\pi}{2}\hat{\alpha}(\hat{\alpha}+2)\sum_{j=1}^{\infty}\mathrm{e}^{2\mathrm{i}X_j/\epsilon}, \tag{2.90}$$

where the index j indicates the number of turning points that contribute a Stokes phenomenon along the real axis. Eq. (2.90) does not explicitly appear in [28] and highlights a typo in the paper for the specific example given by Grimshaw. The subscript G has been used to denote the solution in [28]. Grimshaw's result does not coincide with Meyer's and ours[3]. To see this, we apply R-A to (2.82) to obtain an estimate of the reflected wave. We focus on a single contribution coming from the turning point at X_* and let

$$v(X) \;\sim\; \mathrm{e}^{\mathrm{i}X/\epsilon}\sum_{n=0}^{\infty} a_n(X)\epsilon^n. \tag{2.91}$$

Then, on placing the ansatz above into (2.82), we find

$$2\mathrm{i}a'_{n+1}(X) \;=\; Qa_n - a''_n : \quad a_0(X) \;=\; 1. \tag{2.92}$$

[3]On first inspection it is clear the result in [28] is not acceptable as it is unbounded in $\hat{\alpha}$ (when considering (2.82) independent of (2.7))

Anticipating turning point behaviour, as in (2.67), we let

$$a_n \sim d_n(X - X_*)^{-n},$$

as $X \to X_*$ and follow the same recipe that led to the result in (2.76), which leads to:

$$R \sim -2\mathrm{i}\sin(\hat{\alpha}\pi/2)\mathrm{e}^{2\mathrm{i}X_*/\epsilon}, \quad \hat{\alpha} \notin 2\mathbb{Z}. \tag{2.93}$$

The result above, (2.93), recovers the result of Berry in [4] and hence confirms that the estimate given by [28] is indeed erroneous. The solution when $\hat{\alpha} \in 2\mathbb{Z}$ is a special case, analogous to $\nu_1 \in -(2\mathbb{N}+1)/2$ in (2.40), see the method preceding the result (2.116) for more on this.

Grimshaw's estimate w.r.t (2.7)

We now phrase the estimate of [28] in terms of the original ODE (2.7). Using (2.22) and (2.81):

$$X - X_* \sim \frac{\mathrm{i}^{\alpha_1}}{\gamma(\alpha_1+1)}(x - x_*)^{\alpha_1+1}, \quad x \to x_*.$$

Therefore,

$$\gamma\mathrm{i}^{-\alpha_1}(x - x_*)^{-\alpha_1} \sim \gamma^{\frac{1}{\alpha_1+1}}(\alpha_1+1)^{\frac{-\alpha_1}{\alpha_1+1}}\mathrm{i}^{\frac{-\alpha_1}{\alpha_1+1}}(X - X_*)^{-\alpha_1/(\alpha_1+1)}.$$

With $c(X) = c_1(x)$, comparing the above and (2.87),

$$\hat{\alpha} = \frac{\alpha_1}{\alpha_1+1} \in (-\infty, 0) \cup (0, 1). \tag{2.94}$$

Let $\hat{\alpha} > 0$ (so that the transition point nearest the real axis is a branch point singularity in (2.82) and (2.7)), then the estimate in [28] yields the following estimate for the amplitude of the reflected wave in (2.7):

$$B_{\mathrm{G}}(\epsilon) \sim -\mathrm{i}\pi\frac{\left(3\alpha_1^2 + 2\alpha_1\right)}{2(\alpha_1+1)^2}\mathrm{e}^{2\mathrm{i}g_1(x_*)/\epsilon}, \quad x \to -\infty. \tag{2.95}$$

It is noted that, as $\alpha_1 \to 0$ the estimates of [28] and (2.39) are:

$$\begin{aligned} B_{\mathrm{G}}(\epsilon) &\sim -\mathrm{i}\pi\alpha_1(1 + \mathcal{O}(\alpha_1)\mathrm{e}^{2\mathrm{i}g_1(x_*)/\epsilon}, \quad \alpha_1 \to 0, \\ \text{and} \quad B(\epsilon) &\sim -\mathrm{i}\pi\alpha_1(1 + \mathcal{O}(\alpha_1))\mathrm{e}^{2\mathrm{i}g_1(x_*)/\epsilon}, \quad \alpha_1 \to 0. \end{aligned}$$

Thus, the estimate in [28] appears correct as $\alpha_1 \to 0$ only. This is much to be expected, as the approximation that $v(X) = \mathrm{e}^{\mathrm{i}X/\epsilon}$ is exact when $\hat{\alpha} = 0$. In Figure 2.8 we plot the two estimates (2.39) and (2.95) for several values of α_1, using the techniques of §2.5, highlighting the fact that $B_{\mathrm{G}}(\epsilon)$ appears correct only as $\alpha_1 \to 0$.

2.6.2 Hinch

Our result (2.50) also differs from that in [29] on p137. In this section we follow Hinch's approach but in a significantly more broad setting. That is: we highlight the error by generalising the setup of [29], i.e. [29] deals with the case where $\alpha_1 = 1$ in (2.22) whereas we detail a procedure that deals with $\alpha_1 > 0$, and solve the subsequent problem using a technique that does not appear explicitly in [29]. In this respect the results contained within this section are new. In generalising the approach, we correct a factor ϵ which appears erroneous in [29] and give an analytic expression for the amplitude of the reflected wave. In taking this approach we discover that, although the method employed by Hinch is erroneous, the 'results of Hinch'[4] are remarkably similar to the correct result given in §2.2 for a larger class of wave speed profiles.

[4]Note that these results do not appear in Hinch so what we mean by 'the results of Hinch' is: the results of the apparent method of Hinch as detailed in §2.6.2 not the result that appears in [29].

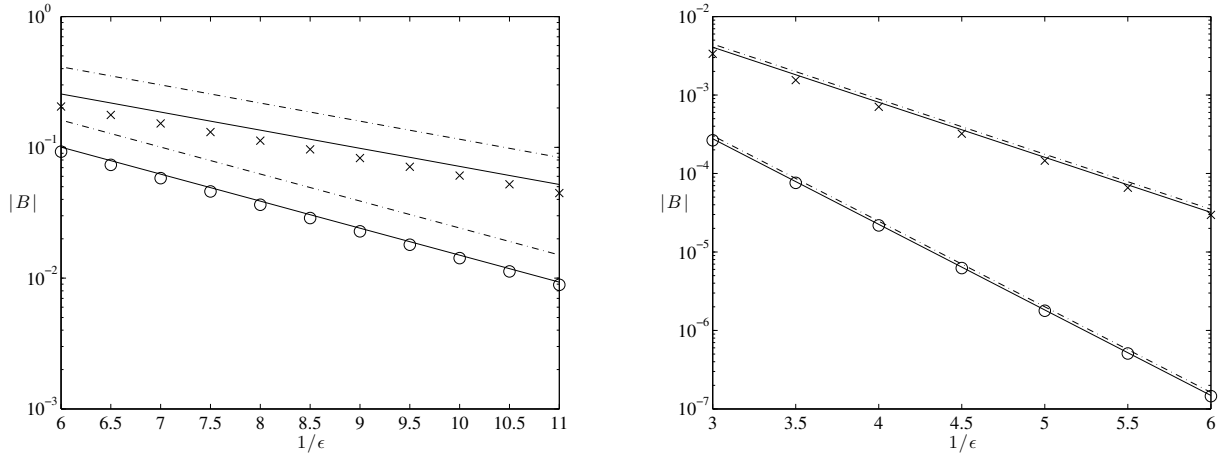

Figure 2.8: Numerical estimate of the amplitude of the reflected wave as a function of $1/\epsilon$ for $\alpha_1 = 2$ (Left) and $\alpha_1 = 1/5$ (Right), with $c_1(x) = \left(\frac{2+x^2}{1+x^2}\right)^2$ crosses and $c_1(x) = (1+\mathrm{sech}(x))^2$ circles. The straight lines show the asymptotic estimate (2.39) and the dash dot (2.87). Figures (a) and (b) highlight the fact that the estimate in [28] appears valid only as $\alpha_1 \to 0$

The approach relies on rewriting (2.7) in terms of two amplitudes $A(x)$ and $B(x)$, with

$$y(x) \;=\; a(x)c_1^{-1/2}(x)\mathrm{e}^{\mathrm{i}g_1(x)/\epsilon} + b(x)c_1^{-1/2}(x)\mathrm{e}^{-\mathrm{i}g_1(x)/\epsilon}.$$

Employing a variation of parameters, it is found that:

$$\begin{aligned} a' \;&=\; -\mathrm{i}\epsilon Q_1(x)\left(a + b\mathrm{e}^{-2\mathrm{i}g_1(x)/\epsilon}\right)/2, \\ \text{and}\quad b' \;&=\; \mathrm{i}\epsilon Q_1(x)\left(b + a\mathrm{e}^{2\mathrm{i}g_1(x)/\epsilon}\right)/2, \end{aligned} \tag{2.96}$$

with

$$Q_1(x) \;=\; \frac{c_1''(x)}{2} + \frac{(c_1'(x))^2}{4c_1(x)},$$

as in (2.54). Introducing,

$$a \;=\; A(x)\mathrm{e}^{-\mathrm{i}\epsilon\phi(x)} \quad \text{and} \quad b \;=\; B(x)\mathrm{e}^{\mathrm{i}\epsilon\phi(x)}, \quad \text{where} \quad \phi(x) \;=\; \int_0^x Q_1(x')dx'/2, \tag{2.97}$$

gives

$$A'(x) \;=\; -\frac{\mathrm{i}\epsilon}{2}Q_1(x)B(x)\mathrm{e}^{-2\mathrm{i}(g_1(x)/\epsilon - \epsilon\phi(x))} \quad \text{and} \quad B'(x) \;=\; \frac{\mathrm{i}\epsilon}{2}Q_1(x)A(x)\mathrm{e}^{2\mathrm{i}(g_1(x)/\epsilon - \epsilon\phi(x))}.$$

It follows that,

$$A''(x) - \left[\frac{Q_1'(x)}{Q_1(x)} + \mathrm{i}\epsilon Q_1(x) - \frac{2\mathrm{i}}{\epsilon c_1(x)}\right]A'(x) - \epsilon^2 Q_1^2(x)A(x)/4 \;=\; 0. \tag{2.98}$$

So far, no approximations have been made. The approach of [29] is then to integrate the equation for $B(x)$, assuming that $A(x)$ is nearly constant[29]. It is clear, however, from (2.98), that away from x_* taking $A(x)$ to be constant is acceptable, an assumption that certainly breaks down in the region of x_*, a branch point singularity or root of $Q_1(x)$. Ignoring this problem

leads to the result

$$B(-\infty) \;=\; -\mathrm{i}\epsilon A(\pm\infty)\int_{-\infty}^{\infty} Q_1(x')\exp\{2\mathrm{i}(g_1(x')/\epsilon - \epsilon\phi(x'))\}dx'/2. \tag{2.99}$$

The integral is then approximated using Laplace's method about x_*. With $c_1(x)$ as in (2.22),

$$g_1(x) \;\sim\; g_1(x_*) + \mathrm{i}^{\alpha_1}\frac{(x-x_*)^{\alpha_1+1}}{\gamma(\alpha_1+1)}, \quad x\to x_*,$$

and (2.65):

$$Q_1(x)/2 \;\sim\; \gamma\mathrm{i}^{-\alpha_1}\frac{\alpha_1}{8}(3\alpha_1+2)(x-x_*)^{-(\alpha_1+2)}, \quad x\to x_*.$$

The integral in (2.99) is deformed to that shown in Figure 2.9 where the contributions coming from the dashed curve (when the phase of the exponential term is $\mathcal{O}(\epsilon^{-1})$) are neglect. Then, the leading order contributions are coming from the contour $\mathcal{C}$, in Figure 2.9, where $x:\; x_*+\delta\mathrm{e}^{\mathrm{i}\theta_1} \to x_*+\delta\mathrm{e}^{\mathrm{i}\theta_2}$, with $\epsilon^{\frac{1}{\alpha_1+1}} < \delta < 1$ and θ_1 and θ_2 are chosen so as to keep the integrand exponentially small at the end points. Letting $\alpha_1 > 0$, it follows that

$$B(-\infty) \sim \mathrm{i}\Lambda\int_{\delta\mathrm{e}^{\mathrm{i}\left(\frac{\pi}{2}+\theta_1\right)}}^{\delta\mathrm{e}^{\mathrm{i}\left(\frac{\pi}{2}+\theta_2\right)}} \frac{\mathrm{e}^{\frac{2}{\epsilon}\frac{\rho^{\alpha_1+1}}{\gamma(\alpha_1+1)} - \frac{\epsilon\alpha_1\gamma}{4}\frac{(3\alpha_1+2)\rho^{-(\alpha_1+1)}}{\alpha_1+1}}}{\rho^{\alpha_1+2}}d\rho, \tag{2.100}$$

$$\text{where} \quad \rho = \mathrm{i}(x-x_*) \quad \text{and} \quad \Lambda = \mathrm{i}\epsilon\frac{\gamma}{8}\alpha_1(3\alpha_1+2)\mathrm{e}^{2\mathrm{i}g_1(x_*)/\epsilon}. \tag{2.101}$$

Now, by setting

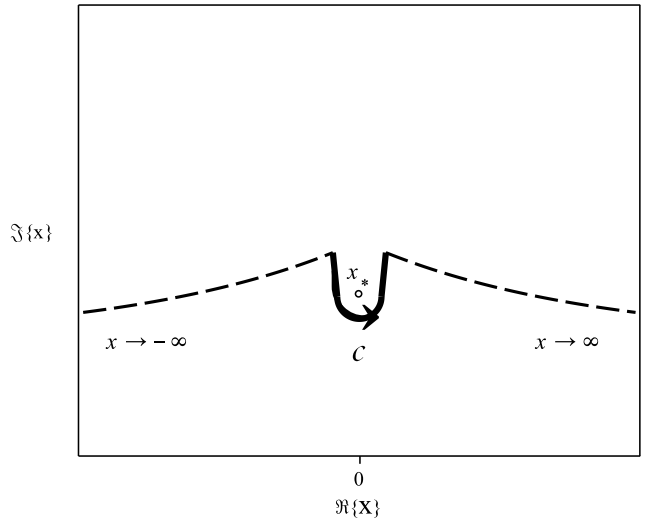

Figure 2.9: Deformed contour of integration in (2.99), the contour $\mathcal{C}$ is given by the solid line.

$$\rho = \mathrm{e}^{\frac{\mathrm{i}\pi}{\alpha_1+1}}Y, \quad \theta_1 \;=\; -\pi\left(\frac{1}{\alpha_1+1}+\frac{1}{2}\right) \text{and} \quad \theta_2 \;=\; \pi\left(\frac{1}{\alpha_1+1}-\frac{1}{2}\right),$$

we extend the path of integration, incurring exponentially small error only, so that

$$B(-\infty) \sim -\mathrm{i}\Lambda\mathrm{e}^{-\mathrm{i}\pi}\int_{\infty\mathrm{e}^{\frac{-2\mathrm{i}\pi}{\alpha_1+1}}}^{\infty} \frac{\mathrm{e}^{-\frac{2}{\epsilon}\frac{Y^{\alpha_1+1}}{\gamma(\alpha_1+1)}+\epsilon\gamma\frac{\alpha_1}{4}\frac{(3\alpha_1+2)}{\alpha_1+1}Y^{-(\alpha_1+1)}}}{Y^{\alpha_1+2}}dY.$$

Hence, let

$$\hat{P} = -\frac{2}{\epsilon}\frac{Y^{\alpha_1+1}}{\gamma(\alpha_1+1)},$$

then

$$B(-\infty) \sim -\mathrm{i}A(\pm\infty)\frac{\alpha_1}{8}\frac{(3\alpha_1+2)}{(\alpha_1+1)^2}\mathrm{e}^{2\mathrm{i}g_1(x_1)/\epsilon}\int_{-\infty}^{(0_+)} 2\mathrm{i}\exp\left\{\hat{P} - \frac{\alpha_1}{2}\frac{(3\alpha_1+2)}{(\alpha_1+1)^2}\hat{P}^{-1}\right\}\frac{d\hat{P}}{\hat{P}^2}. \tag{2.102}$$

Eq(2.102) is a Schläfli integral, see [25], whose solution is

$$J_1(z) = \frac{z}{4\pi\mathrm{i}}\oint \mathrm{e}^{p-z^2/(4p)}\frac{dp}{p^2},$$

where $J_1(z)$ is a Bessel function of the first kind. Let $z = \frac{\sqrt{2\alpha_1(3\alpha_1+2)}}{\alpha_1+1}$, then (2.102) reads

$$B_{\mathrm{H}}(-\infty) \sim \mathrm{i}\pi\frac{\sqrt{\alpha_1(3\alpha_1+2)}}{\sqrt{2}(\alpha_1+1)}J_1\left(\frac{\sqrt{2\alpha_1(3\alpha_1+2)}}{\alpha_1+1}\right)\mathrm{e}^{2\mathrm{i}g_1(x_*)/\epsilon}a(\pm\infty), \tag{2.103}$$

where the subscript H is used to denote Hinch's approximation. It is assumed that (2.103) holds for $\alpha_1 \in (-1, 0)$ as well. We compare (2.40) and (2.103), by first setting

$$\begin{aligned} B_{\mathrm{H}}(-\infty) &\sim K_{\mathrm{H}}\mathrm{e}^{2\mathrm{i}g_1(x_*)/\epsilon}, \\ \text{where} \quad K_{\mathrm{H}}(\epsilon) &\sim \mathrm{i}\pi\frac{\sqrt{\alpha_1(3\alpha_1+2)}}{\sqrt{2}(\alpha_1+1)}J_1\left(\frac{\sqrt{2\alpha_1(3\alpha_1+2)}}{\alpha_1+1}\right). \end{aligned} \tag{2.104}$$

Hinch quotes a result for $\alpha_1 = 1$

$$K_{\mathrm{H}}(-\infty) \sim \mathrm{i}\pi\frac{\sqrt{5}}{2\sqrt{2}}J_1\left(\frac{\sqrt{5}}{\sqrt{2}}\right) = 1.410591902\mathrm{i},$$

which is remarkably similar to (2.39),

$$K(\epsilon) \sim -2\mathrm{i}\cos\left(\frac{3}{4}\pi\right) = \sqrt{2}\mathrm{i}.$$

In fact, the relative error between the Stokes multiplier (2.39) and (2.103) is small for a large range of α_1 values and Figure 2.10 highlights this. The difference is most significant in the region where $-1 < \alpha_1 < 0$. In particular,

$$K(\epsilon) \leq \mathcal{O}(1) \quad \text{and} \quad K_{\mathrm{H}} \to \infty \quad \text{as} \quad \alpha_1 \to -1.$$

2.7 $-1 < \alpha_1 < 0$

The main objective of this section is to find an estimate for the reflected wave when the results in (2.39) and (2.93) do not hold, e.g. $\cos(\nu_1\pi) = 0$ and $\sin(\hat{\alpha}\pi/2) = 0$. This occurs when

$$\alpha_1 \in -1 + \frac{1}{2\mathbb{N}+1} \quad \text{and} \quad \hat{\alpha} \in -2\mathbb{N}/\{0\} \tag{2.105}$$

respectively, whereby the Stokes multiplier is $\mathcal{O}(\epsilon)$ or less. This matter was briefly discussed in the appendix of [38], where it was noted that:

"The exception to [(2.39)] arises for some special values $\leq -4/3$ of $[2\alpha_1]$...for which $[\cos(\nu_1\pi) = 0]$. Then...$[K(\epsilon) = \mathcal{O}(\epsilon)]$."

However, no explicit estimate of the amplitude of the reflected wave was given in [38] and, in

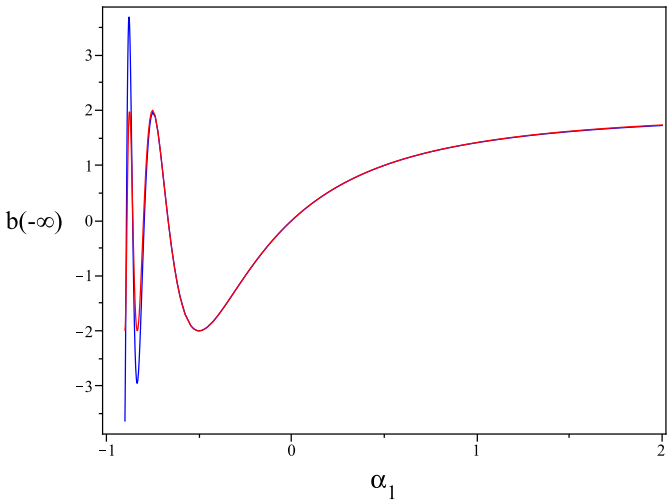

Figure 2.10: Numerical estimate of the pre-factor of the exponentially small term $K(\epsilon)$ and $K_{\rm H}(\epsilon)$ in (2.104), as a function of $\alpha_{_1}$; the blue line is the estimate in (2.103) and the red line is (2.50). The resemblance is remarkable for a large range of $\alpha_{_1}$ values.

fact, the results are somewhat surprising.

Note, in the case of $-1 < \alpha_1 < 0$ the assumption made at the beginning of §2.2 that the nearest transition point to the origin is a branch point singularity is now no longer valid. Instead, the nearest transition point to the real axis is a root of $c_1(x)$.

2.7.1 A calculation of an $\mathcal{O}(\epsilon)$ Stokes multiplier

We begin by investigating the solutions of (2.82) independently of (2.7) whereby the 'special' values of $\hat{\alpha}$ for which (2.93) does not hold are

$$\hat{\alpha} \in 2\mathbb{Z}/\{0\}.$$

It was noted in the paragraph below (2.87) that: the easiest way to confirm an asymptotic result for the Stokes multiplier numerically, when $K(\epsilon) \leq \mathcal{O}(\epsilon)$, is to inspect the solutions of the ODE (2.82) independently of (2.7). This is because, the Stokes geometry associated with the solutions of (2.82) is significantly less detailed than that of (2.7), i.e. the Stokes line is the imaginary axis connecting the points X_* and $\bar{X}_*$. That is, the Stokes lines are clearly the imaginary axis unlike the ODE (2.7) where the Stokes lines were given by (2.23) which are found using (2.11) and (2.17). We first focus on $\hat{\alpha} = 2\mathbb{N}$ in (2.82). Hence, let

$$\hat{\alpha}/2 = p \in \mathbb{N}. \tag{2.106}$$

To find the leading order estimate of the amplitude of the reflected wave it is necessary to consider more terms in the local expansion of $c(X)$ in (2.87). Introducing $z = X - X_*$, let

$$c \sim \hat{\gamma}\mathrm{i}^{-2p} z^{-2p}\,(1 + kz)\,, \quad z \to 0, \tag{2.107}$$

with $\hat{\gamma} > 0$ and k be a non-zero constant. Therefore, (2.88) is

$$\hat{Q} \sim p\,(p+1)\,z^{-2} - kpz^{-1}, \quad z \to 0. \tag{2.108}$$

Recall $a_0 = 1$, from (2.92), and with (2.108) the next term in the recurrence relation is

$$a_1 \sim -\frac{p(p+1)}{2\mathrm{i}z}, \quad z \to 0.$$

To approximate the behaviour of the a_n's for general n, as $z \to 0$, we let:

$$a_n \sim d_n z^{-n} + (e_n \ln(z) + r_n) z^{-(n-1)}, \quad n \geq 2, \tag{2.109}$$

where d_n, e_n and r_n are constants. Note, the logarithm term in (2.109) was determined by calculating the first few coefficients in the ansatz (2.91) via the recurrence relation (2.92) near $z = 0$. Placing (2.109) into (2.92), it is found that

$$d_2 = \frac{p}{2}\frac{(p+2)}{(2\mathrm{i})^2}(p^2-1), \quad e_2 = \frac{kp^2}{(2\mathrm{i})^2}(p+1) \quad \text{and} \quad r_2 = -kp/3,$$

and in general,

$$a_n \sim \frac{U_n}{2\mathrm{i}} d_{n-1} z^{-n} + \frac{V_n}{2\mathrm{i}} e_{n-1} \ln(z) z^{-(n-1)} + \left(kp\frac{d_{n-1}}{n-1} + \left(\frac{2n-3}{n-1} + \frac{V_n}{n-1} \right) e_{n-1} + V_n r_{n-1} \right) \frac{z^{-(n-1)}}{2\mathrm{i}}, \quad n > 2, \tag{2.110}$$

where

$$U_n = \frac{(n+p)(n-p-1)}{n} \quad \text{and} \quad V_n = \frac{(n-p-2)(n+p-1)}{n-1}.$$

Matching (2.110) with (2.109), it follows that

$$d_n = \frac{(n-p-1)\,(n+p)}{n}\frac{d_{n-1}}{2\mathrm{i}}, \tag{2.111}$$

$$\implies \quad d_n = \begin{cases} \frac{(-p)_n (p+1)_n}{(2\mathrm{i})^n n!} & : \quad n \leq p, \\ 0 & : \quad n \geq p+1, \end{cases}$$

$$e_n = \frac{(n-p-2)(n+p-1)}{n-1}\frac{e_{n-1}}{2\mathrm{i}}, \tag{2.112}$$

$$\implies \quad e_n = \begin{cases} (-)^{n-1} \frac{(p+n-1)!}{(p+1-n)!(n-1)!} \frac{kp}{(2\mathrm{i})^n} & : \quad 3 \leq n \leq p+1, \\ 0 & : \quad n \geq p+2, \end{cases}$$

and finally,

$$r_n = \frac{kp}{n-1}\frac{d_{n-1}}{2\mathrm{i}} + \left(\frac{2n-3}{n-1} + \frac{(n-p-2)(n+p-1)}{(n-1)^2} \right) \frac{e_{n-1}}{2\mathrm{i}} + \frac{(n-p-2)(n+p-1)}{n-1}\frac{r_{n-1}}{2\mathrm{i}} \tag{2.113}$$

$$\implies \quad r_n = (-)^p \frac{kp}{(2\mathrm{i})^n} \frac{(n-p-2)!(n+p-1)!}{(n-1)!} \quad : \quad n \geq p+2.$$

Therefore, as $z \to 0$,

$$\begin{aligned} a_n &\sim \frac{(-p)_n (p+1)_n}{n!} (2\mathrm{i}z)^{-n}, \quad n \leq p, \\ a_{p+1} &\sim (-)^p \frac{kp}{2\mathrm{i}} \frac{(2p)!}{p!} \frac{\ln(z)}{(2\mathrm{i}z)^p}, \\ a_n &\sim (-)^p \frac{kp}{2\mathrm{i}} \frac{(n-p-2)!(n+p-1)!}{(n-1)!} (2\mathrm{i}z)^{-(n-1)}, \quad n \geq p+2. \end{aligned} \tag{2.114}$$

The objects $(-p)_n$ and $(p+1)_n$ are Pocchammer rising factorials. Using the identity in (2.72),

$$a_n \sim (-)^p \frac{kp}{2\mathrm{i}} \frac{\Gamma(n-1)}{(2\mathrm{i}z)^{n-1}}, \quad z \to 0,\ n \to \infty. \tag{2.115}$$

With $k \neq 0$, we use the resurgence relation in (2.62) to calculate the leading order estimate of the Stokes multiplier. Placing (2.115), $\chi(X) = 2\mathrm{i}z$ and $b_0(X) = 1$ into (2.62), it is found that,

$$\begin{aligned} &\mu = 1, \\ \text{and} \quad &K(\epsilon) = \left((-)^p \epsilon kp\pi + \mathcal{O}(\epsilon^2) \right), \quad p = \hat{\alpha}/2 \in \mathbb{N}. \end{aligned} \tag{2.116}$$

Hence, the amplitude of the reflected wave is

$$B(\epsilon) \sim (-)^p \epsilon k p \pi \mathrm{e}^{2\mathrm{i}X_*/\epsilon}, \quad X \to -\infty. \tag{2.117}$$

Using the same method that led to (2.116) when $\hat{\alpha} = -2\mathbb{N}$, leads to

$$K(\epsilon) = \left((-)^{p-1}\epsilon k p \pi + \mathcal{O}(\epsilon^2)\right), \quad p = -\hat{\alpha}/2 \in \mathbb{N}. \tag{2.118}$$

Eq. (2.116) and (2.118) highlight that the reflected wave is now smaller by a a factor of ϵ. Note, the most significant difference between (2.116) and (2.118) is that X_* is a zero of $c(X)$, as $\hat{\alpha} \in -2\mathbb{N}$. Thus, one might be tempted to consider (2.118) as the estimate for the leading order Stokes multiplier in (2.7) when α_1 is in (2.105), see §2.7.2.

As an example let, $\hat{\alpha} = 2$ and $c(X) = \left(\frac{2+X^2}{1+X^2}\right)^2$, then $p = 1$ and $k = 5\mathrm{i}$. Therefore,

$$K(\epsilon) \sim -5\epsilon\pi\mathrm{i}.$$

This estimate is confirmed in two ways:

Firstly, we determine the behaviour of the $a_n(X)$ coefficients near X_* by numerically integrating the recurrence relation in (2.92) for $n \gg 1$ and, subsequently, place the leading order result into into the resurgence relation (2.62) for various values of n. It follows that:

$$\begin{aligned}
& K(\epsilon)\epsilon^{-1} \sim -5\pi\mathrm{i}, \quad n \to \infty, \\
& K(\epsilon)\epsilon^{-1} \approx -15.77117439\mathrm{i}, \qquad n = 499 \\
& K(\epsilon)\epsilon^{-1} \approx -15.77104746\mathrm{i}, \qquad n = 500 \\
& K(\epsilon)\epsilon^{-1} \approx -15.75697408\mathrm{i}, \qquad n = 644 \\
\text{and} \quad & K(\epsilon)\epsilon^{-1} \approx -15.75689774\mathrm{i}, \qquad n = 645.
\end{aligned} \tag{2.119}$$

It is evident then, from (2.119), that the pre-factor terms appear to approach the exact value of $-5\pi\mathrm{i}$ as $n \to \infty$.

Secondly, we apply the same numerical scheme as in §2.5. Plotted in Figure 2.11 are the reflected wave amplitude estimates for several speed profiles with $\hat{\alpha} = 2$, indicating that the asymptotic estimate in (2.117) does indeed serve as the leading order estimate of the reflected wave.

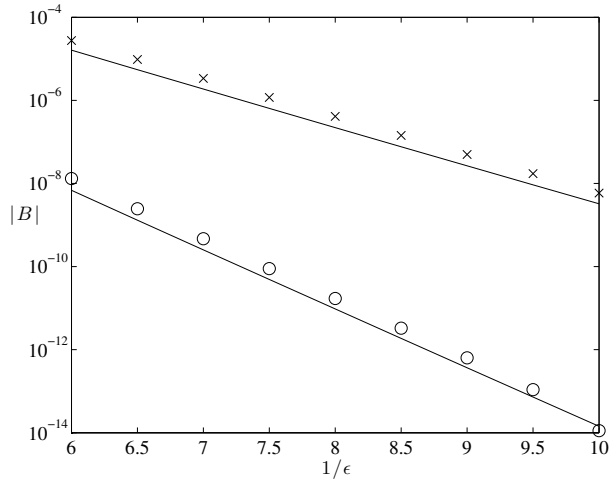

Figure 2.11: Numerical estimate of the amplitude of the reflected wave as a function of $1/\epsilon$ for $c(X) = \left(\frac{2+X}{1+X}\right)^2$ indicated by $\times$ and $c(X) = (1 + \mathrm{sech}(X))^2$ noted by $\circ$. The straight lines represent the asymptotic estimate (2.117) with $\hat{\alpha} = 2 \iff p = 1$.

Note, a faster way with which to ascertain the result in (2.117) is found in Appendix A.

2.7.2 No Stokes phenomena

In this section we highlight the fact that reflections can vanish in two ways. In the first instance we detail the possibility that for certain values of α_1 in (2.22) and $\hat{\alpha}$ in (2.87) the Stokes multiplier associated with x_* and/or X_* is identically zero. The existence of one dimensional potentials in a Schrödinger equation for which there is no reflection was discussed in [5] and subsequently [6]. It shall be shown how the results of this section are related to the aforementioned papers. However, it should be noted that [6] do not deal with the case herein.

A second setup that appears to result in zero reflection can occur when $-1 < \alpha_1 < 0$. In this region there is more than one turning point contributing toward a Stokes phenomenon along the real line. This matter is covered in detail in [13] and as such we merely state that: when $-1 < \alpha_1 < 0$ it is possible for reflections to vanish for special discrete values of the small parameter ϵ and the branch point order α_1. Note that: in this setup both α_1 and $\hat{\alpha}$ are independent of the small parameter ϵ.

The natural conclusion from the result in (2.118) is to assume that: performing the same technique which led to the result in (2.118) furnishes an $\mathcal{O}(\epsilon)$ estimate of the Stokes multiplier in (2.1) when (2.39) fails, e.g. $\cos(\nu_1\pi) = 0$. With this in mind, we let $p \in \mathbb{N}$ and from (2.94) we have that

$$\hat{\alpha} = \frac{\alpha_{_1}}{\alpha_{_1}+1} = -2p \quad \text{and} \quad \alpha_{_1} = -1 + \frac{1}{2p+1}. \tag{2.120}$$

In this scenario, the transition point nearest to the real axis X_* is no longer a branch point singularity but a branch point root of $c(X)$ and thus of $c_1(x)$, noted by (2.81). To find an estimate for the Stokes multiplier in (2.7) additional terms are required in the expansion of $c_1(x)$ near the transition point x_*, than shown in (2.22). In this way the results herein differ from that of [6], as Berry and Howls only consider the leading order terms which is identically zero as the $\sim$ in (2.40) is replaced by $=$, and thus $K(\epsilon) = 0$ identically. Hence, the results presented here are of a qualitatively different nature than that of [6]. We set

$$c_1(x) \approx \gamma \mathrm{i}^{-\alpha_1} Y^{-\alpha_1}\,(1 + k_1 Y) : \quad Y = x - x_*,\, Y \to 0. \tag{2.121}$$

Similarly, we let the local behaviour of $c(X)$, in (2.82), near the transition point X_* be

$$c(X) \approx \hat{\gamma} \mathrm{i}^{2p} z^{2p}\,(1 + k z^q) : \quad z = X - X_*,\, q > 0,\, z \to 0. \tag{2.122}$$

Recalling that $c_1(x) = c(X)$, the factor q has been chosen so as to correctly match the local behaviour of (2.121) and (2.122) as Y, and thus z, tends to zero. From (2.81), it is found that,

$$z \approx \frac{\mathrm{i}^{\alpha_1}}{\gamma(\alpha_{_1}+1)} Y^{\alpha_1+1} \left(1 - k_1 \frac{(\alpha_{_1}+1)}{(\alpha_{_1}+2)} Y\right). \tag{2.123}$$

Connecting the two forms in (2.121) and (2.122) via (2.123) gives

$$q = \frac{1}{\alpha_{_1}+1} = 2p + 1.$$

Therefore, the local behaviour of $c(X)$ is,

$$c(X) \approx \hat{\gamma} \mathrm{i}^{2p} z^{2p} \left(1 + k z^{2p+1}\right), \quad z \to 0, \tag{2.124}$$

and hence, (2.88) near X_* is,

$$Q \approx p(p-1) z^{-2} + 2pk(2p+1) z^{2p-1}, \quad z \to 0. \tag{2.125}$$

Note, the local expansion of Q given by (2.88) should be compared with the function $P^2(z;\epsilon)$ in [6]. To this extent the results presented here and [6] are related.

It should be noted that (2.124) and (2.125) are of a different structure to that of (2.107) and (2.108) and therefore the result in (2.118) is likely not to hold.

Suggested by the form of (2.125), let the coefficients in (2.92) be given by

$$a_n \approx d_n z^{-n} + e_n z^{2p-n+1} \; : \quad 1 \leq n \leq 2p,\; z \to 0, \tag{2.126}$$

where d_n and e_n are constants. Note, the reason for the upper bound of $2p$ on n in (2.126), is due to the potential appearance of logarithm terms beyond this value of n. It is found that:

$$\begin{aligned} d_n \;&=\; \frac{(n-p)(n+p-1)}{n}\frac{d_{n-1}}{2\mathrm{i}} \quad \Longrightarrow \qquad d_n = 0 : \;\; n \geq p \\ \text{and} \quad e_n \;&=\; \frac{(n-3p-1)(n-p-2)}{(n-2p-1)}\frac{e_{n-1}}{2\mathrm{i}} \quad \Longrightarrow \qquad e_n = 0 : \;\; n \geq p+2. \end{aligned} \tag{2.127}$$

Hence, if $p \geq 2$ then,

$$a_n \to \text{constant} \quad \text{as} \quad z \to 0, \quad \forall n \geq p.$$

It is clear from (2.125) that, if $p = 1$ then $a_n \to$ constant for all n. The upshot is that there is no Stokes phenomenon associated with the point at X_*. This recovers the result of [6].

We now extend this result by considering of extra terms in the expansion of (2.125), which, in turn, requires additional terms in (2.126), i.e.

$$a_n \approx d_n z^{-n} + \sum_{m=1} e_n^{(m)} z^{2p-n+m}, \quad z \to 0,\, p \geq 2.$$

Each of the $e_n^{(m)}$ are constant and the extra terms are valid when $n \leq 2p+m$. It follows that

$$e_n^{(m)} = 0 \; : n \geq p+m+2.$$

Hence, consideration of additional terms in (2.125) will not affect the asymptotic behaviour of the coefficients near the transition point. Therefore, the coefficients in (2.91) are non-singular at X_* and the point at $X = X_*$ does not constitute a turning point of (2.82), when $\hat{\alpha} = -2\mathbb{N}$. Hence, there is no Stokes phenomena in this setup and thus no reflected wave. This detail is confirmed numerically by integrating the terms in the recurrence relation (2.92) near X_*.

The fact that there is no Stokes phenomenon in (2.82) due to the point at X_* implies that the point at $x = x_*$ does not constitute a turning point of (2.7) when the behaviour of the speed profile $c_1(x)$ local to a branch point root x_* is given by

$$c_1(x) \;\sim\; \gamma \mathrm{i}^{-\alpha_1/2} Z^{-\alpha_1}\big(1 + k_1 Z + k_2 Z^2 \ldots\big) : \quad Z = x - x_* \quad \text{and} \quad \alpha_1 \in -1 + \frac{1}{2\mathbb{N}+1}. \tag{2.128}$$

Remarkably, this suggest that there is no reflected wave in (2.7) for a countable set of α_1 values given by (2.120). This matter is confirmed, as with the point at X_*, by numerically integrating the terms in (2.57) near x_* (for the speed profiles given in §2.5) which reveals that the coefficients in (2.59) are bounded at x_*. The prediction in [38] that $K(\epsilon) = \mathcal{O}(\epsilon)$ in (2.13), appears incorrect as (it would seem that)

$$K(\epsilon) = 0 \; : \quad \alpha_{_1} = -1 + \frac{1}{2\mathbb{N}+1}, \tag{2.129}$$

in (2.39).

Interesting Stokes geometry and numerical integration

Recalling that each transition point makes an additive contribution, it should be noted that: with $-1 < \alpha_1 < 0$ the dominant transition point[5] switches from a root of $c_1(x)$ to a branch point singularity as α_1 passes some threshold value $\alpha_1 = \alpha_{\mathrm{T}}$. For example, taking the speed profile given in (2.20), there is a branch point root at $x_* = \mathrm{i}$ and a branch point singularity at $x_{\mathrm{bp}} = \sqrt{2}\mathrm{i}$ and if $\alpha_1 < \alpha_{\mathrm{T}} = -1/2$, the dominant contribution to the reflected wave amplitude

[5]The term 'dominant transition point' is used to denote the transition point which contributes to the leading order reflected wave amplitude.

is coming from the branch point at $\sqrt{2}\mathrm{i}$. This detail is determined by solving for

$$\alpha_{\mathrm{T}} : \quad \Im\big(g_1(x_*)\big) = \Im\big(g_1(x_{\mathrm{bp}})\big),$$

in (2.40). The result is that: when $\alpha_1 < \alpha_{\mathrm{T}}$ the contribution coming from the point at $x = \mathrm{i}$ is exponentially smaller than the contribution due to $x = \sqrt{2}\mathrm{i}$. However, the exception to this situation arises for special ϵ values for which there is no contribution to the reflected wave coming from x_{bp}, as noted in [13],
"...[the] reflection coefficient can vanish at an infinite set of values clustering at $\epsilon = 0$."

The reason why there is no Stokes phenomenon associated with the branch point is due to a more complex Stokes geometry than the case where the singularity is positioned above the root as in §2.2. This detail is discussed at length in [13]. We wish to exploit this feature in order to determine the validity of (2.129) numerically, as near a special value of ϵ the dominant contribution will come from the root at x_* provided that x_* is indeed a turning point of (2.7).

For our purposes, it suffices to note that: there is a double contribution toward the amplitude of the reflected wave due to x_{bp} as a result of two Stokes lines crossing the real axis. The upshot is that the Stokes multiplier associated with x_{bp} has an additional cosine pre-factor owing to a phase shift:

$$K_1(\epsilon) \sim 2\mathrm{i}\cos(\nu_1\pi)\left(\mathrm{e}^{2\mathrm{i}\Psi/\epsilon} + \mathrm{e}^{-2\mathrm{i}\Psi/\epsilon}\right)\mathrm{e}^{-2\psi/\epsilon} = 4\mathrm{i}\cos(\nu_1\pi)\cos\left(\frac{2\Psi}{\epsilon}\right)\mathrm{e}^{-2\psi/\epsilon}.$$
$$\text{where} \quad \Psi = \Re\left\{\int_{x_*}^{x_{\mathrm{bp}}} \frac{dx'}{c_1(x')}\right\} \quad \text{and} \quad \psi = \Im\left\{g_1(x_{\mathrm{bp}})\right\}. \tag{2.130}$$

In Figure 2.12 we present numerical and analytical estimates of the reflected wave for several speed profiles whose transition point nearest to the real axis is a root of order $\alpha_1 = 2/3$. In this scenario the dominant contributions toward the reflected wave amplitude come from the branch point singularity, located above the root, at $x_{\mathrm{bp}} = \sqrt{2}\mathrm{i}$, in profile (i), and $x_{\mathrm{bp}} = \pi\mathrm{i}$ in (ii). It is clear from Figure 2.12 that for special values of ϵ the contributions coming from the branch point singularities cancel. Therefore, we focus on the first ($1/\epsilon \approx 2.3$) and third ($1/\epsilon \approx 4$) values of $1/\epsilon$ spotted in Figure 2.12 for which the cosine pre-factor of the amplitude of the reflected wave tends toward zero (for profile (i)). It is expected then, in this region of ϵ if $x_* = \mathrm{i}$ is a turning point of (2.7) then the dominant contribution toward the amplitude of the reflected wave will no longer be from $x_* = \mathrm{i}\sqrt{2}$ and instead will be expected to come from the transition point at $x_* = \mathrm{i}$. However, it is clear from Figure 2.13 that the numerical estimate tends toward zero as ϵ approaches a critical value. Thus, there is no contribution toward the amplitude of the reflected wave coming from the point at $x_* = \mathrm{i}$. Hence, $x_* = \mathrm{i}$ is not a turning point of (2.7) when $\alpha_1 = -2/3$ which supports the result in (2.129).

Note: (2.129) is a recent observation and as such the numerical treatment herein is merely a first inspection.

2.8 $\alpha_1 < -1$

Here we investigate the solutions of (2.7) when $\alpha_1 < -1$ in (2.22). It is noted in [38] that, in this situation the transition point at x_1 cannot be considered a turning point as the exponent of the exponential in (2.40) is $g_1(x_*) = \infty$. We confirm that there is no Stokes phenomenon, in such a scenario, using the methods outlined previously. Note, as $\alpha_1 < -1$, the transition point closest to the real axis is a root of $c_1(x)$. For convenience we set $\alpha = -\alpha_1$.

K–S

We begin with the same set-up that assumes a Stokes phenomenon in (2.12) and (2.13). That is, to the left of a Stokes line the solution of (2.7) is expected to be:

$$y_L \sim c^{-1/2}(x)e^{\mathrm{i}g_1(x)/\epsilon}\left(1 + K(\epsilon)\mathrm{e}^{-\mathrm{i}\chi(x)/\epsilon}\right), \quad \Re(x) < \Re(x_*). \tag{2.131}$$

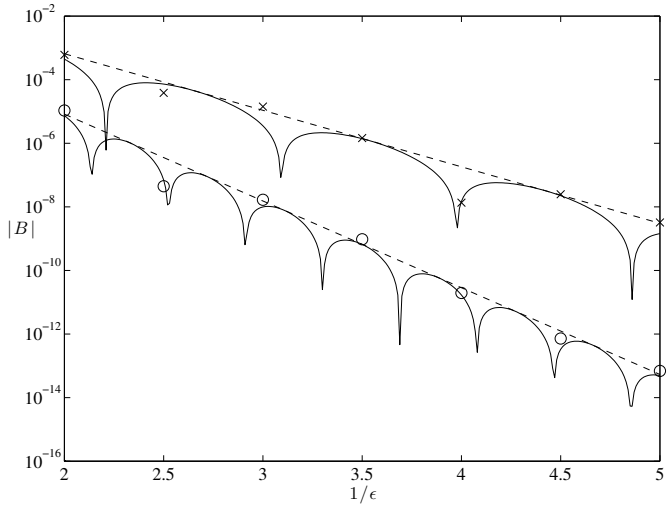

Figure 2.12: Numerical estimate of the amplitude of the reflected wave as a function of $1/\epsilon$ for (i) $c_1(x) = \left(\frac{2+x^2}{1+x^2}\right)^{-2/3}$ ($\times$) and (ii) $c_1(x) = (1+\mathrm{sech}(x))^{-2/3}$ ($\circ$). The straight dashed line represents the asymptotic estimate (2.39) (without phase shift) and the solid lines represent (2.39) pre-factored by a trigonometric function of ϵ deduced in [13]. The diagrams of section 4 example 2 in [13] are helpful in the more difficult case. The active transition point of (i) is $x_* = \mathrm{i}\sqrt{2}$ and of (ii) is $x_* = \mathrm{i}\pi$, where $\alpha_{_1} = 2/3$.

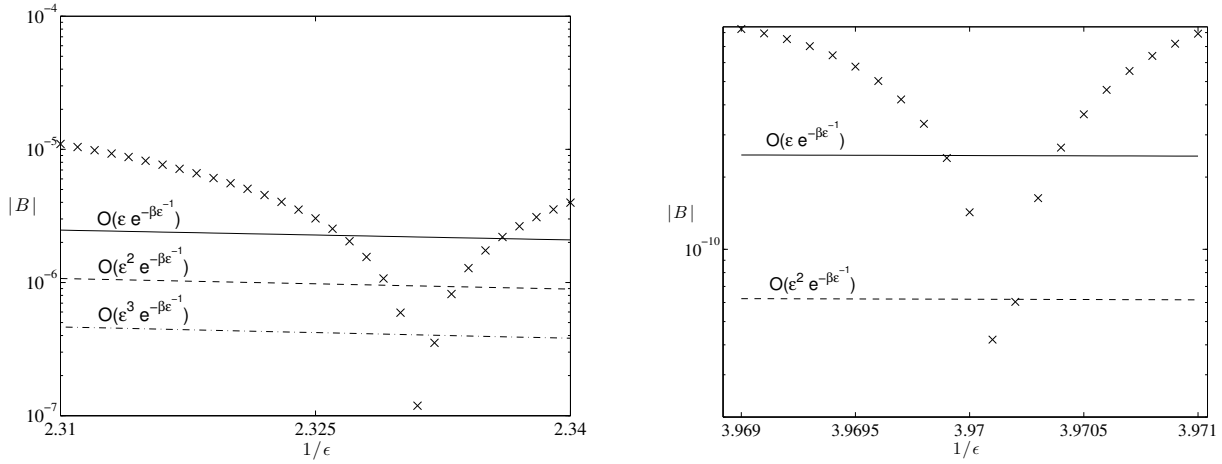

Figure 2.13: Above, we focus on the situation where the wave speed is (i) and on the numerical estimate ($\times$) around the first ($1/\epsilon \approx 2.3$), left panel, and third ($1/\epsilon \approx 4$), right panel, values of $1/\epsilon$ spotted in figure(2.12), for which the cosine pre-factor of the amplitude of the reflected wave tends toward zero. The straight lines of $\mathcal{O}\left(\epsilon^n \mathrm{e}^{-\beta/\epsilon}\right)$ for $n = 1..3$ and $\beta = |2\mathrm{i}g_1(\mathrm{i})|$, have been plotted to indicated where the lower order terms of (2.40) would be expected.

Let $\alpha_{_1} = -\alpha$ and introducing,

$$\eta = \mathrm{i}\epsilon^{-1/(1-\alpha)}(x - x_*), \tag{2.132}$$

the local behaviour of the wave speed, (2.22), is

$$c_1(x) \sim \gamma\epsilon^{\alpha/(1-\alpha)}\eta^\alpha : \quad \alpha > 1 \quad \text{and} \quad \gamma > 0. \tag{2.133}$$

For our proposes it is sufficient to let $g_1(x)$ in (2.11) as $x \to x_*$, be:

$$g_1(x) \approx \mathrm{i}^{-\alpha}(x - x_*)^{1-\alpha}/\gamma(1-\alpha) + \text{l.o.t.} \tag{2.134}$$

When matching solutions along anti-Stokes lines, it is necessary to keep track of the leading order spatially varying term only. Therefore, using (2.132),

$$g_1(x) \sim \mathrm{i}\epsilon\eta^{1-\alpha}/\gamma(\alpha-1), \quad \eta \to 0.$$

Local Solution

Using (2.132) and (2.133), near $x = x_*$ (2.7) is

$$\frac{d}{d\eta}(\eta^{2\alpha}\frac{dy}{d\eta}) - \frac{1}{\gamma^2}y = 0, \tag{2.135}$$

whose solutions can be shown to be

$$y(\eta) \sim \eta^{-\alpha+1/2}\left\{\hat{C}\,H_\nu^{(1)}\left(\frac{\mathrm{i}\eta^{1-\alpha}}{\gamma(\alpha-1)}\right) + \hat{D}\,H_\nu^{(2)}\left(\frac{\mathrm{i}\eta^{1-\alpha}}{\gamma(\alpha-1)}\right)\right\}. \tag{2.136}$$

The objects $\hat{C}$ and $\hat{D}$ are constants, $\nu = \frac{2\alpha-1}{2\alpha-2}$ and $|\eta^{1-\alpha}| \to \infty$. $H_\nu^{(1)}(z)$ and $H_\nu^{(1)}(z)$ are again Hankel functions of the first and second kind whose large-z expansions were given in (2.29) and (2.30). We match along the anti-Stokes lines closest to the (presumed) Stokes line that crosses the real axis. At $x = x_*$, these are lines tangent to

$$\eta_{_R} = \tau\mathrm{e}^{-\mathrm{i}\pi/(2(1-\alpha))} \quad \text{and} \quad \eta_{_L} = \tau\mathrm{e}^{\mathrm{i}\pi/(2(1-\alpha))}, \tag{2.137}$$

where $\tau > 0$. The anti-Stokes lines lie below and above the real axis in the η-plane, from (2.132). The arguments in (2.136), along the anti-Stokes lines, are then

$$\begin{aligned} &\text{(i)}\ \arg\left(\frac{\mathrm{i}{\eta_{_R}}^{1-\alpha}}{\gamma(\alpha-1)}\right) = 0, \\ &\text{(ii)}\ \arg\left(\frac{\mathrm{i}\eta_{_L}^{1-\alpha}}{\gamma(\alpha-1)}\right) = \pi. \end{aligned} \tag{2.138}$$

The argument (i), in (2.136), is within range of (2.29) and (2.30). Therefore, to the right of the Stokes line along $\eta_{_R}$,

$$y_{_R} \sim \ldots\left(\hat{C}\exp\left\{\mathrm{i}\frac{\tau^{\alpha+1}}{\gamma(\alpha+1)}\right\} + \hat{D}\mathrm{e}^{\mathrm{i}\pi(\nu+1/2)}\exp\left\{-\mathrm{i}\frac{\tau^{\alpha+1}}{\gamma(\alpha+1)}\right\}\right). \tag{2.139}$$

Note: the dots here and later in this section represent a constant pre factor to exponential terms. To find the constant we inspect the outer solution.

WKBJ solutions along the anti-Stokes lines

We need only focus on the phase function, $g_1(x)$, in (2.12), to decide which of the coefficients $\hat{C}$ and $\hat{D}$ in (2.136) is zero. With

$$\mathrm{i}g_1(x)/\epsilon \sim \mathrm{i}\left(\frac{\tau^{1-\alpha}}{\gamma(1-\alpha)}\right), \quad \eta = \eta_{_R},$$

$$\implies \quad \hat{D} = 0, \tag{2.140}$$

in (2.139). However, contrary to the situation when the branch point singularity of (2.3) lies below a root, (ii) in (2.138) is within the range of (2.29). As such, on crossing over the imaginary axis and onto the anti-Stokes line, $\eta = \eta_{_L}$, we make no use of the connection relation in (2.34). Thus, there is no additional solution switched on owing to a Stokes phenomenon. That is, to the right of the imaginary axis and below $x = x_*$,

$$y_{_R} \sim \ldots \exp\left\{ \mathrm{i}\frac{\tau^{\alpha+1}}{\gamma(\alpha+1)} \right\}, \quad \Re(x) > 0$$

and to the left of the imaginary axis and below $x = x_*$,

$$y_{_L} \sim \ldots \exp\left\{ -\mathrm{i}\frac{\tau^{\alpha+1}}{\gamma(\alpha+1)} \right\} \quad \Re(x) < 0.$$

It is concluded, as there is no change in the behaviour of the local solution between the anti-Stokes lines $\eta_{_R}$ and $\eta_{_L}$ in (2.137), there must be no Stokes phenomenon due to the point x_*. Therefore,

$$K(\epsilon) = 0, \tag{2.141}$$

in (2.131). Eq. (2.141) holds in a sector local to x_*, bounded by the lines (2.137). One cannot conclude, however, that x_* is certainly not a turning point of (2.7) as there may be other possible regions around x_* where a Stokes line is present and affects the solutions along the real line. To cover all possible sectors surrounding x_* would be time consuming and is therefore a significant set back in the local matching technique. There are no such complications with the method involving late term analysis, as we shall see now.

2.8.1 Inspecting the recurrence relation near x_*

The method of categorising the transition point x_* in the R-A setup is somewhat easier than that of the K–S approach. Here, we investigate the behaviour of coefficients in (2.51), specifically (2.57), as $x \to x_*$. From turning point analysis, see [60] for more information, if $|a_n(x_*)| < \infty \ \forall n$, in (2.57), then the transition point x_* is not of turning point type. It is clear from (2.66), that the behaviour of $a_1(x)$ in (2.51), near x_*, depends on the local behaviour of $Q_1(x)$ in (2.57). Using (2.132) and (2.133), (2.54) local to x_* gives

$$Q_1(x) \sim \ldots \eta^{\alpha-2}, \quad \eta \to 0.$$

Recalling (2.56), as $\eta \to 0$ (2.57) is,

$$a_1(x) = \text{constant} + \mathcal{O}\left(\eta^{\alpha-1}\right).$$

It is apparent from the above that $\alpha = 1$ is a special value, which is discussed later, see §4.2.1. With $\alpha > 1$, $a_1(x)$ is bounded near x_* and in general, it is clear from (2.57) that

$$a_n(x) = \mathcal{O}(1), \quad x \to x_*, \, \forall n.$$

Hence, each $a_n(x)$ is bounded in a region around x_* and, thus, $x = x_*$ does not constitute a turning point of (2.7).

This is a stronger conclusion than that ascertained from the K–S approach. Of course, for a specific $c_1(x)$, one need only consider the lines (2.23) to distinguish regions of validity of the solutions in (2.51). However, this can constitute a study in and of itself, see [30].

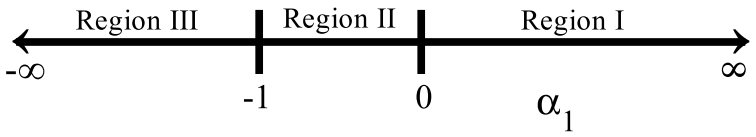

Figure 2.14: The effects of α_1 on wave reflection, where α_1 is the order of the branch point singularity or branch point root of $c_1(x)$ in (2.7). Region I: $\alpha_1 > 0$ and wave reflection occurs. Region II: in this region $-1 < \alpha_1 < 0$ and special phenomena start to appear: a switch in the dominant transition point and no Stoke phenomena for particular values of α_1 : $\alpha_1 \in -1+\frac{1}{2\mathbb{N}+1}$. Region III: here $\alpha_1 < -1$ and there is no Stokes phenomenon and thus no reflected wave.

2.9 Wave reflection: a branch point order perspective

In was noted in §2.2, §2.7 and §2.8 that: a change in the value of the parameter α_1 in (2.22) can affect the amplitude and existence of a reflected wave in (2.7). We now summarise this. Note, α_1 represents the order of the transition (branch) point closest to the real axis x_*.

$\alpha_1 > 0$: here, the closest transition point to the real axis is a branch point singularity. This situation was discussed in §2.2 where it was deduced that an exponentially small reflected wave was generated as a result of a Stokes phenomenon due to point $x = x_*$.

$-1 < \alpha_1 < 0$: here, the closest transition point to the real axis is a root of $c_1(x)$. In this region there are two important details: firstly, there exists a threshold value of α_1, namely α_{T}, whereby if $\alpha_1 < \alpha_{\mathrm{T}} < 0$ then the dominant transition point switches from the transition point closest to the real axis to a neighbouring transition point. Secondly, it was noted in §2.7.1 that for a special set of values, $\alpha_1 \in -1 + \frac{1}{2\mathbb{N}+1}$, no Stokes phenomenon is detected and hence no reflected wave due to the transition point x_*.

$\alpha_1 < -1$: here, the closest transition point to the real axis is a root of $c_1(x)$. It was deduced in §2.8 that there is no reflected wave in this set-up, confirming the prediction of [38].

These results are illustrated in Figure 2.14. Note that, $\alpha_1 = 0$ is trivial and $\alpha_1 = -1$ is a special point which is discussed in §4.2.1.

Chapter 3

Solutions to a wave equation for a spatio-temporal wave speed

Exponentially small reflection is relatively well understood (c.f. [29] & [28]) in the ODE case (corresponding to a continuously forced wave of fixed frequency) but not in the PDE case for an initial-value problem.

In this chapter we consider the PDE (2.1) outlined in §2.1, and present three methods that aim to find the form of the transmitted and reflected waves. Firstly, we use the method of resurgence. Subsequently, we present details of an integral transform that appears to expedite the process of finding the result gained using resurgence. Finally, we employ a Kruskal–Segur matching approach, which closely follows the method of §2.2.1. All three methods return the main result of this thesis (c.f. Eq(3.81)).

Note: a first approach to finding an estimate for the reflected wave amplitude in (2.1) when the wave speed is purely spatially dependent, i.e. $c(x,t) = c_1(x)$, is to apply a spectral analysis (S-A) methodology. We forgo placing the spectral analysis procedure in the main text as: the results are a subset of the case where $c(x,t) = c_1(x)c_2(t)$ with $c_2(t)$ in non-constant and the method lies outwith the theme of the thesis in some respects. Additionally, it is found that the S-A method is more cumbersome than the methods contained within the current chapter and is hence found in Appendix B.

3.1 Preliminary results: leading order 'initial' solution

As noted in §1.5, the scale separation between the $\mathcal{O}(\epsilon^{-1})$ phase and the $\mathcal{O}(1)$ amplitude in (2.2), prompts the use of the slowly varying wave train ansatz to investigate the solutions to (2.1):

$$h(x,t) \sim A(\epsilon)\mathrm{e}^{\mathrm{i}\theta_-(x,t)/\epsilon}\sum_{n=0}^{\infty} a_n(x,t)\epsilon^n + B(\epsilon)\mathrm{e}^{\mathrm{i}\theta_+(x,t)/\epsilon}\sum_{n=0}^{\infty} b_n(x,t)\epsilon^n, \quad \epsilon \to 0. \tag{3.1}$$

The subscripts $-$ and $+$ are used as shorthand to denote the solutions of (2.1) propagating toward decreasing $(-)$ and increasing $(+)$, x. The initial setup, (2.2), implies $B(\epsilon) = 0$ at $t = 0$, and thus a Stokes phenomenon generates (a) reflected wave(s) propagating toward increasing x. The wave propagating towards decreasing x shall be known as the 'initial' solution and upon crossing a Stokes line, the dominant solution. This is because: a dominant solution is deemed dominant only if a subdominant solution is present[1], 'initially' this is not the situation.

We focus on the transition points closest to the real (x,t)plane being a branch point singularity of $c_1(x)$, x_*, and/or a root of $c_2(t)$, t_*, from (2.4).

[1] 'present' is used in the sense that the subdominant solution has a non-zero pre-factor.

Initial and reflected wave phase functions

Substituting (3.1) into (2.1), at $\mathcal{O}(\epsilon^{-2})$:

$$\partial_t\theta_- - c_1(x)c_2(t)\partial_x\theta_- = 0 \quad \text{and} \quad \partial_t\theta_+ + c_1(x)c_2(t)\partial_x\theta_+ = 0. \tag{3.2}$$

The solutions of (3.2) are found via the method of characteristics, giving rise to the following important derivatives:

$$\frac{d}{ds_-} = \partial_t - c_1(x)c_2(t)\partial_x \quad \text{and} \quad \frac{d}{ds_+} = \partial_t + c_1(x)c_2(t)\partial_x. \tag{3.3}$$

The characteristic parameters s_- and s_+ are associated with waves travelling in the direction of decreasing and increasing x. Eq. (3.2) can be rewritten as

$$\frac{d\theta_-}{ds_-} = 0 \quad \text{and} \quad \frac{d\theta_+}{ds_+} = 0. \tag{3.4}$$

From (3.3), we have that

$$ds_\pm = dt = \pm\frac{dx}{c_1(x)c_2(t)} \implies \int_\xi^x \frac{dx'}{c_1(x')} = \mp\int_0^t c_2(t')dt', \tag{3.5}$$

where ξ is a parameter identifying the characteristics. Therefore,

$$x = X(t,\xi) = g_1^{-1}\big(g_1(\xi) \pm g_2(t)\big),$$

which can be inverted to obtain

$$\xi_\pm(x,t) = g_1^{-1}\left(g_1(x) \mp g_2(t)\right) \quad \text{with} \quad \xi(x,0) = x, \tag{3.6}$$

where

$$g_1(x) = \int_0^x 1/c_1(x')dx' \quad \text{and} \quad g_2(t) = \int_0^t c_2(t')dt'. \tag{3.7}$$

By definition, from (3.3):

$$\frac{d\xi_-}{ds_-} = 0 \quad \text{and} \quad \frac{d\xi_+}{ds_+} = 0. \tag{3.8}$$

Thus, the phase of the initial wave in (3.1), using (3.4), is

$$\theta_-(x,t) = \mathcal{D}_-\left(\xi_-(x,t)\right), \tag{3.9}$$

where the arbitrary function $\mathcal{D}_-$ is determined using (2.2). The phase of any reflected wave is then

$$\theta_+(x,t) = \mathcal{D}_+\left(\xi_+(x,t)\right). \tag{3.10}$$

Using (2.2), (3.6) and (3.9), it follows that

$$\mathcal{D}_-(x) = k_0 x.$$

Therefore,

$$\theta_-(x,t) = k_0\xi_-(x,t) = k_0 g_1^{-1}\left(g_1(x) + g_2(t)\right), \tag{3.11}$$

in (3.1).

Recurrence relations

As in (2.52), we determine the recurrence relations of the $a_n(x,t)$ and $b_n(x,t)$ in (3.1) by substituting

$$h(x,t) \sim A(x,t;\epsilon)\mathrm{e}^{\mathrm{i}\theta(x,t)/e}: \quad \theta(x,t) = \theta_\pm(x,t)$$

into (2.1). With $c = c_1(x)c_2(t)$ the l.h.s. of (2.1) is

$$\left(A\mathrm{e}^{\mathrm{i}\theta/\epsilon}\right)_{tt} \;=\; \left(-\frac{\theta_t^2 A}{\epsilon^2} + \frac{\mathrm{i}}{\epsilon}\left[2\theta_t A_t + \theta_{tt}A\right] + A_{tt}\right)\mathrm{e}^{\mathrm{i}\theta/\epsilon}, \tag{3.12}$$

and the r.h.s,

$$\left(c^2\left(A\mathrm{e}^{\mathrm{i}\theta/\epsilon}\right)_x\right)_x \;=\; \left(-\frac{c^2\theta_x^2 A}{\epsilon^2} + \frac{\mathrm{i}}{\epsilon}\left[2c^2\theta_x A_x + \left(c^2\theta_x\right)_x A\right] + \left(c^2 A_x\right)_x\right)\mathrm{e}^{\mathrm{i}\theta/\epsilon}. \tag{3.13}$$

Here and henceforth, subscripts x and t denote differentiation w.r.t. x and t, respectively. On combining the two terms above, at $\mathcal{O}(\epsilon^{-2})$ the equations in (3.4) are recovered. Taking the root pertaining to a leftward propagating wave in (3.2), it is found that

$$\partial_t^2\theta_- - \left(c^2\partial_x\theta_-\right)_x \;=\; \partial_x\theta_-\frac{dc}{ds_-}, \tag{3.14}$$

a similar identity exists for a rightward propagating wave. Equating (3.12) and (3.13) and replacing $A(x,t;\epsilon)$ with $\sum_n a_n\epsilon^n$ or $\sum_n b_n\epsilon^n$, from (3.1), at $\mathcal{O}(\epsilon^{-1})$ gives

$$\frac{da_0}{ds_-} \;=\; -\frac{dc}{ds_-}\frac{a_0}{2c} \tag{3.15}$$

$$\text{and}\quad \frac{db_0}{ds_+} \;=\; -\frac{dc}{ds_+}\frac{b_0}{2c}, \tag{3.16}$$

on using (3.14). It follows that

$$\begin{aligned} a_0(x,t) \;&=\; c^{-1/2}(x,t)\mathcal{F}_-\left(\xi_-(x,t)\right), \\ \text{and}\quad b_0(x,t) \;&=\; c^{-1/2}(x,t)\mathcal{F}_+\left(\xi_+(x,t)\right). \end{aligned} \tag{3.17}$$

The function $\mathcal{F}_-(x)$ is determined using (2.2) and (3.6), where, at $t = 0$ gives

$$\mathcal{F}_-(x) \;=\; c^{1/2}(x,0)f(x - x_0).$$

Therefore,

$$a_0(x,t) \;=\; c^{-1/2}(x,t)c^{1/2}(\xi_-(x,t),0)f(\xi_-(x,t) - x_0). \tag{3.18}$$

The recurrence relations for the coefficients in (3.1) are then,

$$\begin{aligned} 2\mathrm{i}\frac{da_{n+1}}{ds_-} + \mathrm{i}\frac{d\ln c}{ds_-}a_{n+1} \;&=\; \left(\left(c^2\partial_x a_n\right)_x - \partial_t^2 a_n\right)/c\partial_x\theta_-, \\ 2\mathrm{i}\frac{db_{n+1}}{ds_+} + \mathrm{i}\frac{d\ln c}{ds_+}b_{n+1} \;&=\; \left(\left(c^2\partial_x b_n\right)_x - \partial_t^2 b_n\right)/c\partial_x\theta_+. \end{aligned} \tag{3.19}$$

Note, that we have chosen not to replace θ_- or θ_+ with (3.11) or (3.10) for brevity. Following (3.17), let:

$$\begin{aligned} a_n(x,t) \;&=\; c^{-1/2}(x,t)\hat{a}_n(x,t), \\ \text{and}\quad b_n(x,t) \;&=\; c^{-1/2}(x,t)\hat{b}_n(x,t). \end{aligned} \tag{3.20}$$

This reduces the recurrence relations in (3.19) to the more appealing form

$$\begin{aligned} 2\mathrm{i}\frac{d}{ds_-}\hat{a}_{n+1} \;&=\; \left(\left(c\partial_x\hat{a}_n\right)_x - \left(c^{-1}\partial_t\hat{a}_n\right)_t - Q(x,t)\hat{a}_n\right)/\partial_x\theta_-, \\ \text{and}\quad 2\mathrm{i}\frac{d}{ds_+}\hat{b}_{n+1} \;&=\; \left(\left(c\partial_x\hat{b}_n\right)_x - \left(c^{-1}\partial_t\hat{b}_n\right)_t - Q(x,t)\hat{b}_n\right)/\partial_x\theta_+, \end{aligned} \tag{3.21}$$

where,

$$\begin{aligned} Q(x,t) &= \frac{c_{xx}}{2} + \frac{(c_x)^2}{4c} + \frac{3(c_t)^2}{4c^3} - \frac{c_{tt}}{2c^2} \\ &= c_2(t)Q_1(x) - \frac{Q_2(t)}{c_1(x)}. \end{aligned} \tag{3.22}$$

Recalling (2.54) and (2.79), that is,

$$Q_1(x) = \frac{c_1''(x)}{2} + \frac{(c_1'(x))^2}{4c_1(x)} \quad \text{and} \quad Q_2(t) = \frac{c_2''(t)}{2(c_2(t))^2} - \frac{3(c_2'(t))^2}{4(c_2(t))^3}.$$

Here, and henceforth, the prime denotes differentiation w.r.t. the dependent variable. The fact that the coefficient and phase functions in (3.1) are linearly independent makes clear that solutions switched on as the initial solution crosses a Stokes line are not exponentially small 'corrections' to the leading order solution. Rather, they are solutions, generated as a result of a Stokes Phenomenon, which are linearly independent of one another and travelling in opposite directions, as observed from the x axis. Therefore, the two objects in the r.h.s of (3.1) form a basis for the solutions of (2.1) away from any turning points in the system. Hence, the initial solution and any reflected solutions switched on as a result of a Stokes phenomenon are of the same form as the two objects in (3.1), and satisfy (3.17) and (3.19) (or the more convenient (3.21)).

WKBJ solutions

For the purposes of reference in §(3.2), §(3.3) and §(3.4), we present the WKBJ solutions of (2.1) associated with two active turning points: a branch point singularity of $c_1(x)$, x_*, and a root of $c_2(t)$, t_*. Let the subscript $j = 1$ represent a solution switched on due to a spatial turning point and $j = 2$ a temporal turning point, then WKBJ solutions of (2.1) in the real plane are:

$$h(x,t) \sim A(\epsilon)\mathrm{e}^{\mathrm{i}k_0\xi_-/\epsilon}\sum_{n=0}^{\infty} a_n(x,t)\epsilon^n \overset{+}{\sim} \sum_{j=1}^{2} B_j(\epsilon)\mathrm{e}^{\mathrm{i}\mathcal{D}_j(\xi_+)/\epsilon}\sum_{n=0}^{\infty} b_{jn}(x,t)\epsilon^n, \tag{3.23}$$

$$\begin{aligned} a_0(x,t) &= c^{-1/2}(x,t)c^{1/2}(\xi_-(x,t),0)f(\xi_-(x,t)-x_0), \\ b_{j0}(x,t) &= c^{-1/2}(x,t)\mathcal{F}_j\left(\xi_+(x,t)\right), \\ \text{and} \quad \xi_\pm(x,t) &= g_1^{-1}(g_1(x) \mp g_2(t)). \end{aligned}$$

Recalling that,

$$g_1(x) = \int_0^x \frac{dx'}{c_1(x')} \quad \text{and} \quad g_2(t) = \int_0^t c_1(t')dt'.$$

The subscript j has been used as in (3.10) and the function $a_n(x,t)$ and all $b_{jn}(x,t)$ satisfy their respective relations in (3.19). We have introduced the symbol $\overset{+}{\sim}$ to denote that: subdominant solutions switched on via a Stokes phenomenon are only active on the dominant solution crossing a Stokes line/sheet in the real (x,t) plane.

3.1.1 Ray-tubes and localised initial data

Eq(2.1) is a linear hyperbolic second order PDE whose solutions, when pursuing asymptotic solutions of (2.1), can be found via the method of characteristics, a matter that is noted by the fact that the phase (3.4) and all of the coefficients, a_n and b_n, in (3.19) are functions of the characteristic parameters s_- and s_+. This is known as Ray-Tracing, where the solutions of (2.1) are found to follow particular ray paths, or ray-tubes, in the real (x,t) plane given by (3.5)[2]. The upshot is that, any point initially at $x(0,\xi_0)$, can be tracked via (3.3), see [11]. This

[2] The ansatz (3.1), resulting in the so called Ray-Tracing equations, is the standard WKBJ method to finding the leading order solution of (2.1), without a Stokes phenomenon

motivates the idea that: each ray-tube of the initial solution undergoes an individual Stokes phenomenon on crossing a Stokes line in the real (x,t) plane. This detail forms the backbone of the analysis in the case where $c(x,t)$ is an arbitrary function of x and t (c.f. §4.2.3 for further details on this setup), rather than the special case of a separable function studied here.

If the function $f(x-x_0)$ in (2.2) is localised then so too are the ray-tubes. To this extent, we introduce the notion of Dominant Solution Rays (DSR) and Subdominant Solution Rays (SSR), along which the solutions of (2.1) are 'visible'. By localised, we mean: the function $f(x-x_0)$ is chosen such that if $|x-x_0| \geq \delta$, for $\delta \in \mathbb{R} > 0$, then $f(x-x_0)$ will be of order ϵ less that any x satisfying $|x-x_0| < \delta$. With this, we let

$$S = \{x_i : x_i \in (x_0-\delta, x_0+\delta)\}, \quad x_i \in \mathbb{R}, \tag{3.24}$$

then for real x,

$$f(x-x_0) \leq \epsilon : \qquad x \notin S, \tag{3.25}$$

where ϵ is the same small parameter as in (2.2). This detail allows us to identify the location of any ray-tubes, of the initial solution, that are $\leq \mathcal{O}(\epsilon)$.

An example of the function f that is used throughout this section is

$$f(x-x_0) = \mathrm{e}^{-(x-x_0)^2/\sigma^2}.$$

Then, with f as above and a specified σ, we have that

$$\mathrm{e}^{-(\delta/\sigma)^2} \leq \epsilon \quad \Longrightarrow \qquad \delta \geq \sigma\sqrt{\ln(1/\epsilon)}. \tag{3.26}$$

The rays that lie within a δ region of x_0 'initially' (pre-Stokes phenomenon) are the DRS. When the DSR cross a Stokes line subdominant solution rays (SSR) are switched on. Hence, from (3.25), the SSR are localised also. An illustration of these ideas is presented in figure(3.1), whereby each ray tube experiences a Stokes Phenomenon. The characteristic curves are found via (3.6), i.e.

$$\xi_{\pm}(x,t) \;=\; g_1^{-1}\left(g_1(x) \mp g_2(t)\right), \qquad \xi \in S:\; \delta = 1,\; x_0 = 10.$$

In the analysis that follows, referring to the initial solution being to the right (or left) of a Stokes line/sheet is equivalent to requiring that the DSR have not yet crossed the Stokes line in question.

3.2 Exponential asymptotics via resurgent analysis

We closely follow the analysis of §2.4 and w.l.g set $\Re(x_*) = 0$. Throughout this section we intermittently alternate between ds_-, dx and dt using (3.4), i.e.

$$\frac{dx}{ds_-} = -c_1(x)c_2(t) \quad \text{and} \quad ds_- = dt.$$

From (3.23), the solution of (2.1) to the right of a Stokes line (sheet) is

$$\begin{aligned} h(x,t) \;&\sim\; \exp\left(\mathrm{i}k_0\xi_-/\epsilon\right)\sum_{n=0}^{\infty} a_n(x,t)\epsilon^n, \\ \text{with} \quad a_0(x,t) \;&=\; c^{-1/2}(x,t)c^{1/2}(\xi_-(x,t),0)f(\xi_-(x,t)-x_0). \end{aligned} \tag{3.27}$$

3.2.1 Subdominant (reflected) solutions

We focus on a single subdominant solution generated as the initial solution crosses a Stokes sheet due to the spatial turning point x_*. The subdominant solution switched on due to t_* is considered identically.

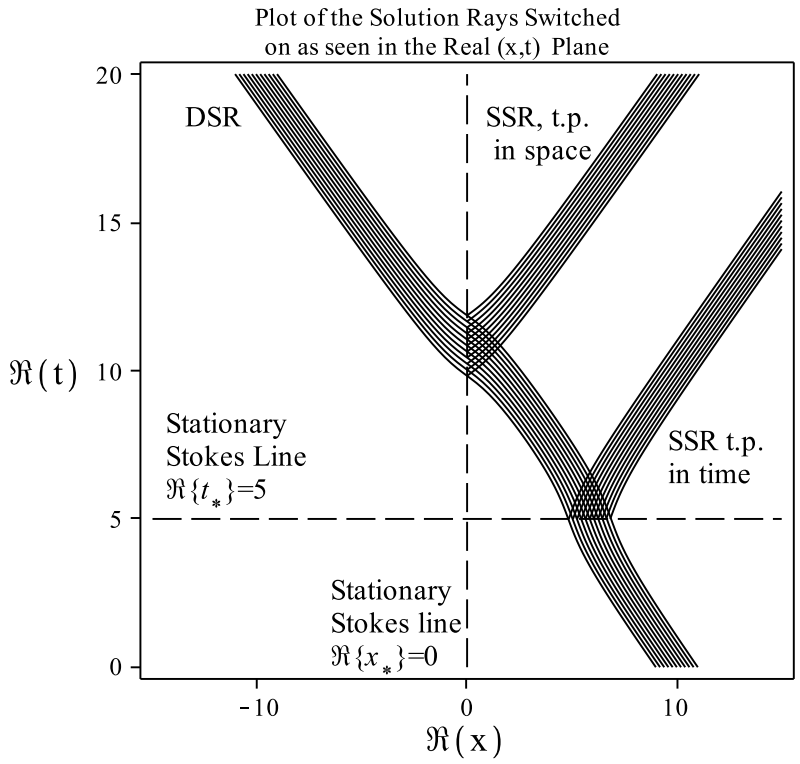

Figure 3.1: With the particular choice of $c(x,t) = \frac{2+x^2}{1+x^2}\frac{1+(t-5)^2}{2+(t-5)^2}$, we plot the Dominant and Subdominant Solution Rays (DSR and SSR), initially around $x_0 = 10$, in the real (x,t) plane. The SSR are generated as the DSR pass Stokes lines due to turning points at $t_* = 5 + \mathrm{i}$ and $x_* = \mathrm{i}$. We use the results of the ODE's (2.7) and (2.47) to guess that the points t_* and x_* are turning points of (2.1).

Upon crossing a Stokes line the solution of (2.1) is

$$h(x,t) \sim \exp\bigl(\mathrm{i}k_0\xi_-/\epsilon\bigr)\left(\underbrace{\sum_{n=0}^{\infty} a_n(x,t)\epsilon^n}_{\text{(i)}} - K_1(\epsilon)\underbrace{\exp\bigl(-\chi_1(x,t)/\epsilon\bigr)\sum_{n=0}^{\infty} b_n(x,t)\epsilon^n}_{\text{(ii)}}\right), \quad x \to \infty. \tag{3.28}$$

Note, $K_1(\epsilon)$ is the Stokes multiplier associated with the spatial turning point.

Phase of subdominant solution

The function $\chi_1(x,t)$ in (3.28) is determined by placing the object (ii) into the differential equation that (i) satisfies, which is deduced from (3.12) and (3.13). Recaling (3.3) and (3.11), let $c = c_1(x)c_2(t)$ then (ii) in (3.28) solves,

$$\frac{\mathrm{i}k_0}{\epsilon}c_1(\xi_-)c_2(t)\left[2\frac{dA}{ds_-} + A\frac{d\ln c}{ds_-}\right] - \bigl(c^2A_x\bigr)_x + A_{tt} = 0,$$

where

$$\frac{\partial\xi_-}{\partial x} = \frac{c_1(\xi_-)}{c_1(x)},$$

has been used. Replacing A with (ii), at $\mathcal{O}(\epsilon^{-2})$:

$$\begin{aligned}
&-2\mathrm{i}k_0 c_1(\xi_-)\,c_2(t)\Big(\partial_t\chi_1 - c\partial_x\chi_1\Big) - c^2\left(\partial_x\chi_1\right)^2 + \left(\partial_t\chi_1\right)^2 \\
&= \Big[\partial_t\chi_1 - c\partial_x\chi_1\Big]\Big[\partial_t\chi_1 + c\partial_x\chi_1 - 2\mathrm{i}k_0 c_1(\xi_-)\,c_2(t)\Big] \\
&= 0. \qquad (3.29)
\end{aligned}$$

Hence, either

$$\frac{d}{ds_-}\chi_1(x,t) = 0 \quad \Longrightarrow \quad \chi_1(x,t) = \mathcal{M}(\xi_-), \qquad (3.30)$$

$$\begin{aligned}
\text{or} \quad \frac{d}{ds_+}\chi_1(x,t) &= 2\mathrm{i}k_0 c_1(\xi_-)\,c_2(t) \\
\Longrightarrow\ \chi_1(x,t) &= \mathrm{i}k_0\int 2c_1(\xi_-)\,c_2(t)ds_+ + \mathcal{N}(\xi_+) \\
&= \mathrm{i}k_0\int d\xi_- + \mathcal{N}(\xi_-) = \mathrm{i}k_0\xi_- + \mathcal{N}(\xi_+), \qquad (3.31)
\end{aligned}$$

where, from (3.3), we have used

$$\frac{d\xi_-}{ds_+} = \frac{d\xi_-}{ds_-} + 2c_1(\xi_-)\,c_2(t) = 2c_1(\xi_-)\,c_2(t).$$

Note that both $\mathcal{M}(\chi_-)$ and $\mathcal{N}(\chi_+)$ are arbitrary functions. The connection between the Stokes phenomenon and the growth of the coefficients in the divergent asymptotic expansions can be expressed using the following, typical, resurgence relation,

$$a_n(x,t) \sim \sum_{j=1}^{2}\frac{K_j(\epsilon)}{2\pi\mathrm{i}}\Gamma(n+\mu)\frac{b_{j0}(x,t)}{\left(\chi_j(x,t)\right)^{n+\mu}}, \quad n\to\infty, \qquad (3.32)$$

where the subscript j has been used to indicate that we expect two solutions to be switched on via a Stokes phenomenon. In the analysis of §2.4, specifically the paragraph preceding (2.63), it was noted that: on approaching a turning point, the exponential pre-factor $\exp\{-\chi_j(x,t)\}$ in (3.28) must be $\mathcal{O}(1)$ for [a similar relation to] (3.32) to hold. Hence, it is required that

$$\chi_j(x,t)\to 0 \ : \quad x\to x_*. \qquad (3.33)$$

The condition in (3.33) implies

$$\mathcal{M}(\xi_-(x_*,t))\to 0, \quad \forall t\in\mathbb{R}>0,$$

in (3.31). Hence, the freedom in the parameter t indicates that $\mathcal{M}(\xi_-)=0$ and (3.30) does not serve as a possible $\chi_1(x,t)$. This could have been spotted immediately as (3.30) represents a wave propagating toward decreasing x. Recall from (3.6) that:

$$\xi_-(x,t) = g_1^{-1}\left(g_1(x)+g_2(t)\right) \quad \text{and} \quad \xi_+(x,t) = g_1^{-1}\left(g_1(x)-g_2(t)\right).$$

Hence, as $x\to x_*$ in (3.31),

$$\mathcal{N}\left(g_1^{-1}(Z)\right) = -\mathrm{i}k_0 g_1^{-1}\left(-Z+2g_1(x_*)\right) \ : \quad Z = g_1(x_*)-g_2(t).$$

Therefore,

$$\begin{aligned}
\mathcal{N}(\xi_+) &= -\mathrm{i}k_0 g_1^{-1}\big(g_2(t)-g_1(x)+2g_1(x_*)\big) \\
\text{and} \quad \chi_1(x,t) &= \mathrm{i}k_0\left[\xi_-(x,t) - g_1^{-1}\big(g_2(t)-g_1(x)+2g_1(x_*)\big)\right]. \qquad (3.34)
\end{aligned}$$

The solution switched on in (3.28) must be subdominant to the initial solution for real x and

t, hence

$$\Re\{\chi_1(x,t)\} < 0 : \quad x,t \in \mathbb{R}. \tag{3.35}$$

Only one of the spatial complex conjugate transition points satisfies (3.35) and hence (3.35) provides a requirement with which to identify the turning point whose Stokes sheet crosses the real (x,t) plane. Comparing (3.23) with (3.28) and (3.34), it is deduced that

$$\mathcal{D}_1(\xi_+) \;=\; k_0 g_1^{-1}\big(2g_1(x_*) - g_1(\xi_+)\big). \tag{3.36}$$

Eq(3.36) displays the form of the phase of the reflected wave in (3.28) due to the spatial turning point. Following the same technique which leads to (3.36) for a temporal turning point, leads to:

$$\begin{aligned} \chi_2(x,t) \;&=\; \mathrm{i}k_0\left[\xi_-(x,t) - g_1^{-1}\big(g_1(x) - g_2(t) + 2g_2(t_*)\big)\right] \\ \text{and} \quad \mathcal{D}_2(\xi_+) \;&=\; k_0 g_1^{-1}\left(2g_1(t_*) - g_1\big(\xi_+\big)\right). \end{aligned} \tag{3.37}$$

Equations (3.28) and (3.34) are compared with (2.60) and (2.64), where it is noticed that: the subdominant solution switched on due to a spatial turning point (along the real axis) in (2.1) is not pre-factored by an exponentially small term. This is in contrast to the results of (2.7), where the solutions switched on are pre-factored by an exponentially small term. See §(4.1) for more.

Symmetric wave speed

Let $c_1(x)$ and $c_2(t)$ be symmetric functions, e.g. (i) or (ii) in (2.20), then complex conjugate transition points arise, e.g. let $x_1 = x_*$ and $x_2 = \bar{x}_*$, and similarly $t_1 = t_*$ and $t_2 = \bar{t}_*$, then it is found that the phase functions of the subdominant solutions, as in (3.28), are:

$$\begin{aligned} \chi_{1l}(x,t) \;&=\; \mathrm{i}k_0\left(\xi_- - g_1^{-1}\left(g_2(t) - g_1(x) + 2g_1(x_l)\right)\right) \\ \text{and} \quad \chi_{2l}(x,t) \;&=\; \mathrm{i}k_0\left(\xi_- - g_1^{-1}\left(g_1(x) - g_2(t) + 2g_1(t_l)\right)\right). \end{aligned} \tag{3.38}$$

The subscript $1l$ pertains to the spatial complex conjugate transition points and $2l$ the temporal. Following the same technique which leads to (3.36), it can be shown that:

$$\begin{aligned} \mathcal{D}_{1l}(\xi_+) \;&=\; k_0 g_1^{-1}\left(2g_1(x_l) - g_1(\xi_+)\right) \\ \text{and} \quad \mathcal{D}_{2l}(\xi_+)(x,t) \;&=\; k_0 g_1^{-1}\left(2g_1(t_l) + g_1(\xi_+)\right). \end{aligned} \tag{3.39}$$

Note, as in the case with the solutions of the ODE (2.7), there is only one possible transition point associated with each complex conjugate pair that satisfies the condition (3.35) or a similar condition for χ_{2l}. Hence, there is only one active transition point (from each pair) that gives rise to a reflected wave in the real plane. It is clear from (3.35) that: a change in sign of k_0 in (2.2) acts to rotate the Stokes lines/sheet which in turn switches the active transition point.

3.2.2 Stokes lines

Along a Stokes line, the initial (dominant) solution must maximally dominate the reflected (subdominant) solution. Hence, from (3.28), (3.36) and (3.37) these are the lines along which

$$\begin{aligned} \Im\{\chi_j(x,t)\} &= 0, \\ \text{and} \quad \Re\{\chi_j(x,t)\} &> 0. \end{aligned} \tag{3.40}$$

There appears to be no apparent way of predicting the location of the Stokes lines that cross the real plane, as in §(2.2.4), without explicit knowledge of $c_1(x)$ and $c_2(t)$.

3.2.3 Recurrence relations near the turning points

Eq. (3.18), (3.19) and (3.22) via (3.21) make clear that the holomorphicity of $a_n(x,t)$ depends upon the behaviour of $c_1(x)$, $c_2(t)$ and $f(x-x_0)$, i.e.

$$\begin{aligned}
&a_0(x,t) \to f(x-x_0), && t \to 0,\ x \in \mathbb{C},\\
&a_0(x,t) \to \infty, && x \to x_*,\ \alpha_1 \in (-1,0),\ t \in \mathbb{R} > 0,\\
&a_1(x,t) \to \infty, && x \to x_*,\ t \in \mathbb{R} > 0,\\
&a_1(x,t) \to \infty, && t \to t_*,\ x \in \mathbb{R},\\
&Q(x,t) \to \infty, && x \to x_* \quad \text{or} \quad t_* \to \infty.
\end{aligned} \tag{3.41}$$

with $\Im\{g_2(t_*) - g_1(x_*)\} \neq 0$, see (3.57). By suitable choice of $f(x-x_0)$ in (2.2) we choose to discount turning points in (2.1) coming from transition points associated with the function $f(x-x_0)$. As such, we let $f(x-x_0)$ be an entire function. Contributions due to transition points in the initial condition are considered in [15].

In the PDE environment, the idea of a discrete turning point promoted from the results of the ODE (2.7) is not valid. That is, $c(x,t) \to \infty$ as $x \to x_*$ for all $t \neq t_*$ and similarly $c(x,t_*) = 0$ for all $x \neq x_*$. Therefore, a nomenclature switch from turning point, valid in the ODE environment, to turning line, in the PDE environment, is required. The turning lines are then

$$(x,t) \;=\; \begin{cases} (x_*,t) : & t \in \mathbb{R} > 0, \\ (x,t_*) : & x \in \mathbb{R}, \end{cases} \tag{3.42}$$

where we expect and confirm that there is no Stokes phenomena at $t = 0$. Note, as the turning points are approached real ranges of t and (subsequently) x are considered as it is the solutions of (2.1) in the real plane that we are interested in.

Arbitrary function of $\xi_-(x,t)$ and the Stokes phenomenon at $t = 0$

It is evident from the recurrence relations in (3.21) that each of the $\hat{a}_n(x,t)$ and $\hat{b}_n$ contain an arbitrary function of ξ_-. Noting that

$$\partial_x \theta_- = k_0 \frac{c_1(\xi_-)}{c_1(x)},$$

from (3.11), the first term in (3.21) reads

$$\hat{a}_1(x,t) \equiv \mathrm{i}\frac{\int^t \zeta_0(x,t')dt'}{2k_0 c_1\,(\xi_-)} + \mathcal{T}_1(\xi_-),$$

on using

$$\zeta_j(x,t) \;=\; -c_1(x)c_2(t)\partial_x\left(c_1(x)\partial_x(\hat{a}_j)\right) + \partial_t\left(\frac{\partial_t(\hat{a}_j)}{c_2(t)}\right) + Q(x,t)\hat{a}_j.$$

We absorb the arbitrary lower bound of integration into the arbitrary function $\mathcal{T}_1(\xi_-)$ and maintain the notation, which gives

$$\hat{a}_1(x,t) \equiv \mathrm{i}\frac{\int_0^t \zeta_0(x(t'),t')dt'}{2k_0 c_1\,(\xi_-)} + \mathcal{T}_1(\xi_-).$$

Therefore, using $\xi(x,0) = x$, $\hat{a}_1(x,t)$ at $t = 0$ is

$$\hat{a}_1(x,0) \;=\; \mathcal{T}_1(x).$$

Applying the same technique to each subsequent $\hat{a}_n(x,t)$, it follows that:

$$\hat{a}_n(x,0) \;=\; \mathcal{T}_n(x).$$

Recalling that $\hat{a}_n(x,t) = c_1^{1/2}(x)c_2^{1/2}(t)a_n(x,t)$, from (3.20), we connect (2.2) with the analytic solution (3.27) at $t = 0$. That is,

$$h(x,0) \;=\; \mathrm{e}^{\mathrm{i}k_0 x/\epsilon} f(x-x_0) \;=\; \mathrm{e}^{\mathrm{i}k_0 x/\epsilon} f(x-x_0) + \sum_{n=1}^{\infty} 0.\epsilon^n, \tag{3.43}$$

and the analytic solution is

$$\begin{aligned} h(x,0) \;&\sim\; \mathrm{e}^{\mathrm{i}k_0 x/\epsilon} \sum_{n=0}^{\infty} a_n(x,0)\epsilon^n \\ &=\; \mathrm{e}^{\mathrm{i}k_0 x/\epsilon} f(x-x_0) + c^{-1/2}(x)c_2^{-1/2}(0) \sum_{n=1}^{\infty} \mathcal{T}_n(x)\epsilon^n. \end{aligned} \tag{3.44}$$

Therefore, matching (3.43) and (3.44) at each order of ϵ gives

$$\mathcal{T}_n(x) \;=\; a_n(x,0) \;=\; 0, \quad \forall\, n \geq 1, \tag{3.45}$$

via the uniqueness of particular asymptotic sequences, see [29]. Hence, we only consider the particular integral at each level of the recurrence relation (3.21):

$$\hat{a}_n(x,t) \;=\; \mathrm{i}\frac{\int_0^t \zeta_{n-1}(x(t'),t')dt'}{2k_0 c_1\left(\xi_-\right)}.$$

Thus, there is no Stokes phenomena at $t = 0$ as

$$a_n(x,0) = 0, \quad \forall\, n > 0.$$

Behaviour of $a_n(x,t)$ near a Turning Point

A more convenient form in which to phrase (3.21), and consequently (3.19), is to make the substitution

$$\hat{a}_n = c_1^{1/2}(\xi_-)c_2^{1/2}(0)f(\xi_- - x_0)\tilde{a}_n. \tag{3.46}$$

Therefore, connecting (3.46), (3.20) and (3.18), it follows that

$$\tilde{a}_0 \;=\; 1 \tag{3.47}$$

and

$$2\mathrm{i}k_0 c_1\left(\xi_-\right)\frac{d\tilde{a}_{n+1}}{ds_-} \;=\; c_1(x)c_2(t)\partial_x\left(c_1(x)\partial_x(\tilde{a}_n)\right) - \partial_t\left(\frac{\partial_t(\tilde{a}_n)}{c_2(t)}\right) - c_1(x)Q(x,t)\tilde{a}_n - W(\xi_-)\frac{d\tilde{a}_n}{ds_-}, \tag{3.48}$$

with,

$$W(\xi_-) \;=\; c_1'(\xi_-) + 2c_1(\xi_-)\frac{f'(\xi_- - x_0)}{f(\xi_- - x_0)}. \tag{3.49}$$

To expedite the recovery of (3.48) it is worth noting that

$$\begin{gathered} \partial_x\xi_- = \frac{c_1(\xi_-)}{c_1(x)}, \quad \partial_t\xi_- = c_2(t)c_1(\xi_-) \\ \text{and} \quad c_1(x)\partial_x L = \frac{\partial_t L}{c_2(t)}, \quad \text{where} \quad L = \sqrt{c_1(\xi_-)c_2(0)}f(\xi_- - x_0). \end{gathered}$$

We use (3.48) to inspect the behaviour of the a_n coefficients near the turning points x_* and t_*, respectively. Recall from (2.22) and (2.48), the behaviour of the spatial and temporal wave speeds near the turning points are:

$$c_1(x) \;\sim\; \gamma\exp\left(-\mathrm{i}\pi\alpha_1/2\right)(x-x_*)^{-\alpha_1}, \qquad x \to x_*, \tag{3.50}$$

$$\text{and} \quad c_2(t) \;\sim\; \sigma\exp\left(\mathrm{i}\pi\alpha_2/2\right)(t-t_*)^{\alpha_2}, \qquad t \to t_*, \tag{3.51}$$

where $\gamma, \sigma \in \mathbb{R} > 0$ and $\alpha_1, \alpha_2 \in (-1, 0) \cup (0, \infty)$. Hence, (3.50) and (3.51), near the turning points are:

$$Q_1 \sim \mathrm{i}^{-\alpha_1}\gamma\frac{\alpha_1}{4}(3\alpha_1+2)(x-x_*)^{-(\alpha_1+2)}, \qquad x \to x_*, \tag{3.52}$$

$$\text{and} \quad Q_2 \sim -\mathrm{i}^{-\alpha_2}\frac{\alpha_2}{4\sigma}(\alpha_2+2)(t-t_*)^{-(\alpha_2+2)}, \qquad t \to t_*. \tag{3.53}$$

$\tilde{a}_1$ in (3.48), using (3.47), is

$$\begin{aligned}\tilde{a}_1 &= \frac{\mathrm{i}}{2}\frac{\int c_1(x(s_-))Q ds_-}{k_0 c_1(\xi_-)} \\ &= -\frac{\mathrm{i}}{2}\frac{\int^t Q_2(t')dt' + \int^x Q_1(x')dx'}{k_0 c_1(\xi_-)}.\end{aligned} \tag{3.54}$$

Hence, with (3.52) and (3.53), it is clear that:

$$\tilde{a}_1 \sim \mathrm{i}\frac{\gamma\alpha_1}{8k_0}\frac{\exp(-\mathrm{i}\pi\alpha_1/2)}{c_1(\xi_-(x_*,t))}\frac{(3\alpha_1+2)}{(\alpha_1+1)}(x-x_*)^{-(\alpha_1+1)}, \qquad x \to x_* \tag{3.55}$$

$$\text{and} \quad \tilde{a}_1 \sim -\frac{\mathrm{i}\alpha_2}{8k_0\sigma}\frac{\exp(-\mathrm{i}\pi\alpha_2/2)}{c_1(\xi_-(x,t_*))}\frac{(\alpha_2+2)}{(\alpha_2+1)}(t-t_*)^{-(\alpha_2+1)}, \qquad t \to t_*. \tag{3.56}$$

We do not allow for the possibility of an additional Stokes phenomenon due to

$$c_1(\xi_-(x,t_*)) \to 0 \quad \Longleftrightarrow \quad x_z = g_1^{-1}(g_1(x)+g_2(t_*)) : \quad x \in \mathbb{R}, \tag{3.57}$$

where x_z is a root of $c_1(x)$. Note that the functions $g_1(x)$ and $g_2(t)$ in (3.7) are bijective, from the definition of the functions $c_1(x)$ and $c_2(t)$ in §2.1, and hence invertible. Hence the function $c_1(\xi_-)$ is regular when $t > 0$. From (3.4), it is noted that

$$k_0 c_1(\xi_-)\frac{d}{ds_-}(\tilde{a}_n) = \frac{d}{ds_-}(k_0 c_1(\xi_-)\tilde{a}_n).$$

Therefore, any temporal or spatial dependence that the leading order term of $a_n(x,t)$ near x_* or t_* may have, appears as a multiplicative pre-factor. Given this, and motivated by (3.55), we trial:

$$\tilde{a}_n(x,t) \sim d_n\frac{(k_0 c_1(\xi_-(x_*,t)))^{-n}}{(x-x_*)^{n(\alpha_1+1)}}, \qquad t > 0,\ x \to x_*, \tag{3.58}$$

$$\text{and} \quad \tilde{a}_n(x,t) \sim e_n\frac{(k_0 c_1(\xi_-(x,t_*)))^{-n}}{(t-t_*)^{n(\alpha_2+1)}}, \qquad x \in \mathbb{R},\ t \to t_*, \tag{3.59}$$

Eq. (3.58) and (3.59) hold by induction and d_n and e_n are constants with

$$d_0 = e_0 = 1, \tag{3.60}$$

on applying (3.47). The fact that the recurrence relation (3.48) is more convenient than its parent form(s) is a product of the succinct (3.47) and that the object $W(\xi_-)\frac{d\tilde{a}_n}{ds_-}$ is expected to be a lower order term, than the other terms as a transition point is approached. We now investigate whether or not this assumption holds. Near the turning points, using (3.58) and (3.59), it follows that

$$\begin{aligned}2\int W(\xi_-)\frac{d\tilde{a}_n}{ds_-}ds_- = 2W(\xi_-)\tilde{a}_n &\sim \begin{cases} W_1(x-x_*)^{-n(\alpha_1+1)}, & x \to x_*, \\ W_2(t-t_*)^{-n(\alpha_2+1)}, & t \to t_*, \end{cases} \\ &< a_{n+1}(x,t).\end{aligned} \tag{3.61}$$

Both $|W_1|, |W_2| < \infty$. Hence, approaching either of the turning points (3.61) is lower order than the other terms in (3.48). Therefore, local to x_* and t_*, (3.48) is

$$\tilde{a}_{n+1} \sim \frac{\mathrm{i}}{2}\left(k_0 c_1\left(\xi_-\right)\right)^{-1} \int \left(\partial_x\left(c_1(x)\partial_x(\tilde{a}_n)\right) - Q_1(x)\tilde{a}_n\right) dx + \text{l.o.t.} \quad x \approx x_*, \tag{3.62}$$

$$\text{and} \quad \tilde{a}_{n+1} \sim \frac{\mathrm{i}}{2}\left(k_0 c_1\left(\xi_-\right)\right)^{-1} \int \left(\partial_t\left(\frac{\partial_t\left(\tilde{a}_n\right)}{c_2(t)}\right) - Q_2(t)\tilde{a}_n\right) dt + \text{l.o.t.} \qquad t \approx t_*. \tag{3.63}$$

Using (3.50)–(3.53), it follows that

$$\begin{aligned}
&\int \left(\partial_x\left(c_1(x)\partial_x(\tilde{a}_n)\right) - Q_1\tilde{a}_n\right) dx \\
&\sim -\frac{d_n\gamma \mathrm{i}^{-\alpha_1}}{\left(k_0 c_1\big(\xi_-(x_*,t)\big)\right)^n} \frac{(\alpha_1+1)}{(n+1)} \left(n - \frac{\alpha_1}{2(\alpha_1+1)}\right)\left(n + \frac{3\alpha_1+2}{2(\alpha_1+1)}\right)(x-x_i)^{-(n+1)(\alpha_1+1)}.
\end{aligned} \tag{3.64}$$

Utilising the reflection formula (2.71) and the identities in (3.60), we connect (3.64) with (3.58), which leads to

$$\begin{aligned}
d_n &= -d_{n-1}\mathrm{i}^{1-\alpha_1}\frac{\gamma}{2}\frac{(\alpha_1+1)}{n}\left(n-1-\frac{\alpha_1}{2(\alpha_1+1)}\right)\left(n-1+\frac{3\alpha_1+2}{2(\alpha_1+1)}\right) \\
&= (-)^n P_1^n \frac{\cos(\nu_1\pi)}{\pi\Gamma(n)}\Gamma\left(n-\nu_1+\frac{1}{2}\right)\Gamma\left(n+\nu_1+\frac{1}{2}\right),
\end{aligned} \tag{3.65}$$

where,

$$\nu_1 = \frac{2\alpha_1+1}{2(\alpha_1+1)} \quad \text{and} \quad \nu_2 = \frac{2\alpha_2+1}{2(\alpha_2+1)}, \tag{3.66}$$

from (2.50). Similarly,

$$\begin{aligned}
&\int \left(\partial_t\left(c_2^{-1}(t)\partial_t\tilde{a}_n\right) - Q_2(t)\tilde{a}_n\right) dt \\
&\sim -\frac{e_n}{\sigma}\frac{\mathrm{i}^{-\alpha_2}}{\left(k_0 c_1\big(\xi_-(x,t_*)\big)\right)^n}\frac{(\alpha_2+1)}{(n+1)}\left(n+\frac{\alpha_2}{2(\alpha_2+1)}\right)\left(n+\frac{\alpha_2+2}{2(\alpha_2+1)}\right)(t-t_{zi})^{-(n+1)(\alpha_2+1)}.
\end{aligned}$$

Following the same process which led to (3.65), leads to:

$$e_n = (-)^{n+1}P_2^n\frac{\cos(\nu_2\pi)}{\pi\Gamma(n)}\Gamma\left(n+\nu_2-\frac{1}{2}\right)\Gamma\left(n-\nu_2+\frac{3}{2}\right). \tag{3.67}$$

In (3.65) and (3.67), we have used

$$P_1 = \frac{\gamma}{2}(\alpha_1+1)\mathrm{i}^{1-\alpha_1} \quad \text{and} \quad P_2 = \frac{(\alpha_2+1)}{2\sigma}\mathrm{i}^{1-\alpha_2}. \tag{3.68}$$

Recalling (2.72), then as $n \to \infty$

$$\tilde{a}_n(x,t) \sim \frac{\Gamma(n)}{\pi}\begin{cases}\left(\frac{-P_1}{k_0 c_1\left(\xi_-(x_*,t)\right)}\right)^n \cos(\nu_1\pi)(x-x_*)^{-n(\alpha_1+1)}, & x \approx x_*, t \in \mathbb{R} > 0, \\ -\left(\frac{-P_2}{k_0 c_1\left(\xi_-(x,t_*)\right)}\right)^n \cos(\nu_2\pi)(t-t_*)^{-n(\alpha_2+1)}, & t \approx t_*,\ x \in \mathbb{R}.\end{cases} \tag{3.69}$$

Combining (3.20) and (3.46), gives

$$a_n(x,t) = c_1^{-1/2}(x)c_2^{-1/2}(t)c_1^{1/2}(\xi_-)c_2^{1/2}(0)f(\xi_- - x_0)\tilde{a}_n,$$

hence, as $n \to \infty$,

$$a_n(x,t) \sim \Gamma(n) \begin{cases} \Delta_1 \left(\frac{-P_1}{k_0 c_1\left(\xi_-(x_*,t)\right)} \right)^n \cos(\nu_1 \pi)(x-x_*)^{-n(\alpha_1+1)+\alpha_1/2}, & x \approx x_*, t \in \mathbb{R} > 0, \\ \Delta_2 \left(\frac{-P_2}{k_0 c_1\left(\xi_-(x,t_*)\right)} \right)^n \cos(\nu_2 \pi)(t-t_*)^{-n(\alpha_2+1)-\alpha_2/2}, & t \approx t_*, \, x \in \mathbb{R}, \end{cases} \tag{3.70}$$

where,

$$\begin{aligned} \Delta_1 &= \frac{\mathrm{i}^{\alpha_1/2}}{\pi\sqrt{\gamma}} c_2^{-1/2}(t) \mathcal{F}_-(\xi_-(x_*,t)), \\ \Delta_2 &= -\frac{\mathrm{i}^{-\alpha_2/2}}{\pi\sqrt{\sigma}} c_1^{-1/2}(x) \mathcal{F}_-(\xi_-(x,t_*)), \\ \text{and} \quad \mathcal{F}_-(\xi_-) &= c^{1/2}(\xi_-,0) f(\xi_- - x_0), \end{aligned}$$

using (3.17).

3.2.4 $b_{j0}(x,t)$ and the Stokes multiplier

The objects denoted (ii) in (3.28) are of the same form as the object pre-factored by $B(\epsilon)$ in (3.1). Hence, the preliminary results of (3.17) and (3.19) apply and using the notation given in (3.23)

$$b_{j0}(x,t) = c^{-1/2}(x,t) \mathcal{F}_j\left(\xi_+(x,t)\right). \tag{3.71}$$

Recall from (3.32), that

$$a_n(x,t) \sim \sum_{j=1}^{2} \frac{K_j(\epsilon)}{2\pi\mathrm{i}} b_{j0}(x,t) \frac{\Gamma(n+\mu)}{(\chi_j)^{n+\mu}} \epsilon^\mu, \quad n \to \infty,$$

which, on inspecting the behaviour of (the late terms of) $a_n(x,t)$ near (2.4), is used to determine the unknown functions $K_j(\epsilon)$ and $\mathcal{F}_j(x)$.

Local to the transition points, the χ_j's are

$$\begin{aligned} \chi_1 &\sim \frac{2k_0 \mathrm{i}^{\alpha_1+1}}{\gamma} c_1 \left(\frac{\mathcal{D}_1\left(\xi_+(x_*,t)\right)}{k_0} \right) \frac{(x-x_*)}{\alpha_1+1}^{\alpha_1+1} \\ &= -\frac{k_0}{P_1} c_1 \left(\frac{\mathcal{D}_1\left(\xi_+(x_*,t)\right)}{k_0} \right) (x-x_*)^{\alpha_1+1}, \quad x \to x_*, \end{aligned} \tag{3.72}$$

$$\begin{aligned} \text{and} \quad \chi_2 &\sim 2\sigma k_0 \mathrm{i}^{\alpha_2+1} c_1 \left(\frac{\mathcal{D}_2\left(\xi_+(x,t_*)\right)}{k_0} \right) \frac{(t-t_*)}{\alpha_2+1}^{\alpha_2+1} \\ &= -\frac{k_0}{P_2} c_1 \left(\frac{\mathcal{D}_2\left(\xi_+(x,t_*)\right)}{k_0} \right) (t-t_*)^{\alpha_2+1}, \quad t \to t_*, \end{aligned} \tag{3.73}$$

having used (3.68), (3.34), (3.36) and (3.37). It is clear then, on comparing (3.70) with (3.71), (3.72) and (3.73) that

$$\mu = 0,$$

in (3.32). Thus, to leading order, the r.h.s. of (3.32) is

$$\begin{aligned} \frac{K_1(\epsilon)}{2\pi\mathrm{i}} b_{10}(x,t) \frac{\Gamma(n+\mu)}{(\chi_1)^{n+\mu}} &\sim \frac{\mathrm{i}^{\alpha_1/2}}{\sqrt{\gamma}} \frac{K_1(\epsilon)}{2\pi\mathrm{i}} \Gamma(n) c_2^{-1/2}(t) \mathcal{F}_1\left(\xi_+(x_*,t)\right) \\ \times \left(\frac{-P_1}{\left(k_0 c_1 \left(\frac{\mathcal{D}_1(t,x_*)}{k_0} \right) \right)} \right)^n &(x-x_*)^{-n(\alpha_1+1)+\alpha_1/2}, \qquad x \to x_*, \, t \in \mathbb{R} > 0, \end{aligned} \tag{3.74}$$

having replaced $b_{10}(x,t)$ with (3.71). Using (3.6) and (3.36), it follows that

$$\xi_-(x_*,t) = \mathcal{D}_1\left(x_*,t\right)/k_{_0}.$$

We therefore connect (3.74) with the appropriate term in (3.70) via the resurgence relation (3.32), which yields

$$2\mathrm{i}\cos(\nu_1\pi)\mathcal{F}_-(\xi_-(x_*,t)) \sim K_1(\epsilon)\mathcal{F}_1\left(\xi_+(x_*,t)\right).$$

Recall that $\xi_-(x,t) = g_1^{-1}\big(g_1(x)+g_2(t)\big)$, from (3.23), then w.l.g we set

$$K_1(\epsilon) \sim 2\mathrm{i}\cos(\nu_1\pi) : \quad \alpha_1 \notin -1+\frac{1}{2\mathbb{N}+1}. \tag{3.75}$$

Therefore, $\mathcal{F}_-\left(\xi_-(x_*,t)\right) = \mathcal{F}_1\left(\xi_+(x_*,t)\right)$ from which it is deduced that

$$\mathcal{F}_1(\xi_+(x,t)) = \mathcal{F}_-\left(\frac{\mathcal{D}_1(\xi_+)}{k_{_0}}\right). \tag{3.76}$$

Similarly, as $t\to t_*$ the rhs of (3.32) is

$$\begin{aligned}
&-\frac{K_2(\epsilon)}{2\pi\mathrm{i}}b_{20}(x,t)\frac{\Gamma(n)}{(\chi_2)^n} \sim -\frac{\mathrm{i}^{-\alpha_2/2}}{\sqrt{\sigma}}\frac{K_2(\epsilon)}{2\pi\mathrm{i}}\Gamma(n)c_1^{-1/2}(x)\mathcal{F}_2\big(\xi_+(x,t_*)\big)\\
&\times\left(\frac{-P_2}{\left(k_{_0}c_1\left(\frac{\mathcal{D}_2(t_*,x)}{k_{_0}}\right)\right)}\right)^n (t-t_*)^{-(n+\mu)(\alpha_2+1)-\alpha_2/2}, \qquad t\to t_*,\ x\in\mathbb{R},
\end{aligned} \tag{3.77}$$

and following the same technique which led to (3.76) and (3.75), leads to:

$$\begin{aligned}
\mathcal{F}_2(\xi_+) &= \mathcal{F}_-\left(\frac{\mathcal{D}_2(\xi_+)}{k_{_0}}\right)\\
\text{and}\quad K_2(\epsilon) &\sim 2\mathrm{i}\cos(\nu_2\pi) : \quad \alpha_2 \neq -1+\frac{1}{2\mathbb{N}+1}.
\end{aligned} \tag{3.78}$$

Hence,

$$b_{j0}(x,t) = c^{-1/2}(x,t)c^{1/2}\left(\frac{\mathcal{D}_j(\xi_+)}{k_{_0}},0\right) f\left(\frac{\mathcal{D}_j(\xi_+)}{k_{_0}}-x_0\right), \tag{3.79}$$

in (3.23). Therefore, the form of the reflected wave packet in (2.1) associated with a spatial turning point is

$$h_{\mathrm{ref}}(x,t) \sim 2\cos(\nu_1\pi)c^{-1/2}(x,t)c^{1/2}\left(\frac{\mathcal{D}_1(\xi_+)}{k_{_0}},0\right) f\left(\frac{\mathcal{D}_1(\xi_+)}{k_{_0}}-x_0\right)\mathrm{e}^{\mathrm{i}\mathcal{D}_1(\xi_+)/\epsilon},$$

where $c(x,t)=c_1(x)c_2(t)$ and $\mathcal{D}_1(\xi_+)$ was given in (3.36).

Stokes multipliers in a symmetric wave speed setup

Maintaining the nomenclature of (3.39), the Stokes multipliers associated with a symmetric wave speed profile, when $\alpha_l \neq -1+\frac{1}{2\mathbb{N}+1}$, are:

$$\begin{aligned}
K_{1l}(\epsilon) &\sim (-)^{l+1}2\mathrm{i}\cos(\nu_1\pi),\\
\text{and}\quad K_{2l}(\epsilon) &\sim (-)^{l+1}2\mathrm{i}\cos(\nu_2\pi).
\end{aligned} \tag{3.80}$$

The terms in (3.80) should be compared with (2.50), where it is noted that: the Stokes multipliers associated with the solutions of (2.1), in the separable wave speed setup, are the same as there respective Stokes multipliers associated with the canonical ODE's in (2.7) and (2.47).

An important detail to note is: with $x_0>0$ in (2.2) the reflected wave exists as $x\to\infty$. In

this situation one must consider the 'initial' solution crossing a Stokes line in a positive sense. To this end a positive $K_j(\epsilon)$ was chosen in (3.32). Thus, a subtle difference between the Stokes multipliers in (2.50) and (3.80) is spotted. That is, in the ODE analysis we were concerned with finding the reflected wave as $x \to -\infty$ and thus a negative sign pre-factored $K(\epsilon)$ in (2.62).

3.2.5 General solution

Connecting (3.23) with (3.36), (3.37), (3.76), (3.75) and (3.78), the solutions of (2.1) are:

$$\boxed{h(x,t) \sim c^{-1/2}(x,t)\left(\mathrm{e}^{\mathrm{i}k_0\xi_-/\epsilon}\mathcal{F}_-\left(\xi_-\right) \overset{+}{\sim} \sum_{j=1}^{2} 2\mathrm{i}\cos(\nu_j\pi)\mathrm{e}^{\mathrm{i}\mathcal{D}_j(\xi_+)/\epsilon}\mathcal{F}_-\left(\frac{\mathcal{D}_j(\xi_+)}{k_0}\right)\right)} \tag{3.81}$$

where $\mathcal{F}_-(x) = c^{1/2}(x,0)f(x-x_0)$.

Eq. (3.81) is the main result of this thesis. The result is unexpected in a number of ways. Firstly, the object $\mathrm{e}^{\mathrm{i}\mathcal{D}_j(\xi_+)/\epsilon}$ cannot be expressed in such a way as to have an exponentially small pre-factor function of ϵ, e.g.

$$\mathrm{e}^{\mathrm{i}\mathcal{D}_j(\xi_+)/\epsilon} \neq \mathrm{e}^{-\beta/\epsilon}\mathrm{e}^{\mathrm{i}\psi(x,t)/\epsilon},$$

where $\psi(x,t)$ is real for real x and t and $\mathrm{e}^{-\beta/\epsilon}$ is exponentially small. This detail might have been anticipated from the results of the ODE's (2.7) and (2.47). In fact, in (3.81) it is the non-trivial object $\mathrm{e}^{\mathrm{i}\mathcal{D}_j(\xi_+)/\epsilon}$ that captures the 'beyond all orders' behaviour of a subdominant solution. A second interesting feature of the result is the existence of a complex argument in the initial function $f(x-x_0)$, i.e.

$$f\left(\frac{\mathcal{D}_j(\xi_+)}{k_0} - x_0\right),$$

in (3.23), which acts to translate the location of the centre of the reflected away from the naive assumption (deduced via the characteristic parameter ξ_+ in (3.6)) that the reflected wave is centred around $g_1(x) + g_2(t) = g_1(x_0)$, for some time $t > 0$.

3.3 Integral transform along the characteristic curve

In the following section we present details of an integral transform that expedites the procedure of finding the form of the reflected waves in (3.81). The transform relates the solutions of (2.1) to that of (2.7) and (2.47) so that much of the important information, like the Stokes lines and Stokes multipliers, is inherited directly from the results of the canonical ODE's (2.7) and (2.47).

We begin by assuming a geometric optics ansatz, see [11], as the 'initial' solution form of (2.1)

$$\begin{aligned} h(x,t) &= c^{-1/2}(x,t)\hat{h}(x,t,\omega)\mathrm{e}^{\mathrm{i}\omega\lambda(x,t)}, \quad \omega \in \mathbb{R}, \\ \text{where} \quad \lambda(x,t) &= g_1(x) + g_2(t), \end{aligned} \tag{3.82}$$

with $g_1(x)$ and $g_2(t)$ given in (3.7), and $\lambda(x,t)$ satisfies the eikonal equation. The pre-factor $c^{-1/2}(x,t)$ is taken a posteriori from (3.17). Let $c_2(t) = 1$, then (3.82) returns the Fourier modes in (2.6). Similarly, $c_1(x) = 1$ returns (2.46). At $t = 0$ we connect (3.82) with (2.2), which reveals that

$$\omega = \mathcal{O}(1/\epsilon). \tag{3.83}$$

Hence, $|\omega| \gg 1$ is considered the large parameter in the following analysis. We expect and confirm that $\hat{h}(x,t,\omega)$ is a localised function of ω owing to $f(x-x_0)$ in (2.2). The equation linking ω and ϵ is a dispersion relation associated with (2.1) and discussed latterly. Summing

across all possible ω, the solution of (2.7) is written as

$$h(x,t) \;=\; c^{-1/2}(x,t)\int_{-\infty}^{\infty}\hat{h}(x,t,\omega)\mathrm{e}^{\mathrm{i}\omega\lambda(x,t)}d\omega. \tag{3.84}$$

Eq(3.84) is regarded as the integral transform along the characteristic parameter, $\xi_-(x,t)$, of $h(x,t)$, in (2.1). Placing (3.84) into the r.h.s. and l.h.s. of (2.1), gives:

$$\begin{aligned}
c^2(x,t)h_x \;&=\; c_1^{1/2}c_2^{3/2}\int_{-\infty}^{\infty}\left(\left(\mathrm{i}\omega-\frac{1}{2}c_1'\right)\hat{h}+c_1\hat{h}_x\right)\mathrm{e}^{\mathrm{i}\omega\lambda(x,t)}d\omega,\\
\left(c^2(x,t)h_x\right)_x \;&=\; c_1^{-1/2}c_2^{3/2}\int_{-\infty}^{\infty}\left(-\omega^2\hat{h}+2\mathrm{i}\omega c_1\hat{h}_x+c_1\left(c_1\hat{h}_x\right)_x-c_1Q_1\hat{h}\right)\mathrm{e}^{\mathrm{i}\omega\lambda(x,t)}d\omega,\\
\text{and}\quad h_{tt} \;&=\; c_1^{-1/2}c_2^{3/2}\int_{-\infty}^{\infty}\left(-\omega^2\hat{h}+2\mathrm{i}\omega c_2^{-1}\hat{h}_t+c_2^{-1}\left(c_2^{-1}\hat{h}_t\right)_t+c_2^{-1}Q_2\hat{h}\right)\mathrm{e}^{\mathrm{i}\omega\lambda(x,t)}d\omega.
\end{aligned} \tag{3.85}$$

The prime denotes differentiation w.r.t. the dependent variable and, $Q_1(x)$ and $Q_2(t)$ were shown in (3.22). Hence, (2.1),

$$h_{tt}-\left(c^2(x,t)h_x\right)_x=0,$$

becomes

$$\begin{aligned}
&c_1^{-1/2}c_2^{3/2}\int_{-\infty}^{\infty}\mathcal{L}(x,t,\omega)\mathrm{e}^{\mathrm{i}\omega\lambda(x,t)}d\omega \;=\; 0,\\
\text{where}\quad &\mathcal{L}(x,t,\omega) \;=\; 2\mathrm{i}\omega c_2^{-1}\left(\hat{h}_t-c_1c_2\hat{h}_x\right)+c_2^{-1}\left\{\left(c_2^{-1}\hat{h}_t\right)_t-c_1c_2\left(c_1\hat{h}_x\right)_x\right\}+\frac{c_1}{c_2}Q(x,t)\hat{h},
\end{aligned} \tag{3.86}$$

with $Q(x,t)$ given in (3.22). We focus on ω positive and aim to solve $\mathcal{L}(x,t,\omega)=0$ for each ω fixed and large. The case where ω is negative is approached similarly. That is, we aim to find an asymptotic approximation to

$$2\mathrm{i}\omega\left(\hat{h}_t-c_1c_2\hat{h}_x\right)+\left\{\left(c_2^{-1}\hat{h}_t\right)_t-c_1c_2\left(c_1\hat{h}_x\right)_x\right\}+c_1Q(x,t)\hat{h} \;=\; 0. \tag{3.87}$$

At first sight, (3.87) appears significantly more complicated than (2.1). However, (3.87) can be approached in the standard way by employing the ansatz

$$\hat{h}(x,t,\omega) \;\sim\; \hat{A}(\omega)\sum_{n=0}^{\infty}\hat{a}_n(x,t)\omega^{-n},\quad \omega\to\infty. \tag{3.88}$$

Recall from (3.3) that

$$\frac{d}{ds_-}=\partial_t-c_1(x)c_2(t)\partial_x\quad\text{and}\quad\frac{d}{ds_+}=\partial_t+c_1(x)c_2(t)\partial_x.$$

Then (3.87) at $\mathcal{O}(\omega)$ is:

$$\begin{aligned}
\partial_t\hat{a}_0-c_1c_2\partial_x\hat{a}_0 \;&=\; \frac{d\hat{a}_0}{ds_-} \;=\; 0.\\
\Longrightarrow\qquad \hat{a}_0(x,t) \;&=\; \mathcal{H}(\lambda(x,t)).
\end{aligned} \tag{3.89}$$

The unknown function $\mathcal{H}$ is determined by applying (2.2). In general, each $\hat{a}_n(x,t)$ in (3.88) is found via the recurrence relation:

$$2\mathrm{i}\frac{d}{ds_-}\hat{a}_{n+1} \;=\; c_1c_2\left(c_1\partial_x\hat{a}_n\right)_x-\left(\frac{\partial_t\hat{a}_n}{c_2}\right)_t-c_1Q(x,t)\hat{a}_n. \tag{3.90}$$

Noting (3.22) and (3.50)-(3.53), it is evident that the singular points of $\hat{a}_n(x,t)$ (and thus

turning points of (2.1)) are the points x_* and t_* in (2.4).

3.3.1 Resurgent analysis and benefits of the integral transform

We apply R-A to the PDE (3.87) and immediately note the benefits of using the transform (3.84): comparing (3.90) with (3.21) it is apparent that approaching the problem of finding solutions to (2.1) via the integral transform (3.84) the difficulties surrounding the regions of holomorphicity of the function $c_1\big(\xi_-(x,t)\big)$, which necessarily appears in (3.21), are bypassed. It was the presence of $c_1\big(\xi_-(x,t)\big)$ which induced a time or spatial dependance to the behaviour of the coefficients, $a_n(x,t)$, in (3.23) as the points at x_* or t_* were approached, see (3.70). The up-shot is: as $x \to x_*$ the recurrence relation (3.90) to leading order is the same as the recurrence relation associated with the canonical ODE's (2.7), e.g.

$$\begin{aligned}
\text{eq. (3.90)}: \quad & 2\mathrm{i}\frac{\partial}{\partial x}\hat{a}_{n+1}(x,t) \sim \left(\frac{(c_1'(x))^2}{4c_1(x)} + c_1''(x)/2)\right)\hat{a}_n(x,t) - \left(c_1\partial_x\hat{a}_n(x,t)\right)_x, \quad x \to x_*, \\
\text{eq. (2.57)}: \quad & 2\mathrm{i}\frac{d}{dx}a_{n+1}(x) = \left(\frac{(c_1')^2}{4c_1} + c_1''/2\right)a_n(x) - \left(c_1 a_n'(x)\right)', \quad x \to x_*.
\end{aligned} \tag{3.91}$$

The situation is similar for (3.90) and (2.78) as $t \to t_*$. The similitude of the two terms in (3.91) motivates the ansatz in (2.67), i.e.

$$\begin{aligned}
\hat{a}_n(x,t) &\sim \hat{d}_n(x-x_*)^{-n(\alpha_1+1)} : && x \to x_*, \\
\hat{a}_n(x,t) &\sim \hat{e}_n(t-t_*)^{-n(\alpha_2+1)} : && t \to t_*,
\end{aligned}$$

where the $\hat{d}_n$ and $\hat{e}_n$ are constant. Hence, as $x \to x_*$ (or $t \to t_*$) the two terms in (3.91) are the same. Whence, details from §(2.4) in chapter are repeated. Therefore, we state the relevant results of (2.73):

$$\begin{aligned}
\hat{a}_n(x,t) &\sim \hat{d}_0(-)^n\frac{\Gamma(n)}{\pi}(P_1)^n\cos(\nu_1\pi)(x-x_*)^{-n(\alpha_1+1)}, && x \to x_*, t \in \mathbb{R} > 0, \\
\text{and similarly} \quad \hat{a}_n(x,t) &\sim \hat{e}_0(-)^{n+1}\frac{\Gamma(n)}{\pi}(P_2)^n\cos(\nu_2\pi)(t-t_*)^{-n(\alpha_2+1)}, && t \to t_*, x \in \mathbb{R},
\end{aligned} \tag{3.92}$$

where P_1 and P_2 where given in (3.68).

Finding $\hat{a}_0(x,t)$ and the Fourier transform in (3.84)

From (3.84), (3.88) and (3.89):

$$h(x,t) = c_1^{-1/2}(x)c_2^{-1/2}(t)\mathcal{H}(g_1(x)+g_2(t))\int_{-\infty}^{\infty}\hat{A}(\omega)\mathrm{e}^{\mathrm{i}\omega\lambda(x,t)}d\omega + \text{l.o.t.}$$

and it is assumed that

$$A(z) = \int_{-\infty}^{\infty}\hat{A}(\omega)\mathrm{e}^{\mathrm{i}\omega z}d\omega. \tag{3.93}$$

Eq. (3.93) is verified in due course. Then, with (3.93) and applying (2.2) gives

$$\begin{aligned}
h(x,0) &\sim c_1^{-1/2}(x)c_2^{-1/2}(0)\mathcal{H}(g_1(x))\int_{-\infty}^{\infty}\tilde{A}(\omega)\mathrm{e}^{\mathrm{i}\omega g_1(x)}d\omega \\
&= c_1^{-1/2}(x)c_2^{-1/2}(0)\mathcal{H}\left(g_1(x)\right)A\left(g_1(x)\right) \\
&= f(x-x_0)\mathrm{e}^{\mathrm{i}k_0 x/\epsilon}.
\end{aligned}$$

We absorb the arbitrary function $\mathcal{H}(g_1(x))$ into $A(g_1(x))$ by letting $\mathcal{H}(x)A(x) = \hat{A}(x)$ and immediately dropping the hat. Therefore,

$$A(z) \;=\; c_1^{1/2}\big(g_1^{-1}(z)\big)c_2^{1/2}(0)f\big(g_1^{-1}(z)-x_0\big)\mathrm{e}^{\mathrm{i}k_0\, g^{-1}(z)/\epsilon}. \tag{3.94}$$

Hence, w.l.g we set

$$\hat{a}_0(x,t) \;=\; 1, \tag{3.95}$$

and therefore $\hat{d}_0 = \hat{e}_0 = 1$ in (3.92). With $A(z)$ given by (3.94), it follows that

$$\hat{A}(\omega) \;= 2\pi \int_{-\infty}^{\infty} \frac{A(g_1(x))}{c_1(x)}\mathrm{e}^{-\mathrm{i}g_1(x)\omega}dx \;=\; 2\pi c_2^{1/2}(0)\int_{-\infty}^{\infty} c_1^{-1/2}(x)f(x-x_0)\mathrm{e}^{\mathrm{i}\left(k_0\, x/\epsilon - g_1(x)\omega\right)}dx, \tag{3.96}$$

having used

$$dg_1(x) \;=\; \frac{dx}{c_1(x)}.$$

The dominant contributions of the integral in (3.96) come from the regions where the rapidly oscillating phase is stationary, i.e. when

$$\frac{d}{dx}\left(\frac{k_0 x}{\epsilon} - g_1(x)\omega\right) = 0 \qquad \Longrightarrow \qquad \omega = \frac{k_0}{\epsilon}c_1(x(\omega)). \tag{3.97}$$

Eq(3.97) justifies the proposal in (3.83). It is clear then, that the sign of ω depends on the sign of k_0 in (2.2). Hence, with $k_0 > 0$ in (2.2), focusing on ω positive is necessary. Evaluation of (3.96), with (3.97), gives

$$\hat{A}(\omega) \;\sim\; 2\pi f\left(x(\omega)-x_0\right)W(\omega), \tag{3.98}$$

where

$$W(\omega) = \mathrm{e}^{\mathrm{i}\pi/4}\sqrt{\frac{\pi c_1\big(x(\omega)\big)c_2(0)}{\omega c_1'\big(x(\omega)\big)}}\exp\left(\mathrm{i}\omega\left[\frac{x(\omega)}{c_1\big(x(\omega)\big)} - g_1\big(x(\omega)\big)\right]\right).$$

Eq(3.98) makes clear that $\hat{A}(\omega)$ is indeed a localised function and related to $f(x-x_0)$, as proposed in (3.88). Additionally, $\hat{A}(\omega) \leq \mathcal{O}(\epsilon)$ when $\big|x(\omega)-x_0\big| > \delta$, from (3.25). Hence, the dominant contributions of the integral in (3.84) are in the neighbourhood of $x(\omega) = x_0$, from (3.98) which highlights, once more, the notion of dominant solution rays (DSR), as discussed in §(3.1.1). We assume the above implies that

$$\hat{h}(x,t,\omega) \to 0 \quad \text{as} \quad \omega \to 0,$$

in (3.88).

One might be concerned by the presence of $c_1'\big(x(\omega)\big)$ in (3.98), however, according to [44], if $c_1'(x(\omega)) = 0$ then we take a 'higher order approximation' in the stationary phase approximation (as the integral is no longer related to a Gaussian integral). Ignoring this, the leading order initial solution to (2.1) is

$$\begin{aligned} h(x,t) \;&\sim\; c_1^{-1/2}(x)c_2^{-1/2}(t)\int_{-\infty}^{\infty}\hat{A}(\omega)\mathrm{e}^{\mathrm{i}\omega\lambda(x,t)}d\omega \\ &=\; c_1^{-1/2}(x)c_2^{-1/2}(t)c^{1/2}\big(\xi_-(x,t),0\big)f\big(\xi_-(x,t)-x_0\big)\mathrm{e}^{\mathrm{i}k_0\,\xi_-(x,t)/\epsilon}. \end{aligned} \tag{3.99}$$

Eq(3.99) is the leading order 'initial' solution to (2.1) and returns (3.27). It may appear that the derivation of (3.99) is somewhat more labour intensive than that of (3.23), however, the benefits are spotted immediately on inspecting the details of the subdominant solutions switched on by (3.84).

3.3.2 Subdominant Solutions

Upon crossing a Stokes line(s), the initial solution (3.99) switches on subdominant solution(s), due to the points at x_* and t_*, so that the solution of (2.1) is:

$$h(x,t) \sim c_1^{-1/2}(x)c_2^{-1/2}(t)\int_{-\infty}^{\infty}\hat{A}(\omega)\mathrm{e}^{\mathrm{i}\omega\lambda(x,t)}\left(\sum_{n=0}^{\infty}\hat{a}_n(x,t)\omega^{-n}\overset{+}{\sim}\sum_{j=1}^{2}K_j(\omega)\mathrm{e}^{-\omega\chi_j(x,t)}\sum_{m=0}^{\infty}\underbrace{b_{jm}(x,t)\omega^{-m+\mu}}_{(\star)}\right)d\omega. \tag{3.100}$$

Again, the $\overset{+}{\sim}$ symbol has been used to pre-factor solutions that are switch on after the dominant solution crosses a Stokes line. $j=1$ represents a solution switched on as a result of the spatial turning point, and $j=2$ a solution as a result of the temporal.

Phase of subdominant solutions

We now aim to find the form of the χ_j's in (3.100). Both objects inside the brackets of (3.100) must satisfy (3.87), hence, placing the subdominant objects into (3.87) at $\mathcal{O}\left(\omega^2\right)$ reads:

$$2\mathrm{i}c_2(t)\Big(\partial_t\chi_j - c_1(x)c_2(t)\partial_x\chi_j\Big) - \Big((\partial_t\chi_j)^2 - c_1(x)^2c_2(t)^2(\partial_x\chi_j)^2\Big) = 0, \tag{3.101}$$

$$\implies \qquad \Big(\partial_t\chi_j - c_1(x)c_2(t)\partial_x\chi_j\Big)\Big(\partial_t\chi_j + c_1(x)c_2(t)\partial_x\chi_j - 2\mathrm{i}c_2(t)\Big) = 0.$$

Therefore, either

$$\text{(i)} \quad \frac{d\chi_j}{ds_-} = 0 \quad \text{or} \quad \text{(ii)} \quad \frac{d\chi_j}{ds_+} = 2\mathrm{i}c_2(t). \tag{3.102}$$

Recalling (3.6) and (3.8), it follows that

$$\begin{aligned} \text{(i)} \quad \frac{d\chi_j}{ds_-} = 0 \qquad &\implies \qquad \chi_j(x,t) = \mathcal{G}_j(g_1(x) + g_2(t)), \\ \text{or} \quad \text{(ii)} \quad \frac{d\chi_j}{ds_+} = 2\mathrm{i}c_2(t) \qquad &\implies \qquad \chi_j(x,t) = \mathcal{H}_j(g_1(x) - g_2(t)) + 2\mathrm{i}g_2(t). \end{aligned} \tag{3.103}$$

The condition in (3.33) requires that:

$$\begin{aligned} \chi_1(x_*,t) &= 0, \qquad \forall t > 0, \\ \text{and} \quad \chi_2(x,t_*) &= 0, \qquad \forall x \in \mathbb{R}. \end{aligned} \tag{3.104}$$

Firstly, we considering χ_j to be of the form (i) in (3.103), then, with the addition of (3.104), we obtain

$$\begin{aligned} \mathcal{G}_1(Y) = 0, \quad Y(t) = g_2(t) - g_1(x_*), \\ \mathcal{G}_2(Z) = 0, \quad Z(t) = g_1(x) - g_2(t_*). \end{aligned}$$

The freedom in t and subsequently x implies that $\mathcal{G}_1 = \mathcal{G}_2 = 0$, which is not viable choice for the χ_j. Hence, $\chi_j(x,t)$ must follow (ii) in (3.103) and with (3.104), it is found that:

$$\begin{aligned} \mathcal{H}_1(Y) = Y - 2\mathrm{i}g_1(x_*), \quad Y(t) = g_1(x_*) - g_2(t). \\ \text{and} \quad \mathcal{H}_2(Z) = -2\mathrm{i}g_2(t_*), \quad Z(x) = g_1(x) - g_2(t_*). \end{aligned} \tag{3.105}$$

Therefore,

$$\chi_1(x,t) = 2\mathrm{i}\Big(g_1(x) - g_1(x_*)\Big), \tag{3.106}$$

$$\chi_2(x,t) = 2\mathrm{i}\Big(g_2(t) - g_2(t_*)\Big). \tag{3.107}$$

The form of $\chi_1(x,t)$ exactly matches that of $\mathrm{i}\chi(x)$ in (2.17). Thus, the condition in (2.19) naturally applies here,

$$\Re\{\mathrm{i}g_1(x_*)\} > 0 \quad \text{and} \quad \Re\{\mathrm{i}g_2(t_*)\} > 0,$$

and is required to verify that the $\mathrm{e}^{-\chi_j/\epsilon}$ are exponentially small. Note, a sign change of k_0 in (2.2) switches the sign of ω, from (3.97), and as ω is a pre-factor to χ_j, in (3.100), therefore, the turning point whose Stokes line crosses the real plane switches from x_* to $\bar{x}_*$ etc.

Active turning points and Stokes lines

We therefore conclude that: the details of §2.2.3 together with equation (2.22) and §2.2.4 are valid in the current problem. Hence, approaching the problem of (2.1) with (2.2) via (3.84), the information on Stokes lines and turning points are, in some sense, inherited. Therefore, in the symmetric wave speed setup there can only be one active turning point whose Stokes line crosses the real plane. See §2.2.4 and Figure 2.2 for an illustration. This is a major simplification as: in §3.2.2 no information on the Stokes lines could be deduced without specifying a $c_1(x)$ and $c_2(t)$ explicitly. Assuming a symmetrical (spatial) wave speed setup, it is confirmed numerically that: if the nearest spatial transition point to the real plane is a branch point singularity at $x = x_*$, a Stokes phenomenon is observed as the dominant solution crosses the Stokes line at $x = \Re\{x_*\}$. The situation is analogous for the transition point t_*. However, in general, $c_1(x)$ and $c_2(t)$ determine the shape of the Stokes curve.

3.3.3 $b_{j0}(x,t)$ and the Stokes multipliers

Placing the object marked $(\star)$ in (3.100) into (3.87), it follows that:

$$\frac{db_{j0}}{ds_+} = \partial_t b_{j0} + c_1(x)c_2(t)\partial_x b_{j0} = 0$$
$$\text{and} \quad 2\mathrm{i}\frac{d}{ds_2}b_{j(m+1)} = c_1c_2\left(c_1\partial_x b_{jm}\right)_x + \left(c_2^{-1}\partial_t b_{jm}\right)_t - c_1 Q(x,t) b_{jm}. \tag{3.108}$$

Therefore,

$$b_{j0}(x,t) \;=\; \mathcal{G}_j(g_1(x) - g_2(t)), \tag{3.109}$$

from (3.6) and (3.8). To determine the form of the arbitrary function $\mathcal{G}$ we employ the use of a resurgence relation similar to (3.32). It is noted from (3.92) that: as $x \to x_*$ and $t \to t_*$ the $\hat{a}_n(x,t)$ coefficients, $\hat{a}_n$ and $\hat{b}_n$, and phase χ_j have no temporal or spatial dependence, respectively. Therefore, on matching both sides of the resurgence relation requires that

$$\begin{aligned} b_{10}(x,t) = \mathcal{G}_1(g_1(x) - g_2(t)) \to \text{constant} \quad &\text{as} \quad x \to x_* \\ \text{and} \quad b_{20}(x,t_*) = \mathcal{G}_2(g_1(x) - g_2(t)) \to \text{constant} \quad &\text{as} \quad t \to t_*. \end{aligned} \tag{3.110}$$

Hence, w.l.g. let

$$b_{j0}(x,t) \;=\; 1.$$

The similitude of the results herein and the results of (2.7) and (2.47), allow for one to immediately conclude that

$$\begin{aligned} K_1(\omega) \;\sim\; 2\mathrm{i}\cos(\nu_1\pi), \quad \alpha_1 \neq -1 + \frac{1}{2\mathbb{N}+1}, \\ \text{and} \quad K_2(\omega) \;\sim\; 2\mathrm{i}\cos(\nu_2\pi), \quad \alpha_2 \neq -1 + \frac{1}{2\mathbb{N}+1}. \end{aligned} \tag{3.111}$$

Eq(3.111) returns the result in (3.80). The solution of (2.1) having crossed a Stokes sheet due to the turning point at x_* reads

$$h(x,t) \;\sim\; c^{-1/2}(x,t)\left(\int_{-\infty}^{\infty}\hat{A}(\omega)\mathrm{e}^{\mathrm{i}\omega\lambda(x,t)}d\omega + 2\mathrm{i}\cos(\nu_j\pi)\int_{-\infty}^{\infty}\hat{A}(\omega)\mathrm{e}^{\mathrm{i}\omega\left(g_2(t)-g_1(x)+g_1(x_i)\right)}d\omega\right)$$

$$= c^{-1/2}(x,t)\left(\mathcal{F}_-\left(\xi_-(x,t)\right)\mathrm{e}^{\mathrm{i}k_0\xi_-(x,t)/\epsilon} + 2\mathrm{i}\cos(\nu_1\pi)\mathcal{F}_-\left(\frac{\mathcal{D}_1(x,t)}{k_0}\right)\mathrm{e}^{\mathrm{i}\mathcal{D}_1(x,t)/\epsilon}\right),$$

using (3.93) and (3.94). In general, we obtain

$$h(x,t) \sim c^{-1/2}(x,t)\left(\mathcal{F}_-\left(\xi_-(x,t)\right)\mathrm{e}^{\mathrm{i}k_0\xi_-(x,t)/\epsilon} + 2\mathrm{i}\sum_{j=1}^{2}\cos(\nu_j\pi)\mathcal{F}_-\left(\frac{\mathcal{D}_j(x,t)}{k_0}\right)\mathrm{e}^{\mathrm{i}\mathcal{D}_j(x,t)/\epsilon}\right). \tag{3.112}$$

Eq(3.112) returns the result in (3.81) with a marked reduction in difficulty, not just in the calculation of the Stokes multipliers but also the location of the relevant Stokes lines.

3.4 Extending K-S (WKBJ) to compute reflection

The usual way of solving (2.1) without wave reflection is to apply the WKBJ method. Hence, here we propose an extension to the method that aims to capture the reflected wave also. In order to apply a K–S approach, as in §(2.2.1), the solutions of (2.1) must be known up to arbitrary functions of ϵ. To do this, we employ a technique outlined previously: we utilise the fact that the two terms in (3.1) form a basis of the solutions to (2.1) away from the points (2.4). Each object in (3.1) satisfies (3.17) and the recurrence relations (3.21). Then, by incorporating details from resurgent analysis (R-A) the phase of the reflected wave can be determined uniquely and the solutions of (2.1) are known up to arbitrary constants.

The key here, is to return the result in (3.81) in a more time efficient fashion than performing late term analysis, as in §3.2.

Throughout the following, the subscripts L and R will be used to denote the solution of (2.1) to the left (post) and right (pre) of a Stokes line. Any use of the subscripts $+$ and $-$ will be used to denote solutions that propagate in the direction of increasing $(+)$ or decreasing $(-)$ x. We assume that the points in (2.4) are the turning points of (2.1) and focus on the situation where the turning point closest to the real axis will be a branch point singularity of $c_1(x)$, x_*, and a root of $c_2(t)$, t_*. Recall the behaviour of the wave speed near the transition points x_* and t_* is:

$$\begin{aligned} c_1(x) &\sim \gamma\exp\left(-\mathrm{i}\pi\alpha_1/2\right)(x-x_*)^{-\alpha_1}, && \gamma\in\mathbb{R}>0,\ \alpha_1\in(-1,0)\cup(0,\infty),\\ c_2(t) &\sim \sigma\exp\left(\mathrm{i}\pi\alpha_2/2\right)(t-t_*)^{\alpha_2}, && \sigma\in\mathbb{R}>0,\ \alpha_2\in(-1,0)\cup(0,\infty). \end{aligned} \tag{3.113}$$

We restate the results in (3.11), (3.17) and (3.23) (for ease of reference throughout this section):

$$\begin{aligned} a_0(x,t) &= c_1^{-1/2}(x)c_2^{-1/2}(t)\mathcal{F}_-(\xi_-(x,t)),\\ b_{j0}(x,t) &= c_1^{-1/2}(x)c_2^{-1/2}(t)\mathcal{F}_j\left(\xi_+(x,t)\right) \end{aligned} \tag{3.114}$$

$$\text{and}\quad h(x,t) \sim A(\epsilon)a_0(x,t)\mathrm{e}^{\mathrm{i}k_0\xi_-(x,t)/\epsilon} \overset{+}{\sim} \sum_{j=1}^{2} B_j(\epsilon)b_{j0}(x,t)\mathrm{e}^{\mathrm{i}\mathcal{D}_j\left(\xi_+(x,t)\right)/\epsilon}. \tag{3.115}$$

The symbol $\overset{+}{\sim}$ has been used as in (3.100) and $\xi_\pm(x,t)$ was given in (3.6). The function $\mathcal{F}_-$ is determined from (2.2), where it follows that

$$\mathcal{F}_-(\xi_-(x,t)) = c^{1/2}(\xi_-(x,t),0)f(\xi_-(x,t)-x_0).$$

Let $A(\epsilon)=1$ in (3.115), then, the initial solution of (2.1), before crossing a Stoke line, is

$$h(x,t) \sim c_1^{-1/2}(x)c_2^{-1/2}(t)\mathcal{F}_-(\xi_-(x,t))\exp\left(\mathrm{i}k_0\xi_-(x,t)/\epsilon\right). \tag{3.116}$$

On crossing a Stokes line, (3.116) switches on (a) subdominant solution(s) as follows:

$$h(x,t) \sim c_1^{-1/2}(x)c_2^{-1/2}(t)\mathrm{e}^{\mathrm{i}k_0\xi_-/\epsilon}\left(\mathcal{F}_-(\xi_-(x,t)) + \sum_{j=1}^{2}K_j(\epsilon)\mathrm{e}^{-\mathrm{i}\chi_j(x,t)/\epsilon}\mathcal{F}_j\left(\xi_+(x,t)\right)\right). \tag{3.117}$$

Reflected wave phase, $\chi_j(x,t)$

We present a method which recovers the phase of the reflected waves in (3.117) in a more streamlined manner than previously. The approach was outlined in §(2.2.2), where it was noted that: the two objects in (3.1) form a basis for the solutions of (2.1) away from the transition points, then, comparing (3.1) and (3.117), with the aid of the condition in (3.33), the phase of the reflected wave can be determined uniquely. Focusing firstly on a spatial turning point, let $B(\epsilon) = B_1(\epsilon)$ in (3.1) and recall that

$$\theta_+(x,t) \;=\; \mathcal{D}_1\big(\xi_+(x,t)\big) \;=\; \mathcal{D}_1\bigg(g_1^{-1}\big(g_1(x) - g_2(t)\big)\bigg).$$

Therefore, connecting (3.1) and (3.117) it follows that

$$B_1(\epsilon)\mathrm{e}^{\mathrm{i}\mathcal{D}_1\left(\xi_+\right)/\epsilon} \;=\; K_1(\epsilon)\mathrm{e}^{\mathrm{i}k_0\xi_-/\epsilon - \chi_j(x,t)/\epsilon}. \tag{3.118}$$

Hence, using (3.33):

$$\begin{aligned} \mathcal{D}_1\bigg(g_1^{-1}\big(g_1(x_*) - g_2(t)\big)\bigg) \;&=\; k_0 g_1^{-1}\bigg(g_1(x_*) + g_2(t)\big)\bigg), \quad x \to x_*. \\ \text{and} \quad B_1(\epsilon) \;&=\; K_1(\epsilon). \end{aligned} \tag{3.119}$$

The freedom in the variable t implies,

$$\mathcal{D}_1\big(\xi_+\big) \;=\; k_0 g_1^{-1}\big(2g_1(x_*) - g_1(\xi_+)\big) \tag{3.120}$$

$$\implies \qquad \chi_1(x,t) \;=\; k_0\xi_-(x,t) - \mathcal{D}_1\big(\xi_+(x,t)\big). \tag{3.121}$$

Note, comparing (3.119) and (3.120) with (2.17) and (2.18) makes clear the differences in form between the solutions to the ODE (2.7) and PDE (2.1). Applying the same technique which led to (3.120), leads to:

$$\begin{aligned} B_2(\epsilon) \;&=\; K_2(\epsilon), \\ \mathcal{D}_2\big(\xi_+\big) \;&=\; k_0 g_1^{-1}\big(2g_2(t_*) + g_1(\xi_+)\big), \\ \text{and} \quad \chi_2(x,t) \;&=\; k_0\xi_-(x,t) - \mathcal{D}_2\big(\xi_+(x,t)\big). \end{aligned} \tag{3.122}$$

3.4.1 K–S Method

Spatial Turning Point

To find the form of $K_1(\epsilon)$ in (3.117) we inspect (2.1) near (x_*, t_s) for fixed $t_s \in \mathbb{C}/\{t_*\}$. In this way we are inspecting the Stokes Phenomenon w.r.t. a ray starting from

$$x = \xi_s \in \mathbb{R} : \quad t_s = g_2^{-1}\left(g_1(\xi_s) - g_1(x_*)\right). \tag{3.123}$$

The specific location of the Stokes surface is determined by noting that the solution ray undergoes a Stokes phenomenon upon crossing a Stokes surface whose location is deduced from:

$$\begin{aligned} k_0\left[\Im\left(\xi_-(x,t) - \mathcal{D}_1(\xi_+)\right)\right] &< 0, \\ \text{and} \quad \Re\left(\xi_-(x,t) - \mathcal{D}_1(\xi_+)\right) \;&=\; 0. \end{aligned} \tag{3.124}$$

Inner Solution: (2.1) Near (x_*, t_s)

Introducing

$$\begin{aligned} X \;&=\; \epsilon^{-1/(\alpha_1+1)}\mathrm{i}\left(x - x_*\right), \\ \text{and} \quad T &= \epsilon^{-1}\left(t - t_s,\right). \end{aligned} \tag{3.125}$$

Note that: we fix t_s and change the large parameter T, it is deduced later that the value one chooses for t_s is arbitrary. The wave speed profiles local to x_* and t_s are

$$\begin{aligned} c_2(t) &\approx c_2(t_s), \\ c_1(x) &\sim \gamma \mathrm{i}^{-\alpha_1}(x-x_*)^{-\alpha_1} \\ &= \gamma \epsilon^{-\alpha_1/(\alpha_1+1)} X_i^{-\alpha_1}, \end{aligned} \tag{3.126}$$

on using (3.113). Hence,

$$\begin{aligned} \partial_t &= \epsilon^{-1}\partial_T, \\ \text{and} \quad \partial_x &= \epsilon^{-1/(\alpha_1+1)}\mathrm{i}\partial_X. \end{aligned} \tag{3.127}$$

Then, from (3.125), (3.126) and (3.127) the $\mathcal{O}(1)$ form of (2.1) near (x_*, t_s) is

$$\frac{\partial_T^2 h}{c_2^2(t_s)} = -\gamma^2 \partial_X \left(X^{-2\alpha_1} \partial_X h \right). \tag{3.128}$$

We solve (3.128), using a Fourier transform:

$$h = \int_{-\infty}^{\infty} \hat{h}(X,\omega) \mathrm{e}^{\mathrm{i}\omega c_2(t_s)T} d\omega. \tag{3.129}$$

It is expected from (2.2) that $\hat{h}(X,\omega)$ is a localised function of ω. Therefore,

$$\int_{-\infty}^{\infty} \left[\partial_X \left(X^{-2\alpha_1} \partial_X \hat{h} \right) - \frac{\omega^2}{\gamma^2} \hat{h} \right] \mathrm{e}^{\mathrm{i}\omega c_2(t_s)T} d\omega = 0.$$

Thus, by holding each ω fixed, we aim to solve

$$\frac{d}{dX}\left(X^{-2\alpha_1} \frac{d}{dX}\hat{h} \right) - \left(\frac{\omega}{\gamma} \right)^2 \hat{h} = 0. \tag{3.130}$$

Eq. (3.130) has the same form as in the ODE case, with the exception that ω changes sign with k_0, deduced a posteriori c.f. (3.151). As in (2.27), the solutions of (3.130) are written as

$$\hat{h} \sim X^{\alpha_1+\frac{1}{2}} \left(\hat{A}(\omega) H_{\nu_1}^{(1)} \left(\mathrm{i}\frac{\omega}{\gamma} \frac{X^{\alpha_1+1}}{(\alpha_1+1)} \right) + \hat{B}(\omega) H_{\nu_1}^{(2)} \left(\mathrm{i}\frac{\omega}{\gamma} \frac{X^{\alpha_1+1}}{(\alpha_1+1)} \right) \right), \tag{3.131}$$

where $\nu_1 = \frac{2\alpha_1+1}{2\alpha_1+2}$ from (3.66) and again $H_{\nu_1}^{(1)}$ and $H_{\nu_1}^{(2)}$ are Hankel functions of the first and second kind. Recall that $H_{\nu_1}^{(1)}$ and $H_{\nu_1}^{(2)}$ have the following large z-asymptotic relations:

$$H_{\nu_1}^{(1)}(z) \sim \sqrt{\frac{2}{\pi z}} e^{i(z - \nu_1 \frac{\pi}{2} - \frac{\pi}{4})} \quad \text{for} -\pi < \arg z < 2\pi, \tag{3.132}$$

$$H_{\nu_1}^{(2)}(z) \sim \sqrt{\frac{2}{\pi z}} e^{-i(z - \nu_1 \frac{\pi}{2} - \frac{\pi}{4})} \quad \text{for} -2\pi < \arg z < \pi. \tag{3.133}$$

It should be noted that a sign change of ω will effect the regions of validity in (3.132) and (3.133). We aim to match (3.131) and (3.117) along anti-Stokes lines, where the arguments in (3.131) are purely real. Thus, from (3.132) and (3.133) we require $X^{\alpha_1+1} \in \mathrm{i}\mathbb{R}$. These are lines tangent to the straight lines:

$$\begin{aligned} X_R &= R\mathrm{e}^{\frac{\mathrm{i}\pi}{2(\alpha_1+1)}}, \quad R > 0, \\ X_L &= R\mathrm{e}^{\frac{-\mathrm{i}\pi}{2(\alpha_1+1)}}, \quad R > 0. \end{aligned} \tag{3.134}$$

The anti-Stokes line when $\Re(x) > \Re(x_*)$ is indicated by the subscript R and the subscript L denotes the anti-Stokes line to the left, $\Re(x) < \Re(x_*)$, of the Stokes line. Note: we have chosen to perform a matching procedure near the point $x = x_*$ and across the Stokes line (which

crosses the real axis), however, a Stokes line starts and finishes at a turning point or infinity, and thus the choice of (complex conjugate) turning point to match near is immaterial. Observe that:

$$\arg\left(\mathrm{i}X_L^{\alpha_1+1}\right) \;=\; 0 \quad \text{and} \quad \arg\left(\mathrm{i}X_R^{\alpha_1+1}\right) \;=\; \pi. \tag{3.135}$$

Therefore, along X_R the arguments in (3.131) fall outside of the range of (3.133). To remedy this, we recall the connection formula (2.34):

$$H^{(2)}_{\nu_1}\left(\frac{\omega R^{\alpha_1+1}}{\gamma(\alpha_1+1)}e^{i\pi}\right) = 2\cos(\nu_1\pi)H^{(2)}_{\nu_1}\left(\frac{\omega R^{\alpha_1+1}}{\gamma(\alpha_1+1)}\right) + e^{i\nu_1\pi}H^{(1)}_{\nu_1}\left(\frac{\omega R^{\alpha_1+1}}{\gamma(\alpha_1+1)}\right). \tag{3.136}$$

Therefore, substituting $X = X_{_R}$, in (3.134), and using (3.136), we obtain

$$h_R \;\sim\; \sqrt{\frac{2\gamma}{\pi\omega}}\sqrt{\alpha_1+1}\mathrm{e}^{\frac{\mathrm{i}\pi\nu_1}{2}}R^{\frac{\alpha_1}{2}}\left[\hat{B}(\omega)\mathrm{e}^{\frac{\mathrm{i}\pi}{4}(2\nu_1-1)}\mathrm{e}^{\mathrm{i}\frac{\omega}{\gamma}\frac{R^{\alpha_1+1}}{\alpha_1+1}} + \hat{Q}(\omega)\mathrm{e}^{-\mathrm{i}\frac{\omega}{\gamma}\frac{R^{\alpha_1+1}}{\alpha_1+1}}\right], \tag{3.137}$$

where $\hat{Q}(\omega) \;=\; \hat{A}(\omega)\mathrm{e}^{-\frac{\mathrm{i}\pi}{4}(2\nu_1+3)} + 2\cos(\nu_1\pi)\hat{B}(\omega)\mathrm{e}^{\frac{\mathrm{i}\pi}{4}(2\nu_1-1)}$.

To determine which of the solutions matches with the outer solution to the right of the Stokes line we inspect (3.117) local to X_R.

WKBJ solutions near (x_*, t_s)

Eq(3.7) near x_* is

$$g_1(x) = g_1(x_*) - \epsilon\mathrm{i}\frac{X^{\alpha_1+1}}{\gamma(\alpha_1+1)} + \text{l.o.t}, \quad x \to x_*,$$

using (3.125), and as $(x,t) \to (x_*, t_s)$

$$\xi_-(x,t) = \xi_-\big(x_*,t_s\big) + \epsilon c_1\left(\big(\xi_-\big(x_*,t_s\big)\right)\left(c_2(t_s)T - \mathrm{i}\frac{X^{\alpha_1+1}}{\gamma(\alpha_1+1)}\right) + \text{l.o.t},$$

$$\text{and} \quad \mathcal{D}_1\big(\xi_+(x,t)\big)/k_0 = \xi_-\big(x_*,t_s\big) + \epsilon c_1\left(\xi_-\big(x_*,t_s\big)\right)\left(c_2(t_s)T + \mathrm{i}\frac{X^{\alpha_1+1}}{\gamma(\alpha_1+1)}\right) + \text{l.o.t},$$

from (3.6) and (3.120). It is convenient to introduce:

$$\mathcal{T}(x) \;=\; \mathcal{F}_-(x)\mathrm{e}^{\mathrm{i}k_0x/\epsilon}, \tag{3.138}$$

$$\text{and} \quad \hat{K}_j(x,t;\epsilon) \;=\; K_j(\epsilon)\frac{\mathcal{F}_j\big(\xi_+(x,t)\big)}{\mathcal{F}_-(\xi_-(x,t))}. \tag{3.139}$$

Then, along $X = X_R$, to the right of the Stokes line, (3.117) is:

$$h_R \;\sim\; \gamma^{-1/2}\epsilon^{\frac{\alpha_1}{2(\alpha_1+1)}}c_2^{-1/2}(t_s)\mathcal{T}\left(\xi_-\big(x_*,t_s\big)\right)\mathrm{e}^{\frac{\mathrm{i}\pi}{4}(2\nu_1-1)}R^{\frac{\alpha_1}{2}}\exp\left\{\mathrm{i}k_0c_1\left(\xi_-\big(x_*,t_s\big)\right)\left[c_2(t_s)T + \frac{R^{\alpha_1+1}}{\gamma(\alpha_1+1)}\right]\right\}, \quad X = X_R. \tag{3.140}$$

On crossing the Stokes line,

$$h_L \;\sim\; \gamma^{-1/2}\epsilon^{\frac{\alpha_1}{2(\alpha_1+1)}}c_2^{-1/2}(t_s)\mathcal{T}\left(\xi_-\big(x_*,t_s\big)\right)\mathrm{e}^{-\frac{\mathrm{i}\pi}{4}(\nu_2-1)}R^{\frac{\alpha_1}{2}}\exp\left\{\mathrm{i}k_\star c_1\left(\xi_-\big(x_*,t_s\big)\right)\left[c_2(t_s)T - \frac{R^{\alpha_1+1}}{\gamma(\alpha_1+1)}\right]\right\}$$
$$\times\left(1 + \hat{K}_1(x_*,t_s;\epsilon)\exp\left\{2\mathrm{i}k_\star c_1\left(\xi_-\big(x_*,t_s\big)\right)\frac{R^{\alpha_1+1}}{\gamma(\alpha_1+1)}\right\}\right), \quad X = X_L. \tag{3.141}$$

Hence, matching (3.137) and (3.140) we find $\hat{Q}(\omega) = 0$. Therefore,

$$\hat{A}(\omega) \;=\; 2\cos(\nu_1\pi)\hat{B}(\omega)\mathrm{e}^{\frac{\mathrm{i}\pi}{2}(2\nu_1+1)}.$$

Thus, (3.137) is

$$\hat{h}_R \sim \hat{B}(\omega)R^{\frac{\alpha_1}{2}}\sqrt{\frac{2}{\pi}\frac{\gamma}{\omega}(\alpha_1+1)}\mathrm{e}^{\mathrm{i}\pi(\nu_1-1/4)}\exp\left\{\mathrm{i}\frac{\omega}{\gamma}\frac{R^{\alpha_1+1}}{(\alpha_1+1)}\right\}, \quad X = X_R. \tag{3.142}$$

As noted in (3.135), on crossing the Stoke line the arguments in (3.131) have

$$\arg\left(\mathrm{i}\frac{\omega_j}{\gamma}\frac{{X_R}^{\alpha_1+1}}{(\alpha_1+1)}\right) = 0.$$

Therefore, both (3.132) and (3.133) can be used. Hence, to the left of the Stokes line

$$\hat{h}_L \sim \hat{B}(\omega)R^{\frac{\alpha_1}{2}}\sqrt{\frac{2}{\pi}\frac{\gamma}{\omega}(\alpha_1+1)}\mathrm{e}^{\mathrm{i}\pi/4}\left(\mathrm{e}^{-\mathrm{i}\frac{\omega}{\gamma}\frac{R^{\alpha_1+1}}{(\alpha_1+1)}} - 2\mathrm{i}\cos(\nu_1\pi)\mathrm{e}^{\mathrm{i}\frac{\omega}{\gamma}\frac{R^{\alpha_1+1}}{(\alpha_1+1)}}\right), \quad X = X_L. \tag{3.143}$$

From (3.129), (3.142) and (3.143), the solutions of (2.1) near (x_*, t_s) are:

$$h_R \sim R^{\frac{\alpha_1}{2}}\sqrt{\frac{2}{\pi}\gamma(\alpha_1+1)}\mathrm{e}^{\mathrm{i}\pi(\nu_1-1/4)}\int_{-\infty}^{\infty}\tilde{B}(\omega)\mathrm{e}^{\mathrm{i}\omega\left(c_2(t_s)T+\left(\frac{R^{\alpha_1+1}}{(\alpha_1+1)}/\gamma\right)\right)}d\omega, \quad X = X_R,$$

and on crossing the Stokes line

$$h_L \sim R^{\frac{\alpha_1}{2}}\sqrt{\frac{2}{\pi}\gamma(\alpha_1+1)}\mathrm{e}^{\mathrm{i}\pi/4}\int_{-\infty}^{\infty}\tilde{B}(\omega)\left(\mathrm{e}^{\mathrm{i}\frac{\omega}{\epsilon}\left(c_2(t_s)T-\left(\frac{R^{\alpha_1+1}}{(\alpha_1+1)}/\gamma\right)\right)} - 2\mathrm{i}\cos(\nu_1\pi)\mathrm{e}^{\mathrm{i}\omega\left(c_2(t_s)T+\left(\frac{R^{\alpha_1+1}}{(\alpha_1+1)}/\gamma\right)\right)}\right)d\omega,$$

along $X = X_R$, with

$$\tilde{B}(\omega) = \frac{\hat{B}(\omega)}{\sqrt{\omega}}: \quad \tilde{B}(0) = 0.$$

Heuristically, we assume that $\tilde{B}(\omega)$ is the Fourier transform of some, to be determined, function. That is,

$$B(x) = \int_{-\infty}^{\infty}\tilde{B}(\omega)\mathrm{e}^{\mathrm{i}\omega x}d\omega. \tag{3.144}$$

Thus,

$$h_R \sim R^{\frac{\alpha_1}{2}}\sqrt{\frac{2}{\pi}\gamma(\alpha_1+1)}\mathrm{e}^{\mathrm{i}\pi(\nu_1-1/4)}B\left(c_2(t_s)T + \frac{R^{\alpha_1+1}}{(\alpha_1+1)}/\gamma\right), \quad X_i = X_R, \tag{3.145}$$

and

$$h_L \sim R^{\frac{\alpha_1}{2}}\sqrt{\frac{2}{\pi}\gamma(\alpha_1+1)}\mathrm{e}^{\mathrm{i}\pi/4}\left[B\left(c_2(t_s)T - \frac{R^{\alpha_1+1}}{(\alpha_1+1)}/\gamma\right) - 2\mathrm{i}\cos(\nu_1\pi)B\left(c_2(t_s)T + \frac{R^{\alpha_1+1}}{(\alpha_1+1)}/\gamma\right)\right], \quad X_i = X_L. \tag{3.146}$$

Matching

Connecting (3.145) with (3.140), and (3.146) with (3.141), we find:

$$B(Y) = \gamma\sqrt{\frac{\pi}{2}}\epsilon^{\frac{\alpha_1}{2(\alpha_1+1)}}c_2^{-1/2}(t_s)\mathrm{e}^{-\mathrm{i}\pi\nu_1/2}\mathcal{T}\left(\xi_-\left(x_*,t_s\right)\right)\exp\left\{\mathrm{i}k_0c_1\left(\xi_-\left(x_*,t_s\right)\right)Y\right\}/\sqrt{\alpha_1+1} \tag{3.147}$$

and

$$\hat{K}_1(x_*,t_s;\epsilon) = K_1(\epsilon)\frac{\mathcal{F}_1\left(\xi_+(x_*,t_s)\right)}{\mathcal{F}_-\left(\xi_-(x_*,t_s)\right)} \sim -2\mathrm{i}\cos(\nu_1\pi).$$

Using (3.120), it is noted that:

$$\xi_-(x,t) \to \frac{\mathcal{D}_1\left(\xi_+(x,t)\right)}{k_0}: \quad x \to x_*, \forall t \in \mathbb{R} > 0.$$

Thus, we let

$$\mathcal{F}_1(x) \;=\; \mathcal{F}_-\left(\frac{\mathcal{D}_1(x)}{k_0}\right). \tag{3.148}$$

Therefore, the Stokes multiplier $K_1(\epsilon)$ is independent of the choice of t_s,

$$K_1(\epsilon) \;\sim\; -2\mathrm{i}\cos(\nu_1\pi), \tag{3.149}$$

holds for all $t \in \mathbb{R} > 0$. The outcome being that: all rays starting along the initial line and that undergo a Stokes phenomena due to the spatial turning point x_*, have the same Stokes multiplier $K_1(\epsilon)$ in (3.149). The results in (3.148) and (3.149) mirror those in (3.81).

From (3.147),

$$\tilde{B}(\omega) \;=\; \ldots \int_{-\infty}^{\infty} \mathrm{e}^{\mathrm{i}\left(k_0 c_1(\xi_-(x_*,t_s))+\omega\right)x} dx \;=\; \ldots\, \delta(k_0 c_1\left(\xi_-(x_*,t_s)\right)+\omega). \tag{3.150}$$

Hence, the assumption that (3.144) be considered a Fourier transform is acceptable and, as anticipated, $\hat{h}(X,\omega)$ in (3.129) is indeed a localised function of ω. Note, ω was scaled by $c_2(t)$ in the exponent of the exponential in (3.129), hence (3.150) implies that

$$\omega \;=\; -k_0 c_2(t_s) c_1\big(\xi_-(x_*,t_s)\big) \;:\quad t_s \;=\; g_2^{-1}\left(g_1(\xi_s)-g_1(x_*)\right), \tag{3.151}$$

having used (3.123). The analysis required that $\omega > 0$ and hence we must pick $k_0 < 0$ in (2.2) to qualify this. From ray-tracing theory:

$$\omega(x,t) \;=\; -\partial_t\theta_-(x,t) \;=\; -k_0 c_2(t) c_1\big(\xi_-(x,t)\big).$$

Therefore, as expected, (3.147) reflects the fact that we have followed a solution ray starting at $x = \xi_s$, when $t = 0$, to the matching region around (x_*, t_s).

The Case of $x_0 > 0$.

With $x_0 > 0$ the reflected wave is expected as $x \to \infty$, therefore, by applying the same technique which lead to (3.149), leads to:

$$\begin{aligned} K_1(\epsilon) \;&\sim\; 2\mathrm{i}\cos(\nu_1\pi), \\ \text{and}\quad K_2(\epsilon) \;&\sim\; 2\mathrm{i}\cos(\nu_1\pi). \end{aligned} \tag{3.152}$$

3.4.2 Temporal Turning Point

Here we aim to find the form of $K_2(\epsilon)$ and $\mathcal{F}_2(x)$ in (3.117) by inspecting (2.1) local to the turning point at t_* with $x \approx x_s \in \mathbb{C}/\{x_*\}$. In this way we inspect the Stokes Phenomenon due to a temporal turning point w.r.t. a ray starting at

$$x = \xi_s \;:\quad x_s = g_1^{-1}\big(g_1(\xi_s) - g_2(t_*)\big).$$

Following the same procedure that lead to the result in (3.149), it is deduced that:

$$\begin{aligned} \mathcal{F}_2(x) \;&=\; \mathcal{F}_-\left(\frac{\mathcal{D}_2(x)}{k_0}\right), \\ \text{and}\quad K_{2l}(\epsilon) \;&\sim\; (-)^{l+1} 2\mathrm{i}\cos(\nu_2\pi), \end{aligned} \tag{3.153}$$

in (3.117).

3.4.3 General solution

With $x_0 > 0$ and $k_0 > 0$, in (2.2) , we connect (3.117) and, (3.120), (3.122), (3.148), (3.152) and (3.153), the solution of (2.1) is

$$h(x,t) \sim c^{-1/2}(x,t)\left(\mathcal{F}_-(\xi_-(x,t))\mathrm{e}^{\mathrm{i}k_0\xi_-(x,t)/\epsilon} + 2\mathrm{i}\sum_{j=1}^{2}\cos(\nu_j)\mathcal{F}_-\left(\frac{\mathcal{D}_j(\xi_+)}{k_0}\right)\mathrm{e}^{\mathrm{i}k_0\mathcal{D}_j(\xi_+)/\epsilon}\right), \quad (3.154)$$

where

$$\begin{aligned} K_j(\epsilon) &\sim 2\mathrm{i}\cos(\nu_j\pi) \\ \text{and} \quad \mathcal{F}_-(x) &= c_1^{1/2}(x)c_2^{1/2}(0)f(x-x_0). \end{aligned}$$

Eq(3.154) repeats the result in (3.81).

3.5 Numerical tests when $c(x,t)$ is separable

We report results obtained for

$$h(x,0) = \mathrm{e}^{\mathrm{i}k_0/\epsilon}\mathrm{e}^{-(x-x_0)/2\sigma^2} \; : \quad k_0 = 1 \quad \text{and} \quad \sigma = 1/\sqrt{2},$$

in (2.2), and several (positive) values of the parameters ϵ and x_0. Note that

$$f(x-x_0) = \mathrm{e}^{-(x-x_0)^2/2\sigma^2},$$

in (2.2). To find a numerical estimate of the reflected wave a third-order Adams–Bashforth (A–B) multistep method was used. That is, let

$$\mathbf{y} = \begin{pmatrix} h(x,t) \\ h_t(x,t) \end{pmatrix},$$

then (2.1) is phrased as

$$\mathbf{y}_t = \begin{pmatrix} 0 & 1 \\ \mathcal{L} & 0 \end{pmatrix}\mathbf{y} = F(t,\mathbf{y}),$$

where

$$\mathcal{L} = c^2(x,t)\partial_x^2 + (c^2(x,t))_x\partial_x.$$

Therefore, the A–B scheme reads

$$\mathbf{y}_{n+3} = \mathbf{y}_{n+2} + \delta\left(\frac{23}{12}F(t_{n+2},\mathbf{y}_{n+2}) - \frac{4}{3}F(t_{n+1},\mathbf{y}_{n+1}) + \frac{5}{12}F(t_n,\mathbf{y}_n)\right).$$

The particular wave speed choices are:

$$\begin{aligned}
&\text{(i)}: \quad c_1(x) = \frac{2+x^2}{1+x^2}, && c_{1_\pm} = 1 \quad \text{and} \quad x_* = \mathrm{i}, \\
&\text{(ii)}: \quad c_1(x) = 1 + \operatorname{sech}(x), && c_{1_\pm} = 1 \quad \text{and} \quad x_* = \frac{\mathrm{i}\pi}{2}, \\
&\text{(iii)}: \quad c_2(t) = \frac{1+(t-3)^2}{2+(t-3)^2}, && c_{2_\pm} = 1 \quad \text{and} \quad t_* = 3+\mathrm{i}, \\
&\text{(iv)}: \quad c(x,t) = \big(1+\operatorname{sech}(x)\big)\frac{1+(t-3)^2}{2+(t-3)^2}, && c_{1_\pm} = c_{2_\pm} = 1 \quad \text{and} \quad x_* = \frac{\mathrm{i}\pi}{2},\ t_* = 3+\mathrm{i}.
\end{aligned} \quad (3.155)$$

Recall that

$$g_1(x) = \int_0^x \frac{dx'}{c_1(x')} \quad \text{and} \quad g_2(t) = \int_0^t c_2(t')dt'.$$

Cubic-spline interpolation was employed to determine the function $g_1^{-1}(x)$ within the numerical test of (3.81).

Two unexpected features arise from the analytical result in (3.81): the exponentially small term in the subdominant solutions cannot be presented as an exponentially small pre-factor function of ϵ only, and the appearance of the function $\mathcal{D}_j(\xi_+)/k_0$ in the localised function $f(x-x_0)$ from (2.2). To highlight the requirement for both features, we introduce two 'naive' leading order solutions to (2.1). These solutions are then noted by the subscripts 1 and 2.

3.5.1 Time independent wave speed

We focus on a spatially dependent wave speed, (i) and (ii) in (3.155), to highlight the interesting features of (3.81), and let $c_2(t)=1$. We introduce,

$$\begin{aligned} \beta &= 2g_1(x_*), \\ \hat{B}(\epsilon) &= \mathrm{e}^{\mathrm{i}\beta/\epsilon}, \\ \hat{\alpha} &= \int_0^\infty \left(\frac{1}{c_1(x)} - \frac{1}{c_{1_\pm}}\right) dx \\ \text{and} \quad \hat{\xi}_\pm(x,t) &= c_{1_\pm}(t \mp g_1(x) - \hat{\alpha}). \end{aligned} \tag{3.156}$$

Note, $\hat{\xi}_\mp(x,t)$ is the approximation of $\xi_\pm(x,t)$ in (3.6) when $x \gg 1$, e.g.

$$\xi_\pm(x,t) \to \hat{\xi}_\pm(x,t), \quad x \to \infty.$$

The asymptotic estimate of the reflected wave in (2.1) was given in (3.81) and is

$$h_{\mathrm{ref}}(x,t) \sim 2\mathrm{i}\cos(\nu_1\pi)c_1^{-1/2}(x)c_1^{1/2}\left(\frac{\mathcal{D}_1(\xi_+)}{k_0}\right) f\left(\frac{\mathcal{D}_1(\xi_+)}{k_0} - x_0\right)\mathrm{e}^{\mathrm{i}\mathcal{D}_1(\xi_+)/\epsilon},$$

where

$$\mathcal{D}_1(\xi_+) = k_0 g_1^{-1}\big(t - g_1(x) + 2g_1(x_*)\big).$$

As noted at the beginning of the current chapter: exponentially small reflection is relatively well understood in the ODE case but not in the PDE case. A naive approach would assume that the exponentially small wave can be computed by simply multiplying the WKBJ solution (3.1) by the exponentially small pre-factor of the ODE (with ω taken to be that of the dominant frequency), e.g. letting

$$B(\epsilon) \sim 2\mathrm{i}\cos(\nu_1\pi)\hat{B}(\epsilon) \quad \text{and} \quad \theta_+(x,t) = k_0\xi_+(x,t),$$

in (3.1). This is not so, and to highlight this we assume a first 'naive' asymptotic approximation of the reflected wave which includes the reflected phase function in the argument of the initial function f but predicts the reflected wave to have an exponentially small pre-factor function of ϵ. In addition, if $x_0 \gg 1$ in (2.2), then we replace ξ_+ with $\hat{\xi}_+$ above. Therefore, let

$$h_1(x,t) \sim 2\mathrm{i}\cos(\nu_1\pi)\,\hat{B}(\epsilon)c_1^{-1/2}(x)c_1^{1/2}\big(\hat{\xi}_+\big) f\left(\hat{\xi}_+ + \mathrm{i}\beta - x_0\right)\mathrm{e}^{\mathrm{i}k_0\hat{\xi}_+/\epsilon}, \tag{3.157}$$

be the first naive approximation for the reflected wave when $x_0 \gg 1$ in (2.2). In the second approximation, we inspect the effects of not having the complex parameter $\mathrm{i}\beta$ in the argument of the function f:

$$h_2(x,t) \sim 2\mathrm{i}\cos(\nu_1\pi)\hat{B}(\epsilon)c_1^{-1/2}(x)c_{1_\pm}^{1/2} f\big(\hat{\xi}_+ - x_0\big)\mathrm{e}^{\mathrm{i}k_0\hat{\xi}_+/\epsilon}. \tag{3.158}$$

Reflected Wave Plots

Figures(3.2) and (3.3) present a numerical estimate together with the asymptotic estimates (3.81), (3.157) and (3.157) of the amplitude of the reflected wave for $c_1(x)$ as (i) and then (ii) in (3.155). It was arbitrarily chosen that the information on the reflected wave would be

taken around the point $x = x_{\rm st} = 8$. Therefore, the simulations were stopped at a time $t_s = \Re\left\{g_2^{-1}\left(g_1(x_0) + g_1(x_{\rm st}) - 2{\rm i}g_1(x_*)\right)\right\}$. It is clear from Figures 3.2 and 3.3 that the estimate in (3.81) appears correctly aligned with the numerical estimate and is the only candidate that maps onto the numerical estimate as $\epsilon \to 0$.

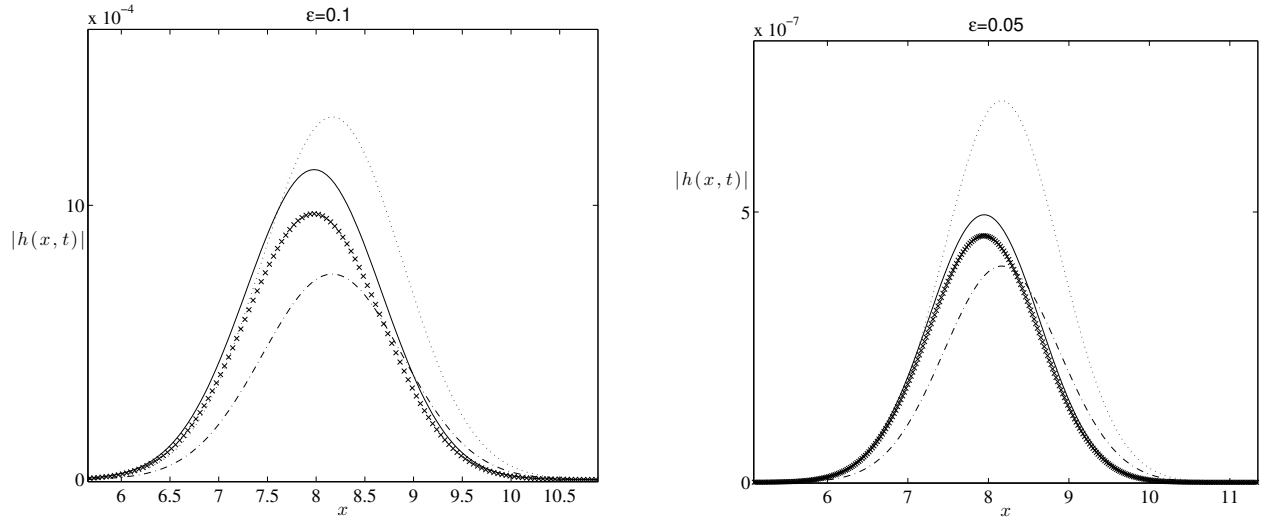

Figure 3.2: Numerical estimate of the amplitude of the reflected wave as a function of x for c_1 given by (i); ($\times$) and $x_0 = 6$. The dashed lines show the asymptotic estimate (3.81) (solid), (3.157) (dash dot) and (3.158) (dots), respectively, for $\epsilon = 0.1$ (left panel) and $\epsilon = 0.05$ (right panel). Note: in the right panel the collection of numerical data points given by $\times$ is discrete. The possible confusion, that the numerical result is continuous, appears as a result of the small step size that is necessary for the A-B scheme to converge.

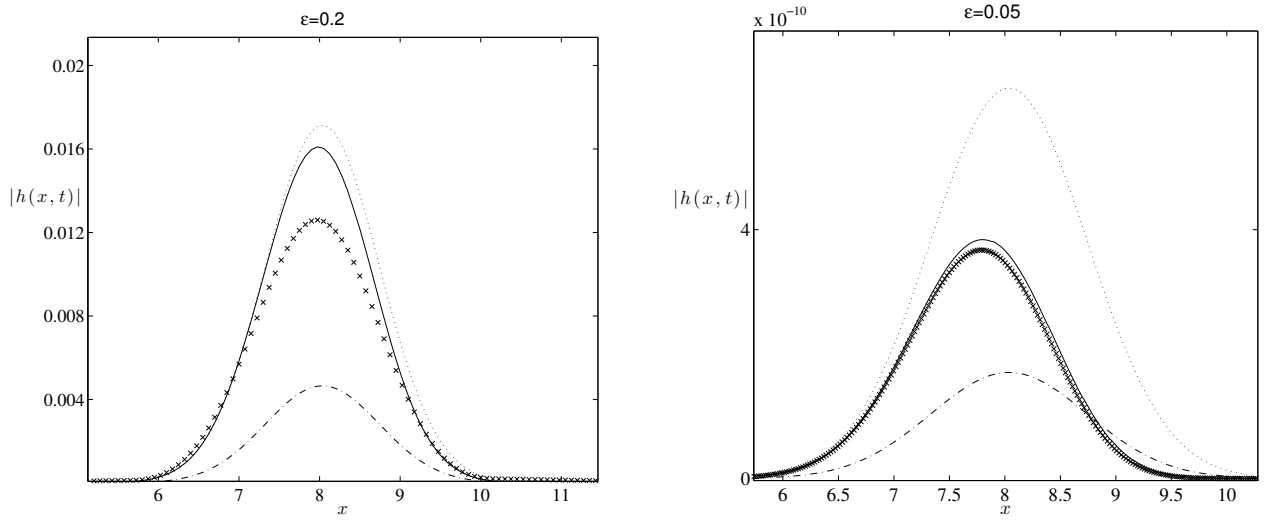

Figure 3.3: Numerical estimate of the amplitude of the reflected wave as a function of x for c_1 given by (ii); ($\times$) and $x_0 = 4$. The dashed lines show the asymptotic estimates (3.81) (solid), (3.157) (dash dot) and (3.158) (dots), respectively, for $\epsilon = 0.2$ (left panel) and $\epsilon = 0.05$ (right panel). Note: in the right panel the collection of numerical data points given by $\times$ is discrete. The possible confusion, that the numerical result is continuous, appears as a result of the small step size that is necessary for the A-B scheme to converge.

Relative error

Presented in Figure 3.4 are estimates of the relative error (of the reflected wave) between the numerical solution h_{N}, and the asymptotic estimates h_{p} (3.81), (3.157) and (3.158), as a function of ϵ. The norm used is

$$|h| = \sup_x |h(x, t_s)|.$$

Figure 3.4 indicates that: as $\epsilon \to 0$ the estimate (3.81) maps onto the numerical estimate. The data was recovered around the point at $x_{\mathrm{st}} = 6$.

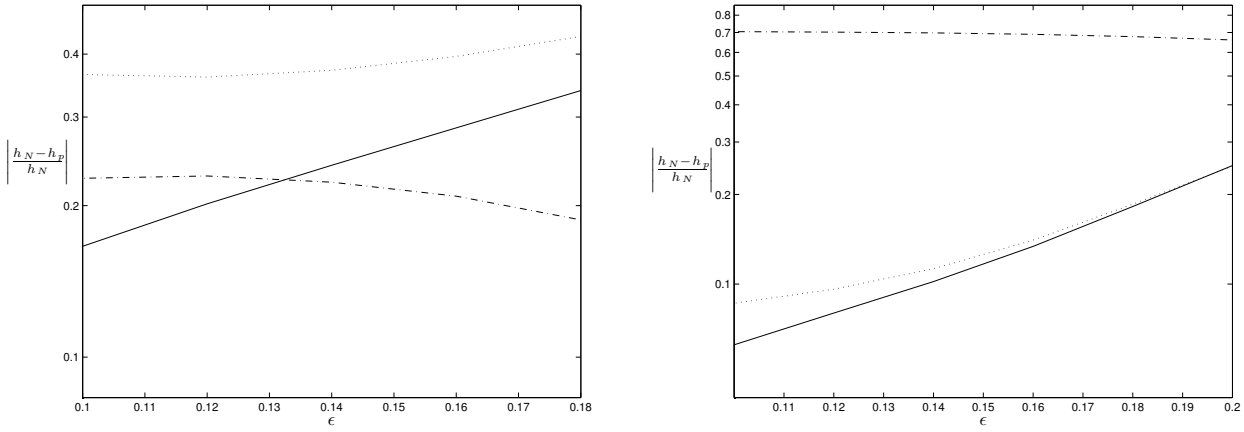

Figure 3.4: Calculation of the relative error between the numerical estimate of the amplitude of the reflected wave and the asymptotic estimates in (3.81), (3.157) and (3.158), as a function of ϵ when $x_0 = 6$. In the left panel $c_1(x)$ is (i). In the right panel $c_1(x)$ is (ii). The asymptotic estimate of (3.81) is given by the solid line and the estimates in (3.157) and (3.158) are given by the dashed and dotted lines respectively.

x_0 dependence

It is noted from the estimate in (3.81) that there is a significant association between the amplitude of the reflected wave and the point around which the initial solution is centred, i.e. $x = x_0$. This detail is explored in Figure 3.5, where it is clear that as x_0 tends toward zero (3.81) captures the behaviour of the numerical estimate indicating the need for the reflected phase in the argument of the function f. The addition of the results presented in Figure 3.4 'guarantees' that the reflected wave maps onto the numerical in Figure 3.5 as $\epsilon \to 0$. All data was recovered around $x_{\mathrm{st}} = 6$.

3.5.2 Spatially independent wave speed

If $c_1(x) = 1$ in (2.1), then $g_1(x) = x$ in (3.7) and therefore the phase of the reflected wave in (3.37) is

$$\mathcal{D}_2(\xi_+) = k_{_0} \left(x - g_2(t) + 2g_2(t_*)\right).$$

Hence, the role of the Stokes multiplier $K_2(\epsilon)$ in (3.81) is the same as in the ODE (2.47), see (2.50). The upshot is that: the modulus of the reflected wave does not change with x or t as in figures(3.2)-(3.5), but instead is a function of ϵ only. Figure 3.87 verifies this and indicates that: as $\epsilon \to 0$ the asymptotic estimate maps onto the numeric estimate. All data was recovered around $x_{\mathrm{st}} = 6$.

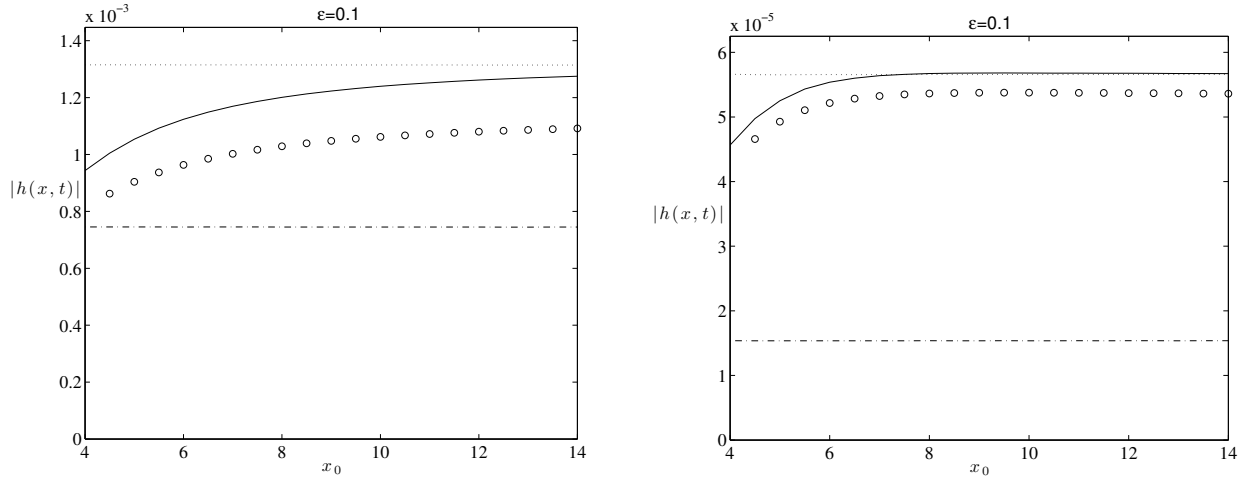

Figure 3.5: Numerical estimate of the amplitude of the reflected wave as a function of x_0 when $\epsilon = 0.1$. In the left panel $c_1(x)$ is (i) and the numerical estimate is shown as $\circ$. In the right panel $c_1(x)$ is (ii) and the numerical estimate is shown as $\circ$. The asymptotic estimate of (3.81) is given by the solid line and the estimates in (3.157) and (3.158) are given by the dotted and dash-dot lines respectively.

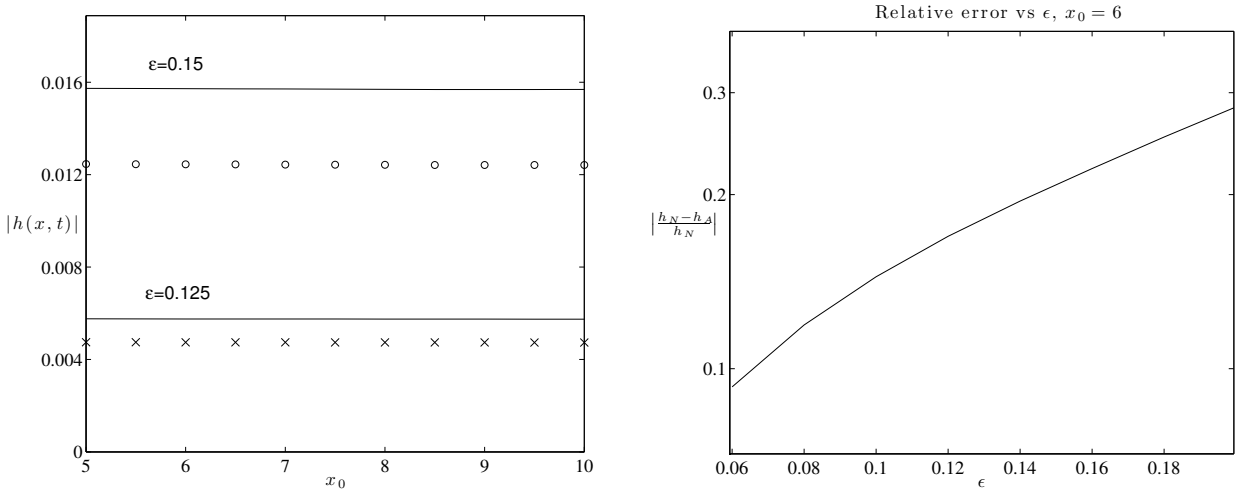

Figure 3.6: Left panel: numerical estimate of the amplitude of the reflected wave as a function of x_0 with $c_2(t)$ as (iii); $\circ$ when $\epsilon = 0.15$ and $(\times)$ when $\epsilon = 0.125$. The straight line denotes the asymptotic estimate in (3.81). Right panel: numerical estimate of the relative error, $\left|\frac{h_{\rm N}-h_{\rm A}}{h_{\rm N}}\right|$, w.r.t. the asymptotic estimate (3.81), with $c_2(t)$ as (iii) and $x_0 = 5$.

3.5.3 Separable wave speed profile

Let $c_1(x)$ and $c_2(t)$ be non-constant. Figure 3.7 presents the numerical and analytical estimates of the reflected waves that appear as a result of a double Stokes phenomena. The first reflected wave appears as a result of the turning point at t_*. A subsequent a reflected wave is generated as a result of a Stokes phenomenon associated with the spatial turning point at $x = x_*$. The characteristic curves (3.6) determine the order in which the reflected waves are detected. We chose to recover information on the spatially reflected wave around the point $x = x_{\rm st} = 5$ and set $x_0 = 6$ in (2.2). Most of the exciting details of the result in (3.81) can be obtained by inspecting a spatially dependent wave speed profile only. Inspection of x_0 dependence in the case

of a separable spatio-temporal wave speed produces similar results to those presented in Figure 3.5. The important detail is that the reflected waves coincides with the numerical estimate in location and amplitude. Therefore, in this segment of the numerical tests we endeavour to verify that the reflected waves are located around the numerical estimate and are similar in amplitude. Figure 3.7 confirms these details.

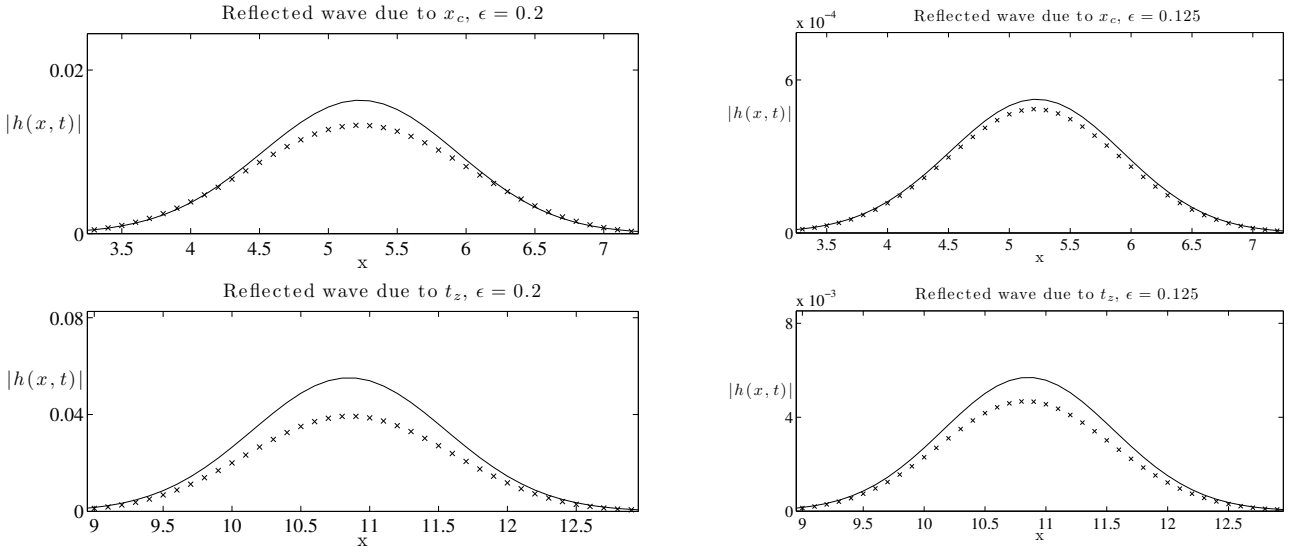

Figure 3.7: Numerical estimate of the reflected waves as a function of x with $c(x,t) = c_1(x)c_2(t)$ as (iv); ($\times$), and $x_0 = 6$. The straight lines denote the asymptotic estimate in (3.81). The varying values of ϵ are noted above each of the plots. The top two panels (left $\epsilon = 0.2$ and right $\epsilon = 0.125$) pertain to the reflected wave as a result of the spatial turning point ant the bottom two panels (left $\epsilon = 0.2$ and right $\epsilon = 0.125$) the temporal turning point.

Chapter 4

Conclusion and future work

4.1 Highlights

The main topic of interest in this thesis was to find an asymptotic estimate of the reflected wave(s) that necessarily appears as a result of a Stokes phenomenon associated with the transition points of $c_1(x)$ and $c_2(t)$ in the slowly varying wave equation (2.1). To achieve this goal we first inspected the canonical ODE's (2.7) and (2.47) that correspond to a continuously forced wave of fixed frequency (Chapter 2). Points of note from Chapter 2 are: the presentation of two methods that appear to expedite the recovery of the results of [13] and [38]. Also of interest in Chapter 2 was the (apparent) discovery of a set of functions, whose behaviour local to a branch point root x_* of $c_1(x)$ was given in (2.128), for which there is no Stokes phenomenon. That is, there exits a countable set of α_1 values, see (2.120), for which there is no wave reflection in (2.7). However, the neighbours of such values e.g.

$$\alpha_1 = -1 - \frac{1}{2\mathbb{N}+1} \pm \delta : \ 0 < \delta \ll 1,$$

do give rise to an exponentially small reflected wave in (2.7). Examples of speed profiles that satisfy the above were given in §2.5.

The main result of the thesis is given in Chapter 3 equation (3.81), where an explicit estimate of the reflected wave in (2.1) was shown. On the whole, (3.81) leads to the conclusion that the results of ODE (2.7) and the PDE (2.1) are markedly different. These details are summarised below.

A note on the differences between the ODE (2.7) and PDE (2.1) environments

We conclude therefore, from the result in (3.81) which is repeated in §3.3 and §3.4, that: for non-constant $c_1(x)$ the idea that a reflected wave, generated by a Stokes phenomenon in (2.1), is pre-factored by an exponentially small function of ϵ as in (2.7) e.g. (2.40), appears to be invalid. Such a conclusion may have been drawn from the results of [13] and [38] on first inspection. It is infact found that a non-trivial phase of the reflected wave, e.g. $\theta_+(x,t)$ in (3.1) where $\theta_+(x,t) = \mathcal{D}_1(\xi_+(x,t))$ given in (3.36), contains the 'beyond all orders' requirement of a subdominant solution.

This idea is highlighted by the role of $B(\epsilon)$ in the WKBJ solutions of (2.7), given in (2.9), and the WKBJ solutions of (2.1), given in (3.1). It has been known for some time (c.f. §1) that $B(\epsilon)$ is exponentially small in, the ODE environment, (2.9), c.f. (2.40). However, in the PDE environment (2.1), $B(\epsilon)$ in (3.1) was given in (3.119) where it was shown that $B(\epsilon) = K_1(\epsilon) \sim -2\mathrm{i}\cos(\nu_1\pi)$ from (3.149) and hence $B(\epsilon) = \mathcal{O}(1)$. Therefore, the exponential smallness of the reflected wave in (2.1) is coming from the object $\mathrm{e}^{\mathrm{i}\theta_+/\epsilon}$ in (3.1) and not the pre factor function of ϵ, $B(\epsilon)$. These ideas are summarised in the table below:

	ODE	PDE
$\lvert B(\epsilon)\rvert$	$\mathcal{O}(\mathrm{e}^{-\beta_1/\epsilon})$	$\mathcal{O}(1)$
$\lvert \mathrm{e}^{\mathrm{i}\theta_+/\epsilon}\rvert$	$\mathcal{O}(1)$	$\leq \mathcal{O}(\mathrm{e}^{-\beta_2/\epsilon})$

where $\beta_1 = 2\big|g_1(x_*)\big|$ and $\beta_2 = \inf\big|\mathcal{D}_1(x,t)\big| : \ (x,t) \in \mathbb{R}^2$. Recalling that the phase of the reflected wave in (2.7) was given by $\theta_+(x) = \int_0^x 1/c_1(x')dx'$ and the phase of the reflected wave in (2.1), $\theta_+(x,t)$, was evaluated in (3.10) where $\mathcal{D}_+ = \mathcal{D}_1$ was given in (3.36) and ξ_+ was given in (3.6). Hence, the notion that the subdominant solutions of (2.1) along the real line are pre-factor by an exponentially small function of ϵ is not valid in the PDE environment (2.1). The exception to this is when $c_1(x)$ is constant, see §3.5.2.

An additional highlight noted from the result (3.81) is the appearance of the reflected phase in the argument of the initial condition function $f(x - x_0)$. This matter spotlights that: the location of the centre of the reflected wave-packet is translated away from the naive assumption (deduced via the characteristic parameter ξ_+ in (3.6)) that the reflected wave is centred around $x = g_1^{-1}\big(g_1(x_0) - g_2(t)\big)$, for some time $t > 0$.

4.2 Future projects

4.2.1 $\alpha_1 = -1$: Chapman and Mahony

Here we highlight an error in the result of [13], via a numerical simulation. The error appears in the calculation for the reflected wave amplitude when the transition point nearest the real axis is a zero (of order 1) of $c_1(x)$, where

$$\begin{aligned} c_1(x) &= \frac{1+x^2}{(1+a)+x^2}, \quad -1 < a, \\ \text{and} \quad g_1(x) &= x + a\arctan(x). \end{aligned} \tag{4.1}$$

Note, when $a > 0$ in (4.1) then the transition point closest to the real axis is a zero of order 1. Using the nomenclature of (2.22), $\alpha_1 = -1$ at the point $x_* = \mathrm{i}$. This situation was not covered in chapter 2, see §2.9. However, [13] reports results for $a \in (-1,0) \cup (0,\infty)$:

$$B(\epsilon) = \mathrm{i}\sqrt{2}\mathrm{e}^{-2g_1\left(\mathrm{i}\sqrt{1+a}\right)/\epsilon}(1+\mathcal{O}(\epsilon)) \qquad -1 < a < 0, \tag{4.2}$$

$$\text{and} \quad B(\epsilon) \sim -\mathrm{i}2\sqrt{2}\mathrm{e}^{-2g_1\left(\mathrm{i}\sqrt{1+a}\right)/\epsilon}\cos(a\pi/\epsilon), \quad a > 0. \tag{4.3}$$

Eq. (4.2) and (4.3) were investigated numerically using the same scheme as §2.5, the results of which are displayed in Figure 4.1. When $-1 < a < 0$, the estimate (4.2) returns the result in (2.50) with $\alpha_1 = 1$. With $a > 0$ the estimate (4.3) appears inaccurate (in general and specifically) when $a = 1/2$ and $a = 1/10$. The only parameter that is changed in the two numerical estimates is a. Hence, with some conviction we can claim that the estimate given in [13] for the case when $a > 0$ requires correction. Interestingly, Figure 4.1 suggests that, for $a = 1/2$ or $a = 1/10$ the leading order amplitude of the reflected wave is ϵ independent.

Possible approach

We aim to find an explicit estimate for the reflected wave that matches the results in Figure 4.1 by switching (2.1) to a related Riccati equation

$$v'(x) + v^2(x) + \left(\frac{1}{c_1^2(x)\epsilon^2} - \frac{c_1''(x)}{c_1(x)}\right) = 0, \tag{4.4}$$

where we have substituted $v(x) = \frac{y'(x)}{y(x)} + \frac{c_1'(x)}{c_1(x)}$ in (2.7). The benefits of performing such a procedure are noted on substitution of the ansatz

$$v(x) = \sum_{n=-1}^{\infty} \kappa_n(x)\epsilon^n, \tag{4.5}$$

into (4.4). Then, the recurrence relation that necessarily appears for the κ_n's does not contain an arbitrary constant of integration like (2.57), therefore, many κ_n coefficients can be computed (near the point of interest). It follows that the point at $x = \mathrm{i}$ is of particular interest as it is a singular point for every odd indexed coefficient in the expansion (4.5). The up-shot is that a resurgence relation, e.g. (2.62), can be employed so as to numerically calculate the Stokes multiplier (associated with the transition point closest to the real axis) for $n \gg 1$. Hence, an estimate for the reflected wave amplitude will hopefully be achieved.

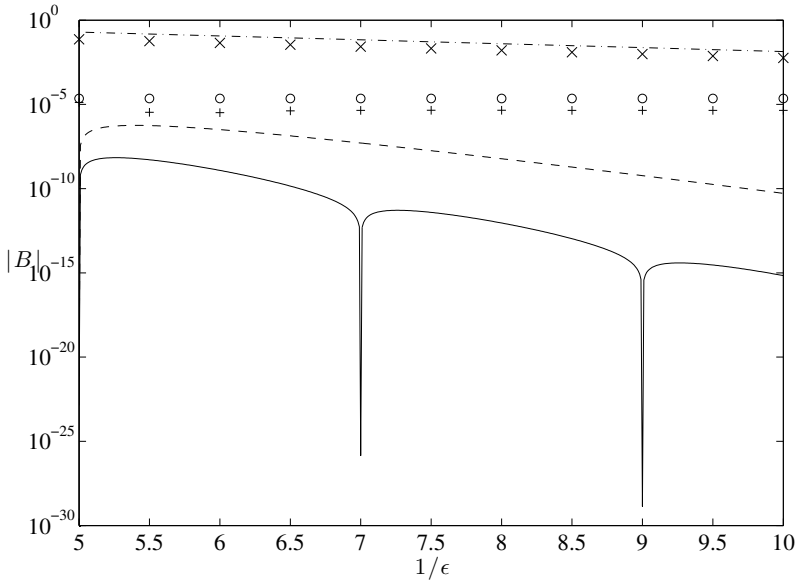

Figure 4.1: Numerical estimate of the amplitude of the reflected wave as a function of $1/\epsilon$ for $c_1(X) = \frac{1+X^2}{(1+a)+X^2}$. (i) $a = -1/2$: $\times$ denote the numerical solution and the asymptotic estimate (4.3)[=(2.40)] is given by the dash dot line. (ii) $a = 1/2$: $\circ$ denote the numerical solution and the asymptotic estimate (4.3) is shown by the solid line. (iii) $a = 1/10$: $+$ denote the numerical solution and the asymptotic estimate (4.3) is given by the dashed line.

4.2.2 No Stokes phenomenon

The main result of §2.7.1 suggests that: if (2.7) contains a speed profile whose behaviour near a branch point root x_* of $c_1(x)$ is given by (2.128), then x_* is not a turning point of (2.7), i.e. no Stokes phenomenon is detected. Although (2.129) was tested numerically for several values of α_1 in (2.120), the analytical result relies on the validity of (2.124). Hence, we wish to find a stronger analytical method that concludes a Stokes phenomenon is not present, possibly by re-scaling the ODE (2.7) in such a way that all of the coefficients of the initial solution in (2.9) are regular at x_*. In this way we could be sure that x_* does not constitute a turning point of (2.7). On first inspection, finding a particular substitution appears to be non-trivial.

4.2.3 Solution of (2.1) for an arbitrary spatio-temporal wave speed

Another project of particular importance is to inspect the solutions of

$$\partial_t^2 h(x,t) = \partial_x\big(c^2(x,t)\partial_x h(x,t)\big), \tag{4.6}$$

with initial conditions

$$\begin{aligned} h(x,0) &= f(x-x_0)\mathrm{e}^{\mathrm{i}k_0 x/\epsilon}, \quad \epsilon \to 0, \\ \text{and} \quad \partial_t h(x,0) &= c(x,0)\partial_x h(x,0), \end{aligned} \tag{4.7}$$

where $c(x,t)$ is an arbitrary function of x and t that is analytic on the real plane and

$$c(x,t) \in \mathbb{R} > 0: \quad x,t \in \mathbb{R}.$$

Again, $f(x-x_0)$ is some localised (entire) function and k_0, $x_0 \in \mathbb{R}/\{0\}$. In addition, $c(x,t)$ has particular (transition) regions where the holomorphicity of $c(x,t)$ and $1/c(x,t)$ is lost. Such regions are similar in nature to the transition points of Chapter 2 and Chapter 3. The aim is then to deduce an estimate for the reflected wave that necessarily appears due to a Stokes phenomenon associated with the 'transition regions' of $c(x,t)$.

Preliminary results

The ansatz (3.1) is trialled as solution to (4.6) and following the same technique that led to the results (3.2), (3.3), (3.18) and (3.21) leads to:

$$\frac{d}{ds_\pm} = \partial_t \pm c(x,t)\partial_x \quad \Longrightarrow \quad ds_\pm = dt \quad \text{and} \quad \frac{dx}{ds_\pm} = \mp c(x,t), \tag{4.8}$$

$$\begin{aligned} \frac{da_0}{ds_-} &= -\frac{dc}{ds_-}\frac{a_0}{2c}, \\ \frac{db_0}{ds_+} &= -\frac{dc}{ds_+}\frac{b_0}{2c}, \end{aligned} \tag{4.9}$$

and

$$\begin{aligned} 2\mathrm{i}\frac{d}{ds_-}\hat{a}_{n+1} &= \left((c\partial_x\hat{a}_n)_x - \left(c^{-1}\partial_t\hat{a}_n\right)_t - Q(x,t)\hat{a}_n\right)/\partial_x\theta_-, \\ 2\mathrm{i}\frac{d}{ds_+}\hat{b}_{n+1} &= \left(\left(c\partial_x\hat{b}_n\right)_x - \left(c^{-1}\partial_t\hat{b}_n\right)_t - Q(x,t)\hat{b}_n\right)/\partial_x\theta_+ \end{aligned} \tag{4.10}$$

where,

$$Q(x,t) = c_{xx}/2 + \frac{(c_x)^2}{4c} + 3\frac{(c_t)^2}{c^3}/4 - c_{tt}/2. \tag{4.11}$$

The parameters $s_\pm$ correspond to the characteristic parameters s_- and s_+, associated with waves travelling in the direction of decreasing, $-$, or increasing, $+$, x. It follows that the phase of the transmitted and reflected waves obey

$$\text{(i)}\ \frac{d\theta_-}{ds_-} = 0, \qquad \text{(ii)}\ \frac{d\theta_+}{ds_+} = 0. \tag{4.12}$$

In the case of a separable wave speed $c(x,t) = c_1(x)c_2(t)$ in Chapter 3 the solutions of (4.8), given by equation (3.3) in Chapter 3, were determined for all points on the initial data line, e.g. $\xi(x,0) = x$ in (3.6). However, in the current set-up this is not possible. To solve (4.8) for

$x(t,\xi)$ an initial value of ξ must be chosen. Therefore, let $x = \xi_0$ at $t = 0$, hence (4.8) reads

$$\int_{\xi_0}^{x} dx' = \int_0^t c(x(t',\xi_0),t')dt' \quad \Longrightarrow \quad x(t,\xi_0) = \xi_0 + \int_0^t c(x(t',\xi_0),t')dt'. \tag{4.13}$$

In this way, (4.13) represents the characteristic curve for a ray starting at ξ_0. The solution of (4.13) is found by employing a Runge–Kutta method. The idea that each ray tube, of the initial solution, undergoes a Stokes Phenomenon on crossing a Stokes line in the real (x,t) plane was discussed in Chapter 3. This detail forms the backbone of the analysis in the case where $c(x,t)$, is some arbitrary function of x and t. The method we propose to solve (4.6) is to concentrate initially on a single ray-tube starting at $x = \xi_0$, e.g. Figure 4.2. The path along which the ray travels is found by solving for the $x(t,\xi_0)$ in (4.13) and the ray experiences a wave speed $c(x,t) = c(x(t,\xi_0),t)$. Hence, we can uniquely identify the transition points of $c(x(t,\xi_0),t)$ as the points where

$$t_* : \quad c(x(t,\xi_0),t) \to \infty \quad \text{as} \quad t \to t_*, \tag{4.14}$$

$$\text{and} \quad t_* : \quad c(x(t,\xi_0),t) \to 0 \quad \text{as} \quad t \to t_*. \tag{4.15}$$

We focus on finding the form of the reflected rays switched on as the DSR, see §3.1.1, cross a Stokes line whose location is determined by (possibly) $\Re\big(x(t_*,\xi_0)\big)$ for every ξ_0 in a localised region of x_0. The solution of (4.6) is then considered by interpolating between each of the DSR and SSR at every time step.

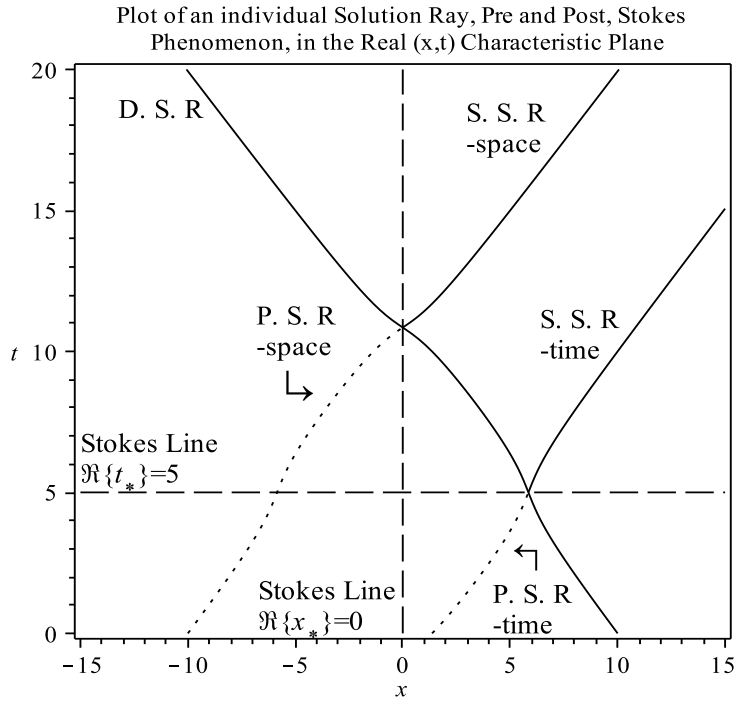

Figure 4.2: The path of a single characteristic initially at $\xi_0 = 10$. The ray experiences a Stokes phenomenon upon crossing Stokes lines in the real x-t plane. D. S. R stands for dominant solution ray, S. S. R is subdominant solution ray and P. S. R is pre-Stokes (phenomenon) ray.

Alternatively, a possible way of determining the form of the reflected wave would be to perform late term analysis on the coefficients in (4.10) directly.

Appendix A

Local matching approach for the case of special $\hat{\alpha}$ values in §2.7.1

Here we present details that return the result of (2.116) more efficiently.

We aim to find the solutions of (2.82) in the case where $\hat{\alpha} = 2p \in \mathbb{N}$ in (2.87). Recall (2.82) and (2.83),

$$v''(X) + \big(\epsilon^{-2} - Q(X)\big)v(X) = 0, \tag{A.1}$$
$$\text{and} \quad Q = \frac{c''(X)}{2c(X)} - \frac{c'(X)}{2c(X)} \quad \text{where} \quad X = \int_0^x \frac{dx'}{c_1(x')}.$$

As discussed in §(2.7.1), (2.87) requires an additional term so as to capture the leading order estimate of the Stokes multiplier in (2.82). Introducing $z = X - X_*$, we let

$$c(X) \sim \gamma \mathrm{e}^{-\mathrm{i}\pi p} z^{-2p}\,(1 + kz): \quad z \to 0,\, k \neq 0,$$

and thus

$$Q \sim p(p+1)z^{-2} - kpz^{-1}.$$

Eq(A.1) near X_* is then

$$v'' + (\epsilon^{-2} - p(p+1)z^{-2} + kpz^{-1})v = 0. \tag{A.2}$$

The solutions of (A.2) can be shown to be

$$v \sim C(\epsilon) M_{-\mathrm{i}kp\epsilon/2,p+1/2}\,(2\mathrm{i}z/\epsilon) + D(\epsilon) W_{-\mathrm{i}kp\epsilon/2,p+1/2}\,(2\mathrm{i}z/\epsilon)\,,$$

where M and W are Whittaker confluent hypergeometric functions. Therefore, by incorporating one additional term in the expansion of $c(X)$ in (2.811), the local form of (2.82) changes from a Bessel equation to a Whittaker equation. From [25],

$$M_{-\mathrm{i}kp\epsilon/2,p+1/2}\,(2\mathrm{i}z/\epsilon) \sim \hat{C}(\epsilon)\mathrm{e}^{\mathrm{i}z/\epsilon} z^{\mathrm{i}kp\epsilon/2} \sum_{s=0}^{\infty} \frac{(-p - \mathrm{i}kp\epsilon/2)_s (1 + p - \mathrm{i}kp\epsilon/2)_s}{s!} \left(\frac{\epsilon}{2\mathrm{i}z}\right)^s,$$

where $(-p - \mathrm{i}kp\epsilon/2)_s$ and $(1 + p - \mathrm{i}kp\epsilon/2)_s$ are Pochhammer symbols. The above is compared with the standard ansatz $v \sim \mathrm{e}^{\mathrm{i}X_*/\epsilon}\mathrm{e}^{\mathrm{i}z/\epsilon} \sum_{n=0}^{\infty} a_n(z)\epsilon^n$ in (2.91). Choosing $\hat{C}(\epsilon)$ appropriately and substituting $z^{\mathrm{i}kp\epsilon/2} = 1 - \mathrm{i}kp\ln(z)\epsilon/2 + \mathcal{O}(\epsilon^2)$, then:

$$a_n \sim \frac{(-p)_n (p+1)_n}{n!} (2\mathrm{i}z)^{-n}, \quad n \leq p,$$
$$a_{p+1} \sim (-)^p \frac{kp}{2\mathrm{i}} \frac{(2p)!}{p!} \frac{\ln(z)}{(2\mathrm{i}z)^p}$$

$$\text{and} \quad a_n \sim (-)^p \frac{kp}{2\mathrm{i}} \frac{(n-p-2)!(n+p-1)!}{(n-1)!} (2\mathrm{i}z)^{-(n-1)}, \quad n \geq p+2. \tag{A.3}$$

The results in (A.3) return (2.114). Hence, as $z \to 0$,

$$a_n \sim (-)^p \frac{kp}{2\mathrm{i}} \frac{\Gamma(n-1)}{(2\mathrm{i}z)^{(n-1)}}, \quad n \to \infty,$$

using (2.72), which recovers the result in (2.115), more efficiently, and leads to (2.116).

Appendix B

Fourier transform of a wave equation with a spatially varying wave speed

Here we consider the 1-dimensional shallow-water equations, without background rotation, linearised about the rest state $h = H(x)$ and $u = 0$,

$$h_t + (H(x)u)_x = 0 \quad \text{and} \quad u_t + g(t)h_x = 0, \tag{B.1}$$

see [12] for more, where the subscripts x and t denote partial differentiation w.r.t. x and t respectively. Note, we consider a time dependent gravity, $g(t)$ (which can be realised experimentally in an accelerated tank). With $c(x,t) = \sqrt{g(t)H(x)}$ denoting the spatio-temporal wave speed, we have,

$$h_{tt} = (c^2(x,t)h_x)_x. \tag{B.2}$$

In what follows, we aim to solve (B.2) with a speed profile $c(x,t)$ that includes, but is not restricted to, $c(x,t) = \sqrt{g(t)H(x)}$. For convenience (2.1) is rearranged into a system of first order PDEs,

$$\mathbf{X}_t = A\mathbf{X}, \tag{B.3}$$

where

$$\mathbf{X} = \begin{pmatrix} h \\ h_t \end{pmatrix},$$

$$A = \begin{pmatrix} 0 & 1 \\ \partial_x(c^2(x,t)\partial_x) & 0 \end{pmatrix} = JH = \begin{pmatrix} 0 & 1 \\ -1 & 0 \end{pmatrix} \begin{pmatrix} -(c^2(x,t)\partial_x)_x & 0 \\ 0 & 1 \end{pmatrix}. \tag{B.4}$$

We examine the propagation of a wavepacket in a slowly varying medium by considering an initial condition of the form

$$h(x,0) = \mathrm{e}^{\mathrm{i}k_0 x/\epsilon} f(x - x_0), \tag{B.5}$$

here $0 < \epsilon \ll 1$ and $f(x - x_0)$ is a localised function (e.g. Gaussian) centred at $x_0 > 0$, and

$$h_t(x,0) = c(x,0)h_x(x,0) = c(x,0)\left(\mathrm{i}k_0/\epsilon + \frac{f'(x-x_0)}{f(x-x_0)}\right) h(x,0), \tag{B.6}$$

which describes an initial wavepacket moving to the left and upon crossing a Stokes-line in the x-t plane produces an exponentially small right propagating reflected wavepacket. We aim to compute the reflected wavepacket using asymptotics.

Spectral analysis

In this section we analyse the case when $c(x,t) = c(x)$, so as to simplify the analysis in the first instance before moving on to the more difficult problem of a general spatio-temporal $c(x,t)$. Note, $c(x)$ is chosen so that the transition point nearest to the real axis is a branch point singularity x_* of $c(x)$. The formal solution of (B.3) is,

$$\mathbf{X}(x,t) = \mathrm{e}^{At}\mathbf{X}(x,0), \quad A = \begin{pmatrix} 0 & 1 \\ \partial_x(c^2(x)\partial_x) & 0 \end{pmatrix}. \tag{B.7}$$

Letting $F(A) = \mathrm{e}^{At}$ we investigate (B.7) using the Riesz-Dunford integral(see [53] searching 'Dunford integral'),

$$F(A) = \frac{1}{2\pi\mathrm{i}}\oint_{\Gamma_c} F(\lambda)(A-\lambda I)^{-1}d\lambda, \tag{B.8}$$

where the contour Γ_c contains all values of λ in the spectrum of A, i.e. $\lambda \in \sigma(A)$ such that $(A-\lambda I)$ is singular, see [53]. Eq. (B.8) is valid since $F(\lambda)$ is holomorphic. With

$$\mathbf{X}(x,t) = F(A)\mathbf{X}(x,0), \tag{B.9}$$

the objective is to find the spectrum of the operator A. To achieve this we evaluate the solutions to

$$(A-\lambda I)^{-1}\begin{pmatrix} p(x) \\ q(x) \end{pmatrix} = \begin{pmatrix} m(x,\lambda) \\ n(x,\lambda) \end{pmatrix}, \tag{B.10}$$

which can be reduced to the following coupled set of equations,

$$\begin{aligned} p(x) &= -\lambda m(x,\lambda) + n(x,\lambda), \\ q(x) &= \frac{d}{dx}(c^2(x)\frac{d}{dx}m(x,\lambda)) - \lambda n(x,\lambda). \end{aligned}$$

Combining the above gives

$$L[m(x,\lambda)] = q(x) + \lambda p(x) = r(x,\lambda), \quad m(\pm\infty,\lambda) \to 0, \tag{B.11}$$

where,

$$L = \frac{d}{dx}\left(c^2(x)\frac{d}{dx}\right) - \lambda^2. \tag{B.12}$$

Eq. (B.11) can be solved using a Green's function, $G(x,x',\lambda)$, defined by

$$L\left\{G(x,x',\lambda)\right\} = \delta(x-x') \quad \text{so that} \quad m(x,\lambda) = \int_{-\infty}^{\infty} G(x,x',\lambda)r(x',\lambda)dx'. \tag{B.13}$$

Finding the Green's function

Let $\phi_i(x,\lambda)$, $\mathrm{i} = 1 \to 4$, be non-trivial solutions to the homogeneous version of (B.11),

$$L[\phi_i(x,\lambda)] = 0, \quad \phi_i(\pm\infty,\lambda) \to 0. \tag{B.14}$$

As $x \to \pm\infty$, the functions $\phi_i(x,\lambda)$ have the following asymptotic relations

$$\begin{aligned} \phi_1(x,\lambda) &\sim c_-^{-1/2}\mathrm{e}^{\frac{\lambda}{c_-}x}, \quad x \to -\infty, \\ \phi_2(x,\lambda) &\sim c_-^{-1/2}\mathrm{e}^{\frac{-\lambda}{c_-}x}, \quad x \to -\infty, \\ \phi_3(x,\lambda) &\sim c_+^{-1/2}\mathrm{e}^{\frac{\lambda}{c_+}x}, \quad x \to +\infty, \\ \text{and} \quad \phi_4(x,\lambda) &\sim c_+^{-1/2}\mathrm{e}^{\frac{-\lambda}{c_+}x}, \quad x \to +\infty, \end{aligned} \tag{B.15}$$

and have following connection relations,

$$\phi_1(x,\lambda) + R(\lambda)\phi_2(x,\lambda) = T(\lambda)\phi_3(x,\lambda), \quad \lambda \in \mathrm{i}\mathbb{R} \tag{B.16}$$

$$\text{and} \quad \phi_4(x,\lambda) + \hat{R}(\lambda)\phi_3(x,\lambda) = \hat{T}(\lambda)\phi_2(x,\lambda), \quad \lambda \in \mathrm{i}\mathbb{R}. \tag{B.17}$$

$R(\lambda)$, $\hat{R}(\lambda)$, $T(\lambda)$ and $\hat{T}(\lambda)$ can be thought of as the reflected and transmitted wave amplitudes.

With $L(G(x,x',\lambda)) = 0$ when $x \neq x'$ in (B.13) and $G(x,x',\lambda)$ continuous, we can construct the Green's function from the homogeneous solutions above, noting that the boundary conditions require

$$G(x,x',\lambda) \to 0 \quad \text{as} \quad x \to \pm\infty. \tag{B.18}$$

We now look at the two cases where $\Re(\lambda) > 0$ and $\Re(\lambda) < 0$. When $\Re(\lambda) > 0$ we have

$$G_+(x,x',\lambda) = \begin{cases} a(x')\phi_1(x,\lambda) & \text{for } x \leq x', \\ b(x')\phi_4(x,\lambda) & \text{for } x \geq x'. \end{cases}$$

However, the continuity condition $G(x'_+,x',\lambda) = G(x'_-,x',\lambda)$, requires $a(x')\phi_1(x',\lambda) = b(x')\phi_4(x',\lambda)$ and thus

$$G_+(x,x',\lambda) = C(x') \begin{cases} \phi_1(x,\lambda)\phi_4(x',\lambda) & \text{for } x \leq x', \\ \phi_4(x,\lambda)\phi_1(x',\lambda) & \text{for } x \geq x'. \end{cases} \tag{B.19}$$

Similarly, for $\Re(\lambda) < 0$,

$$G_-(x,x',\lambda) = D(x') \begin{cases} \phi_2(x,\lambda)\phi_3(x',\lambda) & \text{for } x \leq x', \\ \phi_3(x,\lambda)\phi_2(x',\lambda) & \text{for } x \geq x'. \end{cases} \tag{B.20}$$

Expressions for $C(x')$ and $D(x')$ come from the so called 'jump condition'. To derive this, we return to (B.13) and consider first $\Re(\lambda) > 0$, setting up the following integral to find an expression for $C(x')$,

$$\int_{x'-\hat{\epsilon}}^{x'+\hat{\epsilon}} (c^2(x)G_+(x,x',\lambda)_x)_x - \lambda^2 G_+(x,x',\lambda)dx = \int_{x'-\hat{\epsilon}}^{x'+\hat{\epsilon}} \delta(x-x')dx, \quad \hat{\epsilon} \to 0.$$

With (B.19) and $G(x,x',\lambda)$ continuous,

$$C(x')c^2(x')\left(\phi_4'(x',\lambda)\phi_1(x',\lambda) - \phi_1'(x',\lambda)\phi_4(x',\lambda)\right) = 1.$$

Therefore,

$$C(x') = \frac{1}{c^2(x')W_+(x')} = \frac{1}{V_+(x')} \tag{B.21}$$

in (B.19), where

$$W_+(x') = \begin{vmatrix} \phi_1(x',\lambda) & \phi_4(x',\lambda) \\ \phi_1'(x',\lambda) & \phi_4'(x',\lambda) \end{vmatrix}.$$

Similarly we find

$$D(x') = \frac{1}{c^2(x')W_-(x',\lambda)} = \frac{1}{V_-(x',\lambda)} \tag{B.22}$$

in (B.20), where

$$W_-(x') = \begin{vmatrix} \phi_2(x',\lambda) & \phi_3(x',\lambda) \\ \phi_2'(x',\lambda) & \phi_3'(x',\lambda) \end{vmatrix}.$$

In a Sturm–Liouville problem, as in (B.14), the Green's functions are symmetric, i.e. $G_\pm(x,x',\lambda) = G_\pm(x',x,\lambda)$. To prove this for (B.14), it suffices to show that both $C(x')$ and $D(x')$ are constants, which is shown in Appendix D. In the special situation where $\lambda = \mathrm{i}\omega$ with $\omega \in \mathbb{R}$, it

useful to note that

$$\begin{aligned}\phi_2(x,\omega) &= \bar{\phi}_1(x,\omega),\\ \phi_4(x,\omega) &= \bar{\phi}_3(x,\omega).\end{aligned} \tag{B.23}$$

Additionally, when $\lambda = \mathrm{i}\omega$ it is shown in the Appendix E that

$$V_+(x',\omega) = \bar{V}_-(x',\omega) = -\frac{2\mathrm{i}\omega}{\bar{T}(\omega)}, \tag{B.24}$$

and the Green's function for (B.14) is

$$G_+(x,x',\omega) = \frac{\mathrm{i}\bar{T}(\omega)}{2\omega}\begin{cases}\phi_1(x,\omega)\phi_4(x',\omega) & \text{for } x \le x',\\ \phi_4(x,\omega)\phi_1(x',\omega) & \text{for } x \ge x'.\end{cases} \tag{B.25}$$

$$G_-(x,x',\omega) = -\frac{\mathrm{i}T(\omega)}{2\omega}\begin{cases}\phi_2(x,\omega)\phi_3(x',\omega) & \text{for } x \le x',\\ \phi_3(x,\omega)\phi_2(x',\omega) & \text{for } x \ge x'.\end{cases}$$

In general,

$$G_+(x,x',\lambda) = \frac{1}{V_+(\lambda)}\begin{cases}\phi_1(x,\lambda)\phi_4(x',\lambda) & \text{for } x \le x',\\ \phi_4(x,\lambda)\phi_1(x',\lambda) & \text{for } x \ge x'.\end{cases}$$

$$G_-(x,x',\lambda) = \frac{1}{V_-(\lambda)}\begin{cases}\phi_2(x,\lambda)\phi_3(x',\lambda) & \text{for } x \le x',\\ \phi_3(x,\lambda)\phi_2(x',\lambda) & \text{for } x \ge x',\end{cases}$$

defined piecewise in λ.

Spectral analysis continued

From (B.9) we have that

$$\mathbf{X}(x,t) = F(A)\begin{pmatrix} h(x,0)\\ h_t(x,0)\end{pmatrix} = \frac{1}{2\pi\mathrm{i}}\oint_{\Gamma_c} \mathrm{e}^{\lambda t}(A-\lambda I)^{-1}\begin{pmatrix} h(x,0)\\ h_t(x,0)\end{pmatrix} d\lambda, \tag{B.26}$$

and

$$h(x,t) = \frac{1}{2\pi\mathrm{i}}\oint_{\Gamma_c} \mathrm{e}^{\lambda t}\int_{-\infty}^{\infty} G(x,x',\lambda)(c(x')h_x(x',0) + \lambda h(x',0))dx'd\lambda,$$

using (B.6), (B.10) and (B.11). Residues for the above integral are calculated when $\lambda \in \sigma(A)$. It is clear from (B.10), (B.13), (B.19) and (B.20) that the operator $A - \lambda I$ is singular when $\lambda = \mathrm{i}\omega$, $\omega \in \mathbb{R}$. Therefore, $\sigma(A) = \mathrm{i}\mathbb{R}$. Hence, the contour Γ_c in (B.26) 'loops' around the imaginary axis in the λ plane in a counter clockwise direction. In this case, $G_+(x,x',\lambda)$ is valid in the region to the right of $\lambda \in \mathrm{i}\mathbb{R}$ and $G_-(x,x',\lambda)$ to the left. That is,

$$h(x,t) = \frac{1}{2\pi}\int_{-\infty}^{\infty} \mathrm{e}^{\mathrm{i}\omega t}\int_{-\infty}^{\infty} \left(G_+(x,x',\omega) - G_-(x,x',\omega)\right)\left(\mathrm{i}\omega h(x',0) + h_t(x',0)\right)dx'd\omega. \tag{B.27}$$

We now aim to find an expression for $G_+(x,x',\omega) - G_-(x,x',\omega)$ in terms of the eigenfunctions $\phi_i(x,\omega)$.

Derivation of $G_+ - G_-$

Noting that (B.25) is symmetric in x and x', we proceed with the case when $x \le x'$.

$$G_+(x,x',\omega) - G_-(x,x',\omega) = \left(\frac{1}{V_+}\phi_1(x,\omega)\phi_4(x',\omega) - \frac{1}{V_-}\phi_2(x,\omega)\phi_3(x',\omega)\right)$$

$$= \frac{1}{|V_+|^2}\left(\bar{V}_+\phi_1(x,\omega)\phi_4(x',\omega) - V_+\phi_2(x,\omega)\phi_3(x',\omega)\right)$$
$$= \frac{|T(\omega)|^2}{(2\omega)^2}\left(\frac{2\mathrm{i}\omega}{T(\omega)}\phi_1(x,\omega)\phi_4(x',\omega) + \frac{2\mathrm{i}\omega}{\bar{T}}\phi_2(x,\omega)\phi_3(x',\omega)\right)$$
$$= \frac{\mathrm{i}}{2\omega}\left(\bar{T}(\omega)\phi_1(x,\omega)\phi_4(x',\omega) + T(\omega)\bar{\phi}_1(x,\omega)\bar{\phi}_4(x')\right), \qquad \text{(B.28)}$$

on using (B.24)and (B.23). Then, employing (B.16) and (B.17), it follows that

$$G_+(x,x',\omega) - G_-(x,x',\omega) = \frac{\mathrm{i}}{2\omega}\left(\phi_1(x,\omega)\left(\bar{\phi}_1(x') + \bar{R}(\omega)\phi_1(x',\omega)\right) + \bar{\phi}_1(x,\omega)\left(\phi_1(x',\omega) + R(\omega)\bar{\phi}_1(x')\right)\right)$$
$$= \frac{\mathrm{i}}{2\omega}\Big(\bar{\phi}_1(x,\omega)\phi_1(x',\omega) + \phi_1(x,\omega)\bar{\phi}_1(x')$$
$$+\bar{R}(\omega)\phi_1(x,\omega)\phi_1(x',\omega) + R(\omega)\bar{\phi}_1(x,\omega)\bar{\phi}_1(x')\Big). \qquad \text{(B.29)}$$

Noting that the above is purely imaginary our aim is to have a set up of the form,

$$G_+(x,x',\omega) - G_-(x,x',\omega) = E(\omega)\left(\Phi(x,\omega)\bar{\Phi}(x',\omega) + \bar{\Phi}(x,\omega)\Phi(x',\omega)\right).$$

To achieve this we set

$$\Phi(x,\omega) = \alpha\phi_1(x,\omega) + \beta\bar{\phi}_1(x,\omega).$$

Therefore,

$$\Phi(x,\omega)\bar{\Phi}(x',\omega) + \bar{\Phi}(x,\omega)\Phi(x',\omega)$$
$$= \left(\alpha\phi_1(x,\omega) + \beta\bar{\phi}_1(x,\omega)\right)\left(\bar{\alpha}\bar{\phi}_1(x',\omega) + \bar{\beta}\phi_1(x',\omega)\right) + \left(\bar{\alpha}\bar{\phi}_1(x,\omega) + \bar{\beta}\phi_1(x,\omega)\right)\left(\alpha\phi_1(x',\omega) + \beta\bar{\phi}_1(x')\right)$$
$$= (|\alpha|^2 + |\beta|^2)\left(\phi_1(x,\omega)\bar{\phi}_1(x') + \bar{\phi}_1(x,\omega)\phi_1(x',\omega)\right) + 2\alpha\bar{\beta}\phi_1(x,\omega)\phi_1(x',\omega) + 2\bar{\alpha}\beta\bar{\phi}_1(x,\omega)\bar{\phi}_1(x,\omega). \qquad \text{(B.30)}$$

By comparing (B.30) with (B.29) we find

$$|\alpha|^2 + |\beta|^2 = 1 \quad \text{and} \quad 2\bar{\alpha}\beta = R(\omega). \qquad \text{(B.31)}$$

Combining the above

$$4|\alpha|^4 - 4|\alpha|^2 + |R(\omega)|^2 = 0,$$

and thus,

$$|\alpha|^2 = \frac{4 \pm \sqrt{16 - 16|R(\omega)|^2}}{8} = \frac{1}{2}\left(1 \pm |T(\omega)|\right),$$

where $|R|^2 + |T|^2 = 1$ shown in Appendix F equation (C.14). We choose $\alpha \in \mathbb{R}$ so that $\alpha = \frac{1}{\sqrt{2}}\sqrt{(1 \pm |T(\omega)|)}$ with

$$\beta = \frac{R}{2\alpha} \quad \text{and} \quad |\beta|^2 = \frac{1}{2}\left(1 \mp |T(\omega)|\right).$$

Thus,

$$\Phi(x) = \frac{1}{\sqrt{2}}\sqrt{(1 \pm |T(\omega)|)}\left(\phi_1(x,\omega) + \frac{R(\omega)}{(1 \pm |T(\omega)|)}\bar{\phi}_1(x,\omega)\right). \qquad \text{(B.32)}$$

When $c(x)$ is constant, $R(\omega) = 0$ and $T(\omega) = 1$. Therefore, it is preferential to choose the positive root to avoid $\frac{0}{0}$ on the right hand side of (B.32). This choice is verified by the fact that $\Phi = \phi_1$ in this situation which is exactly what we would have expected. Hence,

$$G_+(x,x',\omega)-G_-(x,x',\omega)=\frac{\mathrm{i}\gamma(\omega)}{4\omega}\left(\Psi(x,\omega)\bar{\Psi}(x',\omega)+\bar{\Psi}(x,\omega)\Psi(x',\omega)\right),\quad x\le x'.$$

The above is symmetric in (x,x') and therefore

$$G_+(x,x',\omega)-G_-(x,x',\omega)=\frac{\mathrm{i}\gamma(\omega)}{4\omega}\left(\Psi(x,\omega)\bar{\Psi}(x',\omega)+\bar{\Psi}(x,\omega)\Psi(x',\omega)\right),\quad \forall x, \tag{B.33}$$

with,

$$\Psi(x,\omega)=\phi_1(x,\omega)+\frac{R(\omega)}{\gamma(\omega)}\bar{\phi}_1(x,\omega)\quad\text{and}\quad\gamma(\omega)=1+|T(\omega)|. \tag{B.34}$$

Spectral Analysis continued

Introducing (B.33) into (B.27) we have

$$h(x,t)=\frac{-\mathrm{i}}{8\pi}\int_{-\infty}^{\infty}\mathrm{e}^{\mathrm{i}\omega t}\frac{\gamma(\omega)}{\omega}\left(\Psi(x,\omega)\int_{-\infty}^{\infty}\bar{\Psi}(x',\omega)\begin{pmatrix}\mathrm{i}\omega & 1\end{pmatrix}\mathbf{X}(x',0)dx'\right.$$
$$\left.+\bar{\Psi}(x,\omega)\int_{-\infty}^{\infty}\Psi(x',\omega)\begin{pmatrix}\mathrm{i}\omega & 1\end{pmatrix}\mathbf{X}(x',0)dx'\right)d\omega. \tag{B.35}$$

Therefore,

$$\mathbf{X}(x,t)=\begin{pmatrix}h(x,t)\\ h_t(x,t)\end{pmatrix}=\frac{-\mathrm{i}}{8\pi}\int_{-\infty}^{\infty}\mathrm{e}^{\mathrm{i}\omega t}\frac{\gamma(\omega)}{\omega}\left(\Psi(x,\omega)\int_{-\infty}^{\infty}\bar{\Psi}(x',\omega)\begin{pmatrix}\mathrm{i}\omega & 1\\ -\omega^2 & \mathrm{i}\omega\end{pmatrix}\mathbf{X}(x',0)dx'\right.$$
$$\left.+\bar{\Psi}(x,\omega)\int_{-\infty}^{\infty}\Psi(x',\omega)\begin{pmatrix}\mathrm{i}\omega & 1\\ -\omega^2 & \mathrm{i}\omega\end{pmatrix}\mathbf{X}(x',0)dx'\right)d\omega.$$

Which can be written as,

$$\mathbf{X}(x,t)\quad=\quad\begin{pmatrix}h(x,t)\\ h_t(x,t)\end{pmatrix}= \tag{B.36}$$

$$-\frac{\mathrm{i}}{8\pi}\int_{-\infty}^{\infty}\mathrm{e}^{\mathrm{i}\omega t}\frac{\gamma(\omega)}{\omega}\int_{-\infty}^{\infty}\left(\mathbf{\Psi}(x,\omega)\otimes\mathbf{\Psi}^{\dagger}(x',\omega)+\mathbf{\Psi}^{\dagger}(x,\omega)\otimes\mathbf{\Psi}(x',\omega)\right)\mathbf{X}(x',0)dx'd\omega,$$

where,

$$\mathbf{\Psi}(x,\omega)=\begin{pmatrix}\Psi(x,\omega)\\ \mathrm{i}\omega\Psi(x,\omega)\end{pmatrix},$$
$$\mathbf{\Psi}^{\dagger}(x,\omega)=\begin{pmatrix}\mathrm{i}\omega\bar{\Psi}(x,\omega)\\ \bar{\Psi}(x,\omega)\end{pmatrix}.$$

Hence, there are two independent eigenvectors for each ω: $\mathbf{\Psi}$ and $\mathbf{\Psi}^{\dagger}$, which are orthogonal. To prove orthogonality, we note

$$\hat{L}[\phi(x,\omega_i)]=-\omega_i^2\phi(x,\omega_i),$$
$$\hat{L}[\bar{\phi}(x,\omega_i)]=-\omega_i^2\bar{\phi}(x,\omega_i),$$
$$\hat{L}[\phi(x,\omega_j)]=-\omega_j^2\phi(x,\omega_j),$$
$$\hat{L}[\bar{\phi}(x,\omega_j)]=-\omega_j^2\bar{\phi}(x,\omega_j),$$

where $\hat{L}=c^2(x)\frac{d^2}{dx^2}+2c(x)\frac{dc(x)}{dx}\frac{d}{dx}$. Therefore, it follows that

$$\int_{-\infty}^{\infty}\bar{\phi}(x,\omega_j)\hat{L}[\phi(x,\omega_i)]-\phi(x,\omega_i)\hat{L}[\bar{\phi}(x,\omega_j)]dx\quad(\star)$$

$$= \left(\omega_i^2 - \omega_j^2\right) \int_{-\infty}^{\infty} \phi(x,\omega_i)\bar{\phi}(x,\omega_j) = 0, \tag{B.37}$$

on performing integration by parts once on the integral ($\star$) and using the initial conditions (B.14). Similarly, without the complex conjugation,

$$\begin{aligned}&\int_{-\infty}^{\infty} \phi(x,\omega_j)\hat{L}[\phi(x,\omega_i)] - \phi(x,\omega_i)\hat{L}[\phi(x,\omega_j)]dx \\ &= \left(\omega_i^2 - \omega_j^2\right) \int_{-\infty}^{\infty} \phi(x,\omega_i)\phi(x,\omega_j) = 0.\end{aligned} \tag{B.38}$$

Thus, with $i \neq j$, we have that

$$\int_{-\infty}^{\infty} \Psi(x,\omega_i)\bar{\Psi}(x,\omega_j)dx \tag{B.39}$$

$$= \int_{-\infty}^{\infty} \phi(x,\omega_i)\bar{\phi}(x,\omega_j) + \frac{\bar{R}(\omega_j)}{\gamma(\omega_j)}\phi(x,\omega_i)\phi(x,\omega_j) + \frac{R(\omega_i)}{\gamma(\omega_i)}\bar{\phi}(x,\omega_i)\bar{\phi}(x,\omega_j) + \left|\frac{R(\omega_i)}{\gamma(\omega_i)}\right|^2 \bar{\phi}(x,\omega_i)\phi(x,\omega_j)dx = 0.$$

Therefore, the $\Psi(x,\omega_i)$ form an orthogonal set which is much to be expected as the method outlined is analogous to the Fourier transform of (2.1). We can phrase (B.39) in terms of tensor products by setting $t = 0$ into (B.36),

$$\mathbf{X}(x,0) =$$

$$\int_{-\infty}^{\infty} \left(\int_{-\infty}^{\infty} \frac{-\mathrm{i}\gamma(\omega)}{8\pi\omega} \big(\mathbf{\Psi}(x,\omega) \otimes \mathbf{\Psi}^\dagger(x',\omega) + \mathbf{\Psi}^\dagger(x,\omega) \otimes \mathbf{\Psi}(x',\omega) \big) d\omega \right) \mathbf{X}(x',0)dx',$$

which reveals,

$$\int_{-\infty}^{\infty} \frac{\gamma(\omega)}{\omega} \left(\mathbf{\Psi}(x,\omega) \otimes \mathbf{\Psi}^\dagger(x',\omega) + \mathbf{\Psi}^\dagger(x,\omega) \otimes \mathbf{\Psi}(x',\omega) \right) d\omega = 8\mathrm{i}\pi\delta(x'-x)\mathbb{I},$$

where $\mathbb{I} = \begin{pmatrix} 1 & 0 \\ 0 & 1 \end{pmatrix}$. Therefore,

$$\int_{-\infty}^{\infty} \frac{\gamma(\omega)}{\omega} \left(\Psi(x,\omega)\bar{\Psi}(x',\omega) + \bar{\Psi}(x,\omega)\Psi(x',\omega) \right) \begin{pmatrix} \mathrm{i}\omega & 1 \\ -\omega^2 & \mathrm{i}\omega \end{pmatrix} d\omega = 8\pi\mathrm{i}\delta\mathbb{I}. \tag{B.40}$$

Comparing with the Fourier Transform

Eq. (B.35) with (B.5) and (B.6) reads as

$$\begin{aligned}h(x,t) \sim \frac{1}{8\pi} \int_{-\infty}^{\infty} \mathrm{e}^{i\frac{\omega'}{\epsilon}t} \frac{\gamma(\omega'/\epsilon)}{\omega'} \Bigg(&\Psi\left(x,\omega'/\epsilon\right) \int_{-\infty}^{\infty} \bar{\Psi}\left(x',\omega'/\epsilon\right) \mathrm{e}^{\mathrm{i}k_0 x'/\epsilon} f(x'-x_0) \left(k_0 c(x') + \omega'\right) dx'/\epsilon \\ &+ \bar{\Psi}(x,\omega'/\epsilon) \int_{-\infty}^{\infty} \Psi\left(x',\omega'/\epsilon\right) \mathrm{e}^{\mathrm{i}k_0 x'/\epsilon} f(x'-x_0) \left(k_0 c(x') + \omega'\right) dx'/\epsilon \Bigg) d\omega',\end{aligned} \tag{B.41}$$

where we have made the substitution $\omega = \frac{\omega'}{\epsilon}$. However, for convenience we shall omit the prime of ω' and x'. The Fourier transform of (2.1) with $c(x,t) = c(x)$, is

$$h(x,t) = \frac{1}{2\pi} \int_{-\infty}^{\infty} \mathrm{e}^{\mathrm{i}\omega t/\epsilon} \left(\hat{A}(\omega/\epsilon)\hat{u}_1(x,\omega/\epsilon) + \hat{B}(\omega/\epsilon)\hat{u}_2(x,\omega/\epsilon) \right) d\omega/\epsilon,$$

where $\hat{A}(\omega/\epsilon)$ and $\hat{B}(\omega/\epsilon)$ are the amplitudes of the linearly independent solutions to (2.1). Hence, with the orthogonal properties in (B.39) we can compare the above with (B.41), the

results of which are

$$\hat{u}_1(x,\omega/\epsilon) = \Psi(x,\omega/\epsilon), \quad \hat{u}_2(x,\omega/\epsilon) = \bar{\Psi}(x,\omega/\epsilon),$$
$$\hat{A}(\omega/\epsilon) \sim \frac{\gamma(\omega/\epsilon)}{2\omega\epsilon}\int_{-\infty}^{\infty} \bar{\Psi}(x,\omega/\epsilon)\,\mathrm{e}^{\mathrm{i}k_0 x/\epsilon} f(x-x_0)\,(k_0 c(x)+\omega)\,dx,$$
$$\text{and} \quad \hat{B}(\omega/\epsilon) \sim \frac{\gamma(\omega/\epsilon)}{2\omega\epsilon}\int_{-\infty}^{\infty} \Psi(x,\omega/\epsilon)\,\mathrm{e}^{\mathrm{i}k_0 x/\epsilon} f(x-x_0)\,(k_0 c(x)+\omega)\,dx.$$

Estimates of $\hat{A}(\omega/\epsilon)$ and $\hat{B}(\omega/\epsilon)$ are calculated by noting that the WKBJ (or Liouville-Green) solution to the problem (B.14), with $\lambda = \frac{\mathrm{i}\omega}{\epsilon}$ and $\omega > 0$, are

$$\phi_1(x,\omega/\epsilon) \sim c^{-1/2}(x)\left(\mathrm{e}^{\mathrm{i}\omega g(x)/\epsilon} + K(\omega/\epsilon)\,H(x-x_*)\mathrm{e}^{-\mathrm{i}\omega g(x)/\epsilon}\right) \quad \epsilon \to 0, \tag{B.42}$$

where

$$g(x) = \int_0^x 1/c(x')dx'. \tag{B.43}$$

$c^{-1/2}(x)\mathrm{e}^{\mathrm{i}\omega g(x)/\epsilon}$ is the dominant $\mathcal{O}(\epsilon)$ acurate solution and $K(\omega/\epsilon)\,H(x-x_*)\mathrm{e}^{-\mathrm{i}\omega g(x)/\epsilon}$ is the $\mathcal{O}(\mathrm{e}^{-\beta/\epsilon})$ 'recessive' solution. The recessive solution is switched on as the dominant solution passes a Stokes line crossing the real axis at $x = \Re(x_*)$, where x_* is a turning point of (2.1). The pre-factor

$$K(\omega/\epsilon) = 2\mathrm{i}\cos(\nu\pi)\mathrm{e}^{-\beta/\epsilon}, \tag{B.44}$$

is the so called Stokes multiplier with $\beta = |2\mathrm{i}g(x_*)|$, $\nu = \frac{2\alpha+1}{2\alpha+2}$ and $H(x-x_*)$ the Heaviside step function. (B.44) is valid for any $c(x)$ that takes the form

$$c(x) \sim \hat{\gamma}\mathrm{i}^{-\alpha/2}(x-x_*)^{-\alpha}, \qquad x \to x_*$$

where $\alpha > 0$ and $\hat{\gamma} \in \mathbb{R}$. It is worth noting that (B.2) contains two linearly independent solutions, as seen in (B.42), and thus the recessive solution does not represent a refinement to the dominant solution but is of a "qualitatively different nature" [38] , giving it dominant importance in some respects. It is shown in §G that

$$K(\omega/\epsilon) = -R(\omega/\epsilon).$$

Without loss of generality we let $\Re(x_*) = 0$ and employ the use of a Heaviside function to represent the switch on of a subdominant solution as the dominant solution crosses the Stokes line at the origin. Therefore,

$$\mathbf{\Psi}(x,\omega/\epsilon) = \begin{pmatrix} \phi_1(x,\omega/\epsilon) + \frac{R(\omega/\epsilon)}{2}\bar{\phi}_1(x,\omega/\epsilon) \\ \frac{\mathrm{i}\omega}{\epsilon}\left(\phi_1(x,\omega/\epsilon) + \frac{R(\omega/\epsilon)}{2}\bar{\phi}_1(x,\omega/\epsilon)\right) \end{pmatrix} \tag{B.45}$$
$$\sim c^{-1/2}(x)\begin{pmatrix} \mathrm{e}^{\mathrm{i}\omega g(x)/\epsilon} + K(\omega/\epsilon)\left(H(x)-\frac{1}{2}\right)\mathrm{e}^{-\mathrm{i}\omega g(x)/\epsilon} \\ \frac{\mathrm{i}\omega}{\epsilon}\left(\mathrm{e}^{\mathrm{i}\omega g(x)/\epsilon} + K(\omega/\epsilon)\left(H(x)-\frac{1}{2}\right)\mathrm{e}^{-\mathrm{i}\omega g(x)/\epsilon}\right) \end{pmatrix},$$

having set $\gamma(\omega/\epsilon) = 2$ in (B.34). Setting $\gamma(\omega/\epsilon) = 2$ is acceptable as

$$|T(\omega/\epsilon)| = 1 + \mathcal{O}\left(\mathrm{e}^{-2\beta/\epsilon}\right),$$

shown in Appendix F. Therefore,

$$\hat{A}(\omega/\epsilon) \sim 1/2\omega\epsilon\int_{-\infty}^{\infty} c^{-1/2}(x)\mathrm{e}^{-\mathrm{i}\omega g(x)/\epsilon}\mathrm{e}^{\mathrm{i}k_0 x/\epsilon} f(x-x_0)\mathrm{i}\,(k_0 c(x)+\omega)\,dx$$

$$+ \bar{K}\left(\omega/\epsilon\right)/2\omega\epsilon \int_{-\infty}^{\infty} \left(H(x) - \frac{1}{2}\right) c^{-1/2}(x) \mathrm{e}^{\mathrm{i}\omega g(x)/\epsilon + \mathrm{i}k_0 x/\epsilon} f(x - x_0)\left(k_0 c(x) + \omega\right) dx. \tag{B.46}$$

and

$$\hat{B}\left(\omega/\epsilon\right) \sim 1/2\omega\epsilon \int_{-\infty}^{\infty} c^{-1/2}(x) \mathrm{e}^{\mathrm{i}\omega g(x)/\epsilon} \mathrm{e}^{\mathrm{i}k_0 x/\epsilon} f(x - x_0)\left(k_0 c(x) + \omega\right) dx$$
$$+ K\left(\omega/\epsilon\right)/2\omega\epsilon \int_{-\infty}^{\infty} \left(H(x) - \frac{1}{2}\right) c^{-1/2}(x) \mathrm{e}^{-\mathrm{i}\omega g(x)/\epsilon + \mathrm{i}k_0 x/\epsilon} f(x - x_0)\left(k_0 c(x) + \omega\right) dx. \tag{B.47}$$

Stationary Phase

We use the method of stationary phase, see [1] or [44], to evaluate (B.41), (B.46) and (B.47), where any stationary points associated with $f(x - x_0)$ are dismissed due to the rapidly oscillating $O(1/\epsilon)$ phase functions $\mathrm{e}^{\pm \mathrm{i}\omega g(x)/\epsilon}$. Again, for convenience we drop the prime in x'. The dominant contribution from the integrals in (B.46) and (B.47) are when

$$\frac{\partial}{\partial x} p_1(x, \omega) = 0 \quad \text{and} \quad \frac{\partial}{\partial x} p_2(x, \omega) = 0,$$

where

$$p_1(x, \omega) = k_0 x - \omega g(x) \quad \text{and} \quad p_2(x, \omega) = k_0 x + \omega g(x).$$

Solving defines the two stationary points:

$$\omega = k_0 c(x_\omega^+) \quad \text{and} \quad \omega = -k_0 c(x_\omega^-). \tag{B.48}$$

As is usual in stationary phase, we compute the Taylor series for p_1 and p_2 about x_{ω_+} and x_{ω_-} respectively,

$$p_1(x, \omega) \approx p_1(x_\omega^+, \omega) + \frac{\partial^2}{\partial x^2} p_1(x, \omega)\bigg|_{x_\omega^+} (x - x_\omega^+)^2 + \mathcal{O}((x - x_\omega^+)^3), \quad x \to x_\omega^+ \tag{B.49}$$

$$p_2(x, \omega) \approx p_2(x_\omega^-, \omega) + \frac{\partial^2}{\partial x^2} q_2(x, \omega)\bigg|_{x_\omega^-} (x - x_\omega^-)^2 + \mathcal{O}((x - x_\omega^-)^3), \quad x \to x_\omega^-, \tag{B.50}$$

and evaluate the Gaussian integral that results, see [1]. Therefore,

$$\hat{A}\left(\omega/\epsilon\right) \sim \mathrm{e}^{\mathrm{i}\pi/2} \frac{\sqrt{2\pi}\gamma(\omega/\epsilon)\epsilon^{-1/2}}{4\sqrt{k_0}} \frac{1}{\sqrt{c'(x_\omega^+)}} f(x_\omega^+ - x_0) \mathrm{e}^{-\mathrm{i}\omega g(x_\omega^+)/\epsilon + \mathrm{i}k_0 x_\omega^+/\epsilon}, \tag{B.51}$$

where the prime denoted differentiation w.r.t. the argument. Note, if $c'\big(x_\omega^+\big) = 0$, then this evaluation fails and one must take higher order terms, see [44]. Similarly,

$$\hat{B}\left(\omega/\epsilon\right) \sim \mathrm{e}^{\mathrm{i}\pi/2} K\left(\omega/\epsilon\right) \left(H(x_\omega^+) - \frac{1}{2}\right) \frac{\sqrt{2\pi}\epsilon^{-1/2}}{\sqrt{k_0}} \frac{f(x_\omega^+ - x_0)}{\sqrt{c'(x_\omega^+)}} \mathrm{e}^{-\mathrm{i}\omega g(x_\omega^+)/\epsilon + \mathrm{i}k_0 x_\omega^+/\epsilon}. \tag{B.52}$$

We avoid the complication of having $c(x) = \text{const}$ in (B.51) and (B.52) by switching the order of integration in (B.46) and (B.47), see §B. Note that

$$\hat{B}(\omega/\epsilon) \;\sim\; \hat{A}\left(\omega/\epsilon\right) K\left(\omega/\epsilon\right) \left(H(x_\omega^+) - \frac{1}{2}\right).$$

Then, (B.41) is

$$h(x,t) \sim \frac{c^{-1/2}(x)}{2\pi}\int_{-\infty}^{\infty} \mathrm{e}^{\mathrm{i}\omega t/\epsilon}\hat{A}\left(\omega/\epsilon\right)\left(\mathrm{e}^{\mathrm{i}\omega g(x)/\epsilon} + K\left(\omega/\epsilon\right)\left(H(x)+H(x_\omega^+)-1\right)\mathrm{e}^{-\mathrm{i}\omega g(x)/\epsilon}\right)d\omega$$
$$\sim \mathrm{e}^{\mathrm{i}\pi/4}\frac{c^{-1/2}(x)}{2\sqrt{2\pi\epsilon k_0}}\int_{-\infty}^{\infty}\gamma\left(\omega/\epsilon\right)\frac{f(x_\omega^+ - x_0)}{\sqrt{c'(x_\omega^+)}}\mathrm{e}^{\mathrm{i}\omega\left(t+g(x)-g(x_\omega^+)\right)/\epsilon+\mathrm{i}k_0 x_\omega^+/\epsilon}d\omega$$
$$+ 2\mathrm{i}\mathrm{e}^{\mathrm{i}\pi/4}\cos\left(\frac{2\alpha+1}{2\alpha+2}\pi\right)\frac{c^{-1/2}(x)}{2\sqrt{2\pi\epsilon k_0}}\int_{-\infty}^{\infty}\left(H(x)+H(x_\omega^+)-1\right)$$
$$\times\ \gamma\left(\omega/\epsilon\right)\frac{f(x_\omega^+ - x_0)}{\sqrt{c'(x_\omega^+)}}\mathrm{e}^{\mathrm{i}\omega\left(t-g(x)-g(x_\omega^+)\right)/\epsilon-|\omega|\beta/\epsilon+\mathrm{i}k_0 x_\omega^+/\epsilon}d\omega. \tag{B.53}$$

The initial condition and choice of k_0 decide how $|\omega|$, in (B.44), is treated. That is, with (B.6), $c(x) > 0$ and the particular choice $k_0 > 0$, the dispersion relation,

$$\omega(x) = k_0 c(x),$$

associated with x_{ω_+}, permits $|\omega| = \omega$ in (B.44), since (B.41), (B.46) and (B.47) are evaluated near (B.48). The dominant contributions from the integral in (B.53) are again found using statioary phase once more. Noting that $x_\omega^+ \equiv x_\omega^+(\omega)$ or $x_\omega^- \equiv x_\omega^-(\omega)$, and with,

$$q_1(\omega) = \mathrm{i}\omega\left(t + g(x) - g(x_\omega^+)\right)/\epsilon + \mathrm{i}k_0 x_\omega^+/\epsilon,$$
$$q_2(\omega) = \mathrm{i}\omega\left(t - g(x) - g(x_\omega^-)\right)/\epsilon - \omega\beta/\epsilon + \mathrm{i}k_0 x_\omega^-/\epsilon,$$

we have,

$$\frac{d}{d\omega}q_1(\omega) = 0 \quad \Rightarrow \quad x_\omega^+ = g^{-1}(t+g(x)),$$
$$\frac{d}{d\omega}q_2(\omega) = 0 \quad \Rightarrow \quad x_\omega^- = g^{-1}(t-g(x)+\mathrm{i}\beta).$$

As such, we can now write (B.41) as

$$h(x,t) \sim \frac{\gamma\left(k_0 c(x_\omega^+)/\epsilon\right)}{2}c^{-1/2}(x)c^{1/2}(x_\omega^+)f(x_\omega^+ - x_0)\mathrm{e}^{\mathrm{i}k_0 x_\omega^+/\epsilon}$$
$$+ 2\mathrm{i}\cos\left(\nu\pi\right)c^{-1/2}(x)c^{1/2}(x_\omega^-)f(x_\omega^- - x_0)\left(H(x)+H(x_\omega^+)-1\right)\mathrm{e}^{\mathrm{i}k_0 x_\omega^-/\epsilon}. \tag{B.54}$$

With $H(x_\omega^+) = 1$, given that $f(x_\omega^+ - x_0)$ is approximately zero except when $x_\omega^+ \approx x_0 > 0$. Therefore,

$$h(x,t) \sim c^{-1/2}(x)c^{1/2}(x_\omega^+)f(x_\omega^+ - x_0)\mathrm{e}^{\mathrm{i}k_0 x_\omega^+/\epsilon} + 2\mathrm{i}\cos\left(\nu\pi\right)c^{-1/2}(x)c^{1/2}(x_\omega^-)f(x_\omega^- - x_0)H(x)\mathrm{e}^{\mathrm{i}k_0 x_\omega^-/\epsilon}. \tag{B.55}$$

This is the main result, it is the leading order asymptotic solution to (2.1) that captures not only the behaviour of the $\mathcal{O}(\epsilon)$ accurate dominant solution (or transmitted wave), but also contains the leading order behaviour of the reflected wave. This result recovers the results of Chapter 3 when $c(x,t) = c_1(x)$. We now propose an alternative route to the solution (B.55) so as to avoid any issues that may arise if $\frac{d}{dx_\omega^+}c(x_\omega^+) = 0$ in (B.51) and (B.52).

Switching the order of integration

Our alternative approach to derive the solution (B.55) is to switch the order of integration in (B.41), from which it follows that

$$h(x,t) = \tag{B.56}$$

$$\frac{1}{8\pi\epsilon}\int_{-\infty}^{\infty}\int_{-\infty}^{\infty}\mathrm{e}^{\mathrm{i}\omega t/\epsilon}\frac{\gamma(\omega/\epsilon)}{\omega}\Psi\left(x,\omega/\epsilon\right)\bar{\Psi}\left(x',\omega/\epsilon\right)\mathrm{e}^{\mathrm{i}k_0x'/\epsilon}f(x'-x_0)\left(k_0c(x')+\omega\right)d\omega dx'$$
$$+\frac{1}{8\pi\epsilon}\int_{-\infty}^{\infty}\int_{-\infty}^{\infty}\mathrm{e}^{\mathrm{i}\omega t/\epsilon}\frac{\gamma(\omega/\epsilon)}{\omega}\bar{\Psi}(x,\omega/\epsilon)\Psi\left(x',\omega/\epsilon\right)\mathrm{e}^{\mathrm{i}k_0x'/\epsilon}f(x'-x_0)\left(k_0c(x')+\omega\right)d\omega dx'.$$

The asymptotic behaviour of $\Psi\left(x,\omega/\epsilon\right)$ was given in (B.45). Thus,

$$h(x,t)\sim\frac{2}{8\pi}c^{-1/2}(x)\int_{-\infty}^{\infty}c^{-1/2}(x')f(x'-x_0)\mathrm{e}^{\mathrm{i}k_0x'/\epsilon}\,I\,dx' \tag{B.57}$$
$$+\frac{2\mathrm{i}k_0}{8\pi\epsilon}c^{-1/2}(x)\int^{t}\int_{-\infty}^{\infty}c^{1/2}(x')f(x'-x_0)\mathrm{e}^{\mathrm{i}k_0x'/\epsilon}\,I\,dx'dt.$$

where we have taken the time derivative of any integral that contained a $1/\omega$ factor, that is

$$I=\left(I_1+I_2+2\mathrm{i}\cos\left(\nu\pi\right)\left(H(x)+H(x')-1\right)\left(I_3+I_4\right),\right.$$

such that,

$$\begin{aligned}
I_1 &= \int_{-\infty}^{\infty}\mathrm{e}^{\mathrm{i}\omega\left(t+g(x)-g(x')\right)/\epsilon}d\omega/\epsilon,\\
I_2 &= \int_{-\infty}^{\infty}\mathrm{e}^{\mathrm{i}\omega\left(t-g(x)+g(x')\right)/\epsilon}d\omega/\epsilon,\\
I_3 &= \int_{-\infty}^{\infty}\mathrm{e}^{-\frac{|\omega|}{\epsilon}\beta}\mathrm{e}^{\mathrm{i}\omega\left(t-g(x)-g(x')\right)/\epsilon}d\omega/\epsilon,\\
I_4 &= -\int_{-\infty}^{\infty}\mathrm{e}^{-\frac{|\omega|}{\epsilon}\beta}\mathrm{e}^{\mathrm{i}\omega\left(t+g(x)+g(x')\right)/\epsilon}d\omega/\epsilon.
\end{aligned}$$

Using the standard identity

$$\delta(x)=\int_{-\infty}^{\infty}\mathrm{e}^{-2\pi\mathrm{i}nx}dn,$$

gives

$$I_1=-2\mathrm{i}\pi\delta(t+g(x)-g(x')),$$

and I_2 follows. To determine I_3 and thus I_4 we inspect

$$\begin{aligned}
I_3 &= \int_0^{\infty}\mathrm{e}^{\omega(\mathrm{i}N-\beta)/\epsilon}d\omega/\epsilon+\int_{-\infty}^{0}\mathrm{e}^{\omega(\mathrm{i}N+\beta)/\epsilon}d\omega/\epsilon\\
&= -2\beta\epsilon/(\mathrm{i}N-\beta)(\mathrm{i}N+\beta),
\end{aligned}$$

where $N=t-g(x)-g(x')$. I_4 is found similarly. We now drop the Heaviside function, $H(x')$, in the integration. This is because the region of integration is localised around $x'=x_0>0$, and the function $f(x'-x_0)$ is approximately zero everywhere, except near x_0. A discussion on dropping the Heaviside function in this way is found in §H. With,

$$h(x,t)\sim \tag{B.58}$$
$$\frac{1}{2}c^{-1/2}(x)\int_{-\infty}^{\infty}c^{1/2}(g^{-1}(v))f(g^{-1}(v)-x_0)\mathrm{e}^{\mathrm{i}k_0g^{-1}(v)/\epsilon}\left\{\delta(v-j_1)+\delta(v-j_2)\right\}dv$$
$$+\frac{\beta}{\pi}\mathrm{i}\cos\left(\nu\pi\right)c^{-1/2}(x)H(x)\int_{-\infty}^{\infty}\frac{c^{1/2}(g^{-1}(v))}{(v-l_1)(v-\bar{l}_1)}f(g^{-1}(v)-x_0)\mathrm{e}^{\mathrm{i}k_0g^{-1}(v)/\epsilon}dv\quad(*)$$
$$-\frac{\beta}{\pi}\mathrm{i}\cos\left(\nu\pi\right)c^{-1/2}(x)H(x)\int_{-\infty}^{\infty}\frac{c^{1/2}(g^{-1}(v))}{(v-l_2)(v-\bar{l}_2)}f(g^{-1}(v)-x_0)\mathrm{e}^{\mathrm{i}k_0g^{-1}(v)/\epsilon}dv\quad(*)$$

$$\frac{\mathrm{i}k_0}{2\epsilon}c^{-1/2}(x)\int\int_{-\infty}^{\infty}c^{3/2}(g^{-1}(v))f(g^{-1}(v)-x_0)\mathrm{e}^{\mathrm{i}k_0g^{-1}(v)/\epsilon}\left\{\delta(v-j_1)+\delta(v-j_2)\right\}dvdt$$

$$-\frac{k_0\beta}{\pi\epsilon}\cos(\nu\pi)\,c^{-1/2}(x)H(x)\int\int_{-\infty}^{\infty}\frac{c^{3/2}(g^{-1}(v))}{(v-l_1)(v-\bar{l}_1)}f(g^{-1}(v)-x_0)\mathrm{e}^{\mathrm{i}k_0 g^{-1}(v)/\epsilon}dvdt \quad (*)$$

$$+\frac{k_0\beta}{\pi\epsilon}\cos(\nu\pi)\,c^{-1/2}(x)H(x)\int\int_{-\infty}^{\infty}\frac{c^{3/2}(g^{-1}(v))}{(v-l_2)(v-\bar{l}_2)}f(g^{-1}(v)-x_0)\mathrm{e}^{\mathrm{i}k_0 g^{-1}(v)/\epsilon}dvdt, \quad (*)$$

where the substitutions $x' = g^{-1}(v)$, $j_1 = g(x) + t$, $j_2 = g(x) - t$, $l_1 = t - g(x) + \mathrm{i}\beta$ and $l_2 = -t - g(x) + \mathrm{i}\beta$ have been made. We deform the contour of integration in the integrals marked $(*)$ above, so as take into account the contributions coming from the poles at $v = l_1$ and $v = l_2$. The deformed contour is shown in Figure B.1. Note, k_0 in (2.2) is taken to be positive here. Should k_0 be negative, the contour would be reflected along the real axis and poles at $v = \bar{l}_1$ and $v = -\bar{l}_2$ would be considered.

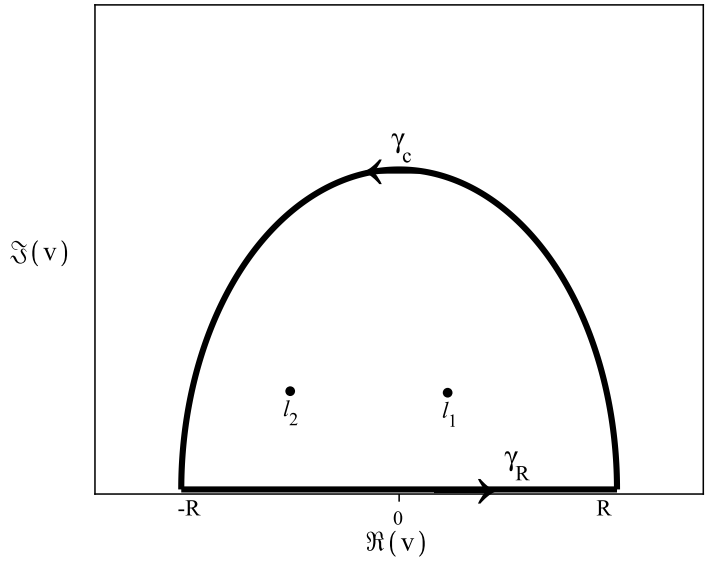

Figure B.1: Deformed contour containing the poles at $v = l_1$ and $v = l_2$.

$$\begin{aligned}\gamma_R: &\quad v; &&\{-R \le v \le R\} \quad \text{and} \quad R \to \infty,\\ \gamma_c: &\quad v = R\mathrm{e}^{\mathrm{i}\theta}; &&\{0 < \theta < \pi\}.\end{aligned}$$

Deforming the contour in this way is discussed in Appendix I. Progressing, we note that we can use Cauchy's integral theorem and that the main contributions will come from the poles at $v = l_1$ and $v = -l_2$. Therefore,

$$\begin{aligned}h(x,t) \sim\ & J_1 + J_2 + J_3 + J_4\\ &+ \frac{\mathrm{i}k_0}{2\epsilon}c^{-1/2}(x)\int^t c^{3/2}(g^{-1}(j_1))f(g^{-1}(j_1)-x_0)\mathrm{e}^{\mathrm{i}k_0 g^{-1}(j_1)/\epsilon}dt\\ &+ \frac{\mathrm{i}k_0}{2\epsilon}c^{-1/2}(x)\int^t c^{3/2}(g^{-1}(j_2))f(g^{-1}(j_2)-x_0)\mathrm{e}^{\mathrm{i}k_0 g^{-1}(j_2)/\epsilon}dt\\ &- \frac{k_0}{\epsilon}\cos(\nu\pi)\,H(x)c^{-1/2}(x)\int^t c^{3/2}(g^{-1}(l_1))f(g^{-1}(l_1)-x_0)\mathrm{e}^{\mathrm{i}k_0 g^{-1}(l_1)/\epsilon}dt\\ &+ \frac{k_0}{\epsilon}\cos(\nu\pi)\,H(x)c^{-1/2}(x)\int^t c^{3/2}(g^{-1}(\bar{l}_2))f(g^{-1}(\bar{l}_2)-x_0)\mathrm{e}^{\mathrm{i}k_0 g^{-1}(\bar{l}_2)/\epsilon}dt \qquad \text{(B.59)}\end{aligned}$$

where,

$$J_1 = \frac{c^{-1/2}(x)}{2}c^{1/2}(g^{-1}(j_1))f(g^{-1}(j_1)-x_0)\mathrm{e}^{\mathrm{i}k_0 g^{-1}(j_1)/\epsilon},$$

$$
\begin{aligned}
J_2 &= \frac{c^{-1/2}(x)}{2} c^{1/2}(g^{-1}(j_2)) f(g^{-1}(j_2) - x_0) \mathrm{e}^{\mathrm{i}k_0 g^{-1}(j_2)/\epsilon}, \\
J_3 &= \mathrm{i}\cos(\nu\pi)\, H(x) c^{-1/2}(x) c^{1/2}(g^{-1}(l_1)) f(g^{-1}(l_1) - x_0) \mathrm{e}^{\mathrm{i}k_0 g^{-1}(l_1)/\epsilon}, \\
J_4 &= -\mathrm{i}\cos(\nu\pi)\, H(x) c^{-1/2}(x) c^{1/2}(g^{-1}(\bar{l}_2)) f(g^{-1}(\bar{l}_2) - x_0) \mathrm{e}^{\mathrm{i}k_0 g^{-1}(\bar{l}_2)/\epsilon},
\end{aligned}
\tag{B.60}
$$

Focusing on the terms involving integration across t, integration by parts gives,

$$
\begin{aligned}
&\frac{\mathrm{i}k_0}{2\epsilon} c^{-1/2}(x) \int^t c^{3/2}(g^{-1}(j_1)) f(g^{-1}(j_1) - x_0) \mathrm{e}^{\mathrm{i}k_0 g^{-1}(j_1)/\epsilon} dt \\
&\quad = \frac{c^{1/2}(g^{-1}(j_1))}{2} f(g^{-1}(j_1) - x_0) \mathrm{e}^{\mathrm{i}k_0 g^{-1}(j_1)/\epsilon} \;=\; J_1, \\
&\frac{\mathrm{i}k_0}{2\epsilon} c^{-1/2}(x) \int^t c^{3/2}(g^{-1}(j_2)) f(g^{-1}(j_2) - x_0) \mathrm{e}^{\mathrm{i}k_0 g^{-1}(j_2)/\epsilon} dt \\
&\quad = -\frac{c^{1/2}\left(g^{-1}(j_2)\right)}{2} f(g^{-1}(j_2) - x_0) \mathrm{e}^{\mathrm{i}k_0 g^{-1}(j_2)/\epsilon} \;=\; -J_2,
\end{aligned}
$$

$$
\begin{aligned}
&-\frac{k_0}{\epsilon} \cos(\nu\pi)\, H(x) c^{-1/2}(x) \int^t c^{3/2}(g^{-1}(l_1)) f(g^{-1}(l_1) - x_0) \mathrm{e}^{\mathrm{i}k_0 g^{-1}(l_1)/\epsilon} dt \\
&= \mathrm{i}\cos(\nu\pi)\, H(x) c^{-1/2}(x) c^{1/2}(g^{-1}(l_1)) f(g^{-1}(l_1) - x_0) \mathrm{e}^{\mathrm{i}k_0 g^{-1}(l_1)/\epsilon} \;=\; J_3,
\end{aligned}
$$

and

$$
\begin{aligned}
&\frac{k_0}{\epsilon} \cos(\nu\pi)\, H(x) c^{-1/2}(x) \int^t c^{3/2}(g^{-1}(-l_2)) f(g^{-1}(-l_2) - x_0) \mathrm{e}^{\mathrm{i}k_0 g^{-1}(-l_2)/\epsilon} dt \\
&= \mathrm{i}\cos(\nu\pi)\, H(x) c^{-1/2}(x) c^{1/2}(g^{-1}(-l_2)) f(g^{-1}(-l_2) - x_0) \mathrm{e}^{\mathrm{i}k_0 g^{-1}(-l_2)/\epsilon} \;=\; -J_4.
\end{aligned}
$$

Therefore $h(x,t) \sim 2J_1 + 2J_3$ and with,

$$
g^{-1}(j_1) = x_\omega^+, \quad g^{-1}(l_1) = x_\omega^-,
$$

we have that

$$
h(x,t) \sim c^{-1/2}(x) c^{1/2}\left(x_\omega^+\right) f(x_\omega^+ - x_0) \mathrm{e}^{\mathrm{i}k_0 x_\omega^+/\epsilon} + 2\mathrm{i}\cos(\nu\pi)\, H\left(x - \Re(x_*)\right) c^{-1/2}(x) c^{1/2}\left(x_\omega^-\right) f(x_\omega^- - x_0) \mathrm{e}^{\mathrm{i}k_0 x_\omega^-/\epsilon}.
\tag{B.61}
$$

Eq. (B.61) repeats the result given in (B.55) without the complications encountered when $c'(x_\omega^+) = 0$ in the stationary phase approach.

Appendix C

Conservation laws, amplitudes and general identities

D Showing $C(x')$ is constant in (B.21)

For convenience we drop the prime in the argument of C so that all uses of the prime denote differentiation w.r.t. x. From (B.12) and (B.14) we have that

$$\begin{aligned} (c^2\phi_4')' &= \lambda^2\phi_4 \\ \text{and} \quad (c^2\phi_1')' &= \lambda^2\phi_1. \end{aligned}$$

Therefore, (B.21) reads

$$\begin{aligned} \frac{d}{dx}\left(\frac{1}{C(x)}\right) &= \frac{d}{dx}\left(c^2(x)W_+(x)\right) \\ &= \phi_1(c^2\phi_4')' + \phi_1'(c^2\phi_4') - \phi_4(c^2\phi_1')' - \phi_4(c^2\phi_1') \\ &= 0, \end{aligned} \tag{C.1}$$

and hence,

$$c^2(x')W_+(x) = \frac{1}{C(x)} = \text{constant}.$$

A simlar argument shows that $D(x) = \text{constant}$ in (B.22). Thus, we have two constants given by

$$V_+(x,\omega) = c^2(x)W_+(x,\omega) \quad \text{and} \quad V_-(x,\omega) = c^2(x)W_-(x,\omega),$$

noted in (B.21) and (B.22) respectively. We aim to calculate values for both. To do this we must first connect the Wronskians above.

Relationship between the Wronskians

If an initial solution wave propagates from $-\infty \to +\infty$ the solutions of (B.14) have the following connection relation,

$$\phi_1(x,\lambda) + R(\lambda)\phi_2(x,\lambda) = T(\lambda)\phi_3(x,\lambda), \tag{C.2}$$

where $R(\lambda)$ and $T(\lambda)$ are the reflected and transmitted wave amplitudes. Similarly, if the initial solution wave wave propagates from $+\infty \to -\infty$, then

$$\phi_4(x,\lambda) + \hat{R}(\lambda)\phi_3(x,\lambda) = \hat{T}(\lambda)\phi_2(x,\lambda), \tag{C.3}$$

where again $\hat{R}(\lambda)$ and $\hat{T}(\lambda)$ represent the reflected and transmitted wave amplitudes. Recall that

$$W_+(x,\lambda) = \begin{vmatrix} \phi_1(x,\lambda) & \phi_4(x,\lambda) \\ \phi_1'(x,\lambda) & \phi_4'(x,\lambda) \end{vmatrix} \tag{C.4}$$

and

$$W_-(x,\lambda) = \begin{vmatrix} \phi_2(x,\lambda) & \phi_3(x,\lambda) \\ \phi_2'(x,\lambda) & \phi_3'(x,\lambda) \end{vmatrix}. \tag{C.5}$$

Therefore, using (C.2) and (C.3) it is possible to derive a relationship between $W_+(x)$ and $W_-(x)$. Note that when $\lambda = \mathrm{i}\omega$ in (B.12) the solutions (B.14) are related by

$$\phi_2(x,\omega) = \bar{\phi}_1(x,\omega), \quad \phi_3(x,\omega) = \bar{\phi}_4(x,\omega), \tag{C.6}$$

where the bar denotes complex conjugation. Therefore,

$$W_-(x,\omega) = \phi_3'(x,\omega)\phi_2(x,\omega) - \phi_2'(x,\omega)\phi_3(x,\omega) \tag{C.7}$$

$$= \bar{\phi}_4'(x,\omega)\bar{\phi}_1(x,\omega) - \bar{\phi}_1'(x,\omega)\bar{\phi}_4(x,\omega) = \bar{W}_+(x,\omega).$$

Now, by using (C.2), (C.3) and (C.6) the above reduces to,

$$W_+(x,\omega) = \frac{1}{\hat{\bar{T}}}\big(\phi_4'(x,\omega)\bar{\phi}_4(x,\omega) - \bar{\phi}_4'(x,\omega)\phi_4(x,\omega)\big), \tag{C.8}$$

valid to the right of the transition point x_* and

$$W_+(x,\omega) = \frac{1}{\bar{T}}\left(\bar{\phi}_1'(x,\omega)\phi_1(x,\omega) - \phi_1'(x,\omega)\bar{\phi}_1(x,\omega)\right), \tag{C.9}$$

valid to the left of the transition point.

E Finding the constant V_+

Recall that the elements of W_+ as $x \to \pm\infty$ are given by (B.15) and that $c(x) \to c_\pm$ as $x \to \pm\infty$, where $c_\pm$ are real positive constants. Letting $x \to \pm\infty$ and using (C.8) and (C.9), it follows that

$$V_+(x,\omega) \sim \frac{c_+^2}{\hat{\bar{T}}}\left(-\frac{\mathrm{i}\omega}{c_+^2}\mathrm{e}^{-\mathrm{i}\omega\frac{x}{c_+}}\mathrm{e}^{\mathrm{i}\omega\frac{x}{c_+}} - \frac{\mathrm{i}\omega}{c_+^2}\mathrm{e}^{\mathrm{i}\omega\frac{x}{c_+}}\mathrm{e}^{-\mathrm{i}\omega\frac{x}{c_+}}\right) = -\frac{2\mathrm{i}\omega}{\hat{\bar{T}}}, \quad x \to \infty \tag{C.10}$$

and

$$V_+(x,\omega) \sim \frac{c_-^2}{\bar{T}}\left(-\frac{\mathrm{i}\omega}{c_-^2}\mathrm{e}^{-\mathrm{i}\omega\frac{x}{c_-}}\mathrm{e}^{\mathrm{i}\omega\frac{x}{c_-}} - \frac{\mathrm{i}\omega}{c_-^2}\mathrm{e}^{\mathrm{i}\omega\frac{x}{c_-}}\mathrm{e}^{-\mathrm{i}\omega\frac{x}{c_-}}\right) = -\frac{2\mathrm{i}\omega}{\bar{T}}, \quad x \to -\infty. \tag{C.11}$$

Given that $V_+(x,\omega)$ is constant it is required that

$$\hat{T} = T. \tag{C.12}$$

Using the same method that leads to (C.10) and (C.11), leads to

$$V_-(x,\omega) = \bar{V}_+(x,\omega) = \frac{2\mathrm{i}\omega}{T}.$$

F Conservation Law

The flux of the wave energy constant, see [29]. This detail is found on replacing $\lambda = \mathrm{i}\omega$ and letting $\phi_j = \phi$ in (B.14), whence

$$c^2\bar{\phi}_{xx} + c_x^2\bar{\phi}_x + \omega^2\bar{\phi} = 0$$

and

$$c^2\phi\bar{\phi}'' + c_x^2\phi\bar{\phi}' + \omega^2\phi\bar{\phi} = \left(c^2\phi\bar{\phi}'\right)' - c^2|\phi'|^2 + \omega^2|\phi|^2 = 0. \tag{C.13}$$

Therefore,

$$\Im\big(c^2\phi\bar{\phi}'\big)' = 0.$$

Thus, the energy conservation law is found by applying the boundary conditions at $\pm\infty$, whereby

$$\Im\big(c^2\phi\bar{\phi}_x\big)\Big|_{\infty} = \Im\big(c^2\phi\bar{\phi}_x\big)\Big|_{-\infty}.$$

Using (B.15), (C.2) and (C.3) it follows that

$$\Im\left(c_+^2|T|^2\phi_3\bar{\phi}_3'\right)\Big|_{\infty} = \Im\left(c_-^2(\phi_1+R\phi_2)(\bar{\phi}_1'+\bar{R}\bar{\phi}_2')\right)\Big|_{-\infty}.$$

on following an initial solution wave from $-\infty \to \infty$. Note that,

$$R\phi_2\bar{\phi}_1' = -\overline{\bar{R}\phi_1\bar{\phi}_2'}, \quad x \to \infty,$$

from (B.15). Thus,

$$1 = |T|^2 + |R|^2. \tag{C.14}$$

Following the same process for an initial wave travelling from $\infty \to -\infty$, gives

$$1 = |\hat{T}|^2 + |\hat{R}|^2.$$

Hence,

$$|\hat{R}| = |R|,$$

on using (C.12). Therefore, the transmitted and reflected amplitudes for a non symmetric wave speed are connected by the following relations,

$$\hat{T} = T \quad \text{and} \quad |\hat{R}| = |R|. \tag{C.15}$$

G Reflected wave amplitude and the Stokes multiplier

Focusing on $\omega \gg 1$, the solution of (B.14) is

$$\phi_1(x,\omega) \sim c^{-1/2}(x)\left(\mathrm{e}^{\mathrm{i}\omega g(x)} + K(\omega)\mathrm{e}^{-\mathrm{i}\omega g(x)}\right), \quad \omega \to \infty,$$

where $g(x)$ and the (exponentially small) Stokes multiplier were given in (B.43) and (B.44) respectively. Note, the above relation takes into account that the Stokes multiplier is zero to the right of the Stokes line. Placing the above into (C.2) and using (B.15),

$$\begin{aligned} T\phi_3(x,\omega) &= \phi_1(x,\omega) + R\phi_2(x,\omega) \\ &= \phi_1(x,\omega) + R\bar{\phi}_1(x,\omega) \\ &\sim\ c^{-1/2}(x)\left(\left(1+R(\omega)\bar{K}(\omega)\right)\mathrm{e}^{\mathrm{i}\omega g(x)} + \left(R(\omega)+K(\omega)\right)\mathrm{e}^{-\mathrm{i}\omega g(x)}\right) \end{aligned} \tag{C.16}$$

Letting $x \to -\infty$ and using (B.15) yields

$$T\mathrm{e}^{\mathrm{i}\frac{\omega x}{c_+}} \ \sim\ \big(1+R(\omega)\bar{K}(\omega)\big)\mathrm{e}^{\mathrm{i}\omega\left(\frac{x}{c_+}+\hat{\alpha}\right)} + \big(R(\omega)+K(\omega)\big)\mathrm{e}^{-\mathrm{i}\omega\left(\frac{x}{c_+}+\hat{\alpha}\right)}, \tag{C.17}$$

where,

$$\hat{\alpha} = \int_0^{\infty} \frac{1}{c(x')} - \frac{1}{c_{\max}}dx' \in \mathbb{R} > 0.$$

See §I for details on $\hat{\alpha}$. Connecting both sides of (C.17) reveals that $R(\omega) = -K(\omega)$ and $|T| = 1 + \mathcal{O}(\mathrm{e}^{-2\beta/\epsilon})$ as required.

Note, with (C.15) and $R = -K$ it is spotted that a change in the direction of the initial wave amounts to a change in the sign of the Stokes multiplier, this detail was noted in Chapters

2 and 3.

H Dropping the Heaviside function

By dropping the Heaviside function in (B.57), we reduce the labour costs of finding the leading order solution (inc. reflection) of (B.2). To achieve this we require that,

$$|f(x-x_0)| \leq \mathrm{e}^{-\xi|x-x_0|^2}, \tag{C.18}$$

so that the error in removing $H(x)$ is $\mathcal{O}\left(\mathrm{e}^{-\xi {x_0}^2}\right)$, where $x_0 > 0$ and $\xi \geq 1$. Then, by setting

$$\mathrm{e}^{-\xi {x_0}^2} \leq \epsilon, \tag{C.19}$$

so that any contribution to (B.57) that is lost by removing $H(x)$ is no longer relevant in the leading order expansion of (B.56), it follows that

$$x_0 \geq \left(\ln \epsilon^{-1}\right)^{1/2} / \sqrt{\xi}.$$

An alternative approach would have been to require that

$$x_0 = \mathcal{O}(\epsilon^{-1}).$$

However, this clearly restricts the domain of the initial data and a greater range of x_0 values is necessary to elucidate the behaviour of the reflected near a Stokes line, the figures in §3.5.1 illustrate this point.

I Deforming the contour in (B.58)

We focus on wave speed profiles that have the properties outlined in §2.1 and

$$\lim_{R\to\infty} c(R\mathrm{e}^{\mathrm{i}\theta}) = c_{\max} = \text{constant} > 0 : \quad \theta \in [0, 2\pi), \tag{C.20}$$

in (B.2). Examples of speed profiles that satisfy this were used in §3.5. With (C.20) it follows that

$$\lim_{R\to\infty} g(R\mathrm{e}^{\mathrm{i}\theta}) \sim \frac{R\mathrm{e}^{\mathrm{i}\theta}}{c_{\max}} + \hat{\alpha} \quad \text{and} \quad \lim_{R\to\infty} g^{-1}(R\mathrm{e}^{\mathrm{i}\theta}) \sim c_{\max}(R\mathrm{e}^{\mathrm{i}\theta} - \hat{\alpha}), \tag{C.21}$$

where

$$\hat{\alpha} = \int_0^{\infty \mathrm{e}^{\mathrm{i}\theta}} \frac{1}{c(x')} - \frac{1}{c_{\max}} dx' \in \mathbb{R} > 0,$$

and the contour avoids any singular points of $1/c(x)$. Recall that the exponential term in the integrand of (B.58) is $\mathrm{e}^{\mathrm{i}k_0 g^{-1}(v)/\epsilon}$ where $k_0 > 0$. Then, along γ_c where $\theta = (0, \pi)$ (shown in Figure B.1) it follows that

$$\mathrm{e}^{\mathrm{i}k_0 g^{-1}(v)/\epsilon} \leq \mathcal{O}\left(\mathrm{e}^{-k_0 R \sin(\theta)/\epsilon}\right). \tag{C.22}$$

Additionally, when $\theta \approx 0$ or $\theta \approx \pi$ the function $f(x - x_0)$ in the initial condition has the property:

$$\lim_{R\to\infty} f(R\mathrm{e}^{\mathrm{i}\theta} - x_0) \leq \mathcal{O}\left(\mathrm{e}^{-\xi R^2}\right) \quad \text{as} \quad \theta \to 0_+ \quad \text{or} \quad \theta \to \pi, \tag{C.23}$$

on using (C.18). Hence, deforming the contour in (B.58) to include γ_c, the error incurred is exponentially small. Moreover, the error is exponentially smaller than the subdominant solution switched on via the Stokes phenomenon and hence neglected.

It is noted that the deformed contour γ_R and γ_c contains a singular point of $c(x)$ at $v = g(x_*)$. However, it can be shown that the contribution coming from the point at $g(x_*)$ is exponentially smaller than than the contributions from l_1 and l_2 and is therefore neglected to leading order.

Bibliography

[1] M. J. Ablowitz and A. S. Fokas. *Complex Varialbes: Introduction and Applications.* Cambridge University Press; 2 edition, 2003.

[2] W. Balser. *Formal power series and linear systems of meromorphic ordinary differential equations.* Springer–Universitext–New York, 2000.

[3] M. V. Berry and K. E. Mount. Semiclassical approximations in wave mechanics. *Rep. Prog. Phys.* **35**, 315-397 (1972)

[4] M. V. Berry. Semiclassical weak reflections above analytic and non-analytic potential. barriers J. Phys. A: Math. Gen. 15 3693 (1982)

[5] M. V. Berry. Quantum phase corrections from adiabatic iteration. *Proc. R. Soc.* A414, 31-46 (1987)

[6] M .V .Berry and C. J. Howls. Fake Airy functions and the asymptotics of reflectionlessness. J. Phys. A: Math. Gen. 23, L243-L 246 (1990)

[7] M. V. Berry and C. J. Howls Hyperasymptotics. *Proc. R. Soc. Lond.* A (1990)

[8] M. V. Berry. Waves near Stokes Lines. *Proc. Roy. Soc. Lond.* A **427**. 265-280 (1990)

[9] M. V. Berry. Uniform asymptotic smoothing of stokes' discontinuities. *Proc. Roy. Soc. Lond*, pages 635–668, 1990.

[10] J .P. Boyd. The Devils Invention: Asymptotic, Superasymptotic and Hyperasymptotic Series. Acta Applicandae Mathematica, March 1999, Volume 56, Issue 1, pp 1-98.

[11] O . Bühler. Introduction Classical and Statistical Mechanics. *Courant Lecture Notes,* vol. 13, 2006.

[12] O . Bühler. Waves and Mean Flows. Cambridge Monogr. Mech. Cambridge, UK: Cambridge Univ. Press, 2009.

[13] P. B. Chapman J. J. Mahony. Reflection of Waves in a Slowly Varying Medium. *SIAM J. APPL. Math* Vol. 34, No. 2, March 1978.

[14] S. J. Chapman and D. B. Mortimer. Exponential asymptotics and Stokes lines in a partial differential equation. Proc. R. Soc. A 2005 461, doi: 10.1098/rspa.2005.1475, 2005.

[15] S. J. Chapman C. J. Howls J. R. King A .B. Olde Daalhuis. Why is a shock not a caustic? The higher-order Stokes phenomenon and smoothed shock formation. *Nonlinearity 20*, 2007, 2425–2452.

[16] S. J. Chapman and D. B. Mortimer. Exponential asymptotics and Stokes lines in a partial differential equation. *Proc. R. Soc.* A (2005) **461**, 2385–2421.

[17] O. Costin, G. Luo and S. Tanveer. Divergent expansion, Borel summability and three-dimensional NavierStokes equation. *Phil. Trans. R. Soc.* A (2008) **366**, 2775–2788.

[18] R. B. Dingle. *Appl. Sci. Res.* B **5** 345-67.

[19] R. B. Dingle. Asymptotic Expansions and Converging Factors. I. General Theory and Basic Converging Factors. *Proc. Roy. Soc. Lon* Vol. 244, No. 1239 (Apr. 22, 1958), pp. 456-475.

[20] R. B. Dingle. *Asymptotic expansions: Their derivation and interpretation.* New York– Academic Press, 1973.

[21] NIST Digital Library of Mathematical Functions. http://dlmf.nist.gov/5.5E3, Release 1.0.6 of 2013-05-06.

[22] NIST Digital Library of Mathematical Functions. http://dlmf.nist.gov/10.11E4, Release 1.0.6 of 2013-05-06.

[23] NIST Digital Library of Mathematical Functions. http://dlmf.nist.gov/10.17E5, Release 1.0.6 of 2013-05-06.

[24] NIST Digital Library of Mathematical Functions. http://dlmf.nist.gov/10.17E6, Release 1.0.6 of 2013-05-06.

[25] NIST Digital Library of Mathematical Functions. http://dlmf.nist.gov/13.19E1, Release 1.0.5 of 2012-10-01

[26] N. Fröman and P. O. Fröman *JWKB Approximation*. Amsterdam: North-Holland (1965).

[27] R. Grimshaw and N. Joshi. Weakly Nonlocal Solitary Waves in a Singularly Perturbed KortewegDe Vries Equation. *SIAM J.Appl.Math.,* 55(1) (1995), pp. 124-135.

[28] R. Grimshaw. Asymptotic Methods in Fluid Mechanics: Survey and Recent Advances, Exponential Asymptotics and Generalized Solitary Waves. Springer Vienna, 2011. url=http://dx.doi.org/10.1007/978-3-7091-0408-83, isbn=978-3-7091-0407-1.

[29] E. J. Hinch. Perturbation methods. Cambridge University Press, 1991

[30] T. Kawai. On the Stokes Geometry of Higher Order Painlev Equations. *Kyto Daigaku Sri Kaiseki Kenkyjo*, 2004.

[31] M. D. Kruskal and H. Segur. Asymptotics beyond all orders in a model of crystal growth. *Stud. Appl. Math. ,* **85** (1991), 129-181.

[32] R. E. Langer. On the asymptotic solutions of ordinary differential equations, with an application to Bessel functions of large order. *Trans. Amer. Math. Soc.,* **33**, pp. 23-64. (1931).

[33] R. E. Langer. On the asymptotic solutions of differential equations, with an application to the Bessel functions of large complex order. *Trans. Amer. Math. Soc.,* **34** (1932), 447-480.

[34] R. E. Langer. On the asymptotic solutions of differential equations, with reference to the Stokes' phenomenon about a singular point, *Trans. Amer. Math. Soc.,* **37** (1935), 397-416.

[35] R. E. Langer. *Phys. Rev* **51**, 669-76 (1937).

[36] P. J. Langman C. J. Howls and A. B. Olde Daalhuis. On the higher-order stokes phenonmenon. *R. Soc. Lond*, 460:2285–2303, 2004.

[37] J. J. Mahony. The reflection of short waves in a variable medium. *Quart. Appl. Math.,* 25 (1967), pp. 313-316.

[38] R. E. Meyer. Gradual Reflection of Short Waves. *SIAM J. Appl. Math.,* 29(3) (1975), 481492.

[39] R. E. Meyer. A simple explanation of the Stokes phenomenon. *SIAM Rev.,* 31(1989), pp.435-445

[40] S. C. Miller and R. H. Good. *Phys. Rev.* **91** 174-9 (1953)

[41] E. I. Òlafsdòttir A. B. Olde Daalhuis and J. Vanneste. Stokes-multiplier expansion in am inhomogeneous differential equation with a small parameter. *Proc. Roy. Soc. Lond*, 461:2243–2256, 2005.

[42] A. B. Olde Daalhuis and F. W. J. Olver. 1994, Exponentially improved asymptotic solutions of ordinary differential equations. II. Irregular singularities of rank one. equations with a singularity of rank 1. *Proc. R. Soc. London Ser.* A **445**, 39-56.

[43] A. B. Olde Daalhuis. Hyperasymptotic solutions of higher order linear differential equations with a singularity of rank 1. *Proc. R. Soc*, 454:1–29, 1998.

[44] F. W. J. Olver. Asymptotics and Special Functions. *New York: Academic Press*, 1974.

[45] F. W. J. Olver. On an asymptotic expansion of a ratio of gamma functions. *Proceedings of the Royal Irish Academy. Section A: Mathematical and Physical Sciences*, 95.

[46] F. W. J. Olver. Uniform, exponentially improved asymptotic expansions for the the generalised exponential integral. *SIAM J. Math.*, 22:1460–1489, 1991.

[47] J. Painter and R. Meyer. Turning-Point Connection at Close Quarters. *SIAM J. Math. Anal.,* 13 (1982), pp. 541-554.

[48] R. B. Paris and A. D. Wood. Stokes phenomenon demystified. 33(3), 1995.

[49] V. L. Pokrovskii, S. K. Savvinykh and F. R. Ulinich. 1958 *Sov. Phys.-JETP***34** 879-82.

[50] V. L. Pokrovskii, F. R. Ulinich and S. K. Savvinykh. 1958 *Sov. Phys.-JETP***34** 1119-20.

[51] V. L. Pokrovskii and I. M. Khalatnikov 1961 *Sov. Phys.-JETP***13** 1207-10.

[52] H. Segur et al Proceedings of a NATO Advanced Research Workshop on Asymptotics beyond All Orders, (1991 : La Jolla, San Diego, Calif.) VI. Series.

[53] V. S. Shul'man (originator). Spectrum of an operator, Encyclopedia of Mathematics. http://www.encyclopediaofmath.org/index.php?title=Spectrum_of_an_operator&oldid=11393

[54] B. Y. Sternin and V. E. Shatalov. Borel-Laplace Transform and Asymptotic Theory. *CRC Press*, 1996.

[55] G. G. Stokes. On the discontinuety of arbitrary constants that appear in divergent developments. *Trans. Cam. Phil. Soc*, 10:106–128, 1857.

[56] G. G. Stokes. Supliment to a paper on the discontinuety of arbitrary constants that appear in divergent developments. *Trans. Cam. Phil. Soc*, 11:412–423, 1868.

[57] G. G. Stokes. On the discontinuety of arbitrary constants that appear as multipliers of semi convergent series. *Acta Mathematica*, 26:393–397, 1902.

[58] P. H. Trinh, S. J. Chapman and J. Vanden-Broeck Do waveless ships exist? Results for single-cornered hulls. *J. Fluid Mech.* (2011), *vol.* 685, pp. 413439.

[59] J. Vanneste. Reflected wave in a slowly varying medium. Unpublished, PDF available on request by emailing: j.vanneste@ed.ac.uk.

[60] W. R. Wasow. Linear Turning Point Theory. *Springer-Verlag*, 1985.

[61] A. Zwaan . Intensitaeten im Ca-Funkenspectrum. Arch. Needandaises Sci. Exactes Natur. Set. 3A, 12, pp. 1-76 (1929).